University of Southern Queensland

Faculty of Engineering and Surveying

Design of a High-Shear Geopolymer Concrete Mixer

A dissertation submitted by

Steven Jon Brown

in fulfilment of the requirements of

Courses ENG4111 and 4112 Research Project

towards the degree of

Bachelor of Mechanical Engineering

Submitted: October 2011

ABSTRACT

Concrete is a well known and understood product used extensively in the building and construction industry however there are ecological drawbacks associated with its use. Geopolymer concrete has been presented as a comparatively environmentally friendly alternative; replacing traditional aggregate with an alumino-silicate material (i.e. fly-ash) and the traditional OPC (ordinary Portland cement) binder with an alkaline solution. Preliminary research performed by HALOK identified deficiencies in the existing mixing techniques and suggested that a high-shear mixer may significantly improve the mechanical strength characteristics of aerated geopolymer concrete.

This study involves the development of a conceptual high-shear mixer suitable for the preparation of aerated geopolymer concrete samples. *ANSYS-CFX* computational fluid dynamics (CFD) software has been used in conjunction with *Solidworks* 3D modelling software to model the behaviour of the tradition 'paddle mixer' and proposed high-shear mixer, to permit a comparison between the two, and ultimately verify the validity of the concept.

The conceptual mixer utilises a rotor-stator arrangement to impart the required shear into the fluid and develop sufficient pressure to promote recirculation of the fluid. Also key to the performance of the mixer is a fly-ash injection system, which is intended to permit greater control over the water/solid ratio of the paste, without compromising workability.

Modelling techniques employed to conduct the steady state analyses include *multiple frame of reference* and *multiphase analysis*. Variables used in assessing the suitability of the high-shear mixer include *velocity*, *pressure* and *shear strain rate*.

Results from the CFD analysis conducted indicate a significant increase in average *shear strain rate* compared to the traditional 'paddle' style mixer. This is expected to result the mixer being able to produce a more homogenous geopolymer paste, ultimately resulting in an increase in strength of aerated geopolymer concrete.

University of Southern Queensland

Faculty of Engineering and Surveying

ENG4111 Research Project Part 1 &
ENG4112 Research Project Part 2

Limitations of Use

The Council of the University of Southern Queensland, its Faculty of Engineering and Surveying, and the staff of the University of Southern Queensland, do not accept any responsibility for the truth, accuracy or completeness of material contained within or associated with this dissertation.

Persons using all or any part of this material do so at their own risk, and not at the risk of the Council of the University of Southern Queensland, its Faculty of Engineering and Surveying or the staff of the University of Southern Queensland.

This dissertation reports an educational exercise and has no purpose or validity beyond this exercise. The sole purpose of the course pair entitled "Research Project" is to contribute to the overall education within the student's chosen degree program. This document, the associated hardware, software, drawings, and other material set out in the associated appendices should not be used for any other purpose: if they are so used, it is entirely at the risk of the user.

Professor Frank Bullen

Dean

Faculty of Engineering and Surveying

CERTIFICATION

I certify that the ideas, designs and experimental work, results, analyses and conclusions set out in this dissertation are entirely my own effort, except where otherwise indicated and acknowledged.

I further certify that the work is original and has not been previously submitted for assessment in any other course or institution, except where specifically stated.

Steven Jon Brown

Student Number: W0049767

Signature

Thursday 27th October 2011

Date

TABLE OF CONTENTS

LIST OF FIGURES

LIST OF TABLES

NOMENCLATURE AND ACRONYMS

The following symbols have been used throughout the text:

$\mathbf{d_{50}}$	median particle diameter
$\boldsymbol{\eta}$	coefficient of rigidity (or plastic viscosity)
m	mass / molar mass / meter
$\boldsymbol{\mu}$	dynamic viscosity
$\boldsymbol{\rho}$	density
$\boldsymbol{\tau}$	shear stress
$\boldsymbol{\tau_0}$	yield stress
$\boldsymbol{\nu}$	velocity
X	mass fraction

The following abbreviations have been used throughout the text:

3D	three dimensional
ATM	atmosphere (101.15 kPa)
AU	Australian
CFD	computational fluid dynamics
CO_2	carbon dioxide
HALOK	Halok Pty Ltd
ID	inside diameter
LHS	left hand side
LSS	liquid sodium silicate
NaOH	Sodium hydroxide
OD	outside diameter
OPC	ordinary Portland Cement
RHS	right hand side
RPM	revolutions per minute
US	United States of America

1. INTRODUCTION

1.1 Introduction

The construction industry and society in general, is beginning to place increased emphases on sustainability. With comparatively lower embodied energy and CO_2 emissions during manufacture, geopolymer concrete is being considered an attractive alternative to traditional Ordinary Portland Cement (OPC) concrete. While there are many potential uses for geopolymer concrete, this study is concerned with the development of a fly-ash-based lightweight geopolymer building material to be used in a modular housing application.

Cellular, or lightweight, concrete has been widely used in Scandinavia for some time but has proved less popular in Australia. It can be manufactured using several different techniques; an additional lightweight aggregate, such as polystyrene, can be added to the mixture or air pockets can be formed either chemically or mechanically.

There have been numerous literary works published which investigate non-aerated geopolymer concrete, however very little research has been conducted investigating aerated geopolymer concrete. One company which has conducted significant research into this developing field of late is Brisbane based HALOK, It has investigated the effect of the chemical composition & mixture ratios of aerated geopolymer concrete and therefore the optimization of these characteristics to gain the required mechanical strength. An example of the samples being produced by HALOK is shown in Figure 1.

Figure 1 - HALOK Fly-Ash-Based Geopolymer Samples

The ultimate objective for HALOK is to produce a fly-ash-based lightweight geopolymer material which may be used in the manufacture of precast panels. It is expected that these panels will be well suited to the ever expanding modular housing sector. A conceptual drawing of such a panel is given in Figure 2 below.

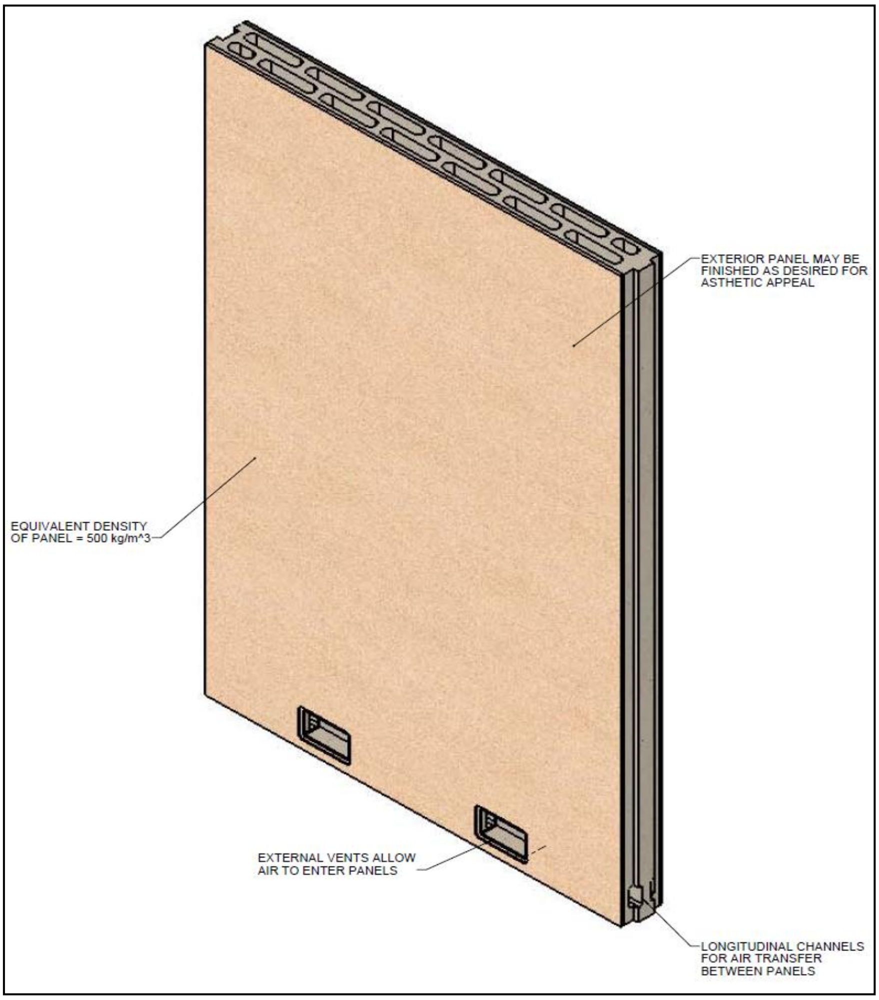

Figure 2 - Precast Lightweight Geopolymer Panel (HALOK Pty Ltd)

During the research conducted by HALOK, some problems have been identified with the mixing process. Mixing has been performed using a traditional paddle mixer and has resulted in the samples often exhibiting non-homogeneous tendencies; thought to be detrimental to the strength of the aerated geopolymer sample.

This study is designed to complement the research already conducted by HALOK by investigating the use of a high-shear mixer to prepare aerated geopolymer concrete samples for testing. A combination of 3D modelling and Computational Fluid Dynamics (CFD) software packages have been used to verify the potential of the conceptual high-shear mixer.

1.2 The Problem

Preliminary mixing trials, by HALOK and other researchers, have generally been performed using a planetary paddle mixer. It has been observed that a homogeneous mixture is not always obtained using this mixing technique. Research into cellular concrete also suggests that strength is affected not only by the microstructure (chemistry) of the concrete but also the macrostructure.

Figure 3 is a magnified image of a sample of aerated geopolymer concrete prepared by HALOK in 2009 where the dark areas represent air voids (pores). The small pores are desirable because they make the material comparatively lightweight. It is clear from this image that there are also some extremely large pores present in the sample. These large pores are thought to significantly reduce the compressive strength of the material.

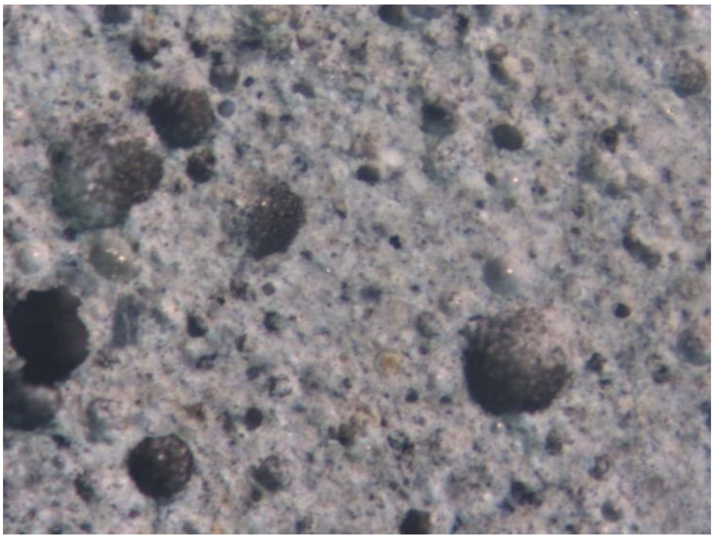

Figure 3 - Aerated Geopolymer – 28x Magnification

If aerated geopolymer concrete is to gain recognition as a reliable construction material into the future, it is critical not only to optimise the chemical composition of the material, but also to optimise the macroscopic properties. The first step in achieving this goal is to design a high-shear mixing device which is suitable for the ongoing research into the viability of the product; essentially the objective of this research project.

1.3 Research Objectives

As noted in the previous section, there is currently a need to improve the mixing process employed in the manufacture of fly-ash-based geopolymer concrete. To achieve this, an appropriate mixing devise must be designed. This research project has been carried out to perform the preliminary design of a high-shear mixer, which may be used in ongoing research by HALOK Pty Ltd.

It is important to note that due to the many unknown variables associated with this fluid, the 'solution' identified in this study is only the first step. A rigorous testing and optimisation program is also required to verify the numerical results obtained to date and this falls outside of the scope of this work.

The primary objectives of this research project are as follows:

1. Research OPC concrete and geopolymer concrete fundamentals
2. Research high-shear mixers used in other industries
3. Develop a conceptual high-shear mixer design
4. Verify the potential of the conceptual design through the use of Computational Fluid Dynamics (CFD) numerical analysis software

1.4 Dissertation Arrangement

The remainder of this dissertation is set out as follows;

- Section 2 - provides some background information on geopolymer concrete including; what it is and why it appeals as a construction material. Cellular concrete is also explained, as are the common mixing techniques currently employed during concrete manufacture
- Section 3 - sets out the design parameters used throughout the research project
- Section 4 - describes the conceptual design phase of the project and provides some explanation as to which design features are considered critical
- Sections 5 & 6 - walk through the process of CFD analysis including; geometry, meshing, analysis setting and results
- Section 7 - discusses the results obtained from all analysis conducted and draws conclusions accordingly. Future work is also discussed

2. LITERATURE REVIEW

2.1 Concrete and the Environment

Concrete is a well known and understood building product which has been used extensively in the building and construction industry since the early 1900's. It's use has become so prevalent that it is now considered a major cause of global ecological problems (Pulselli et al. 2008).

The energy intensive nature of the cement production process is the primary environmental concern. Cement is the binder used in concrete to hold the aggregate together, of which OPC is the most common. The embodied energy in cement accounts for approximately 94% of the total embodied energy in concrete (BuildingGreen.com 1993). This is due to the high temperature (up to 1480 °C) rotating kilns used to mix the cement and also drive the chemical reactions required to make them able to react together through hydration. In 1992 in the United States, cement production required about 0.6% of total US energy use while contributing only 0.06% of the gross domestic product (BuildingGreen.com).

In more recent times, carbon emissions have come onto the environmental radar due to their breaking down of the ozone layer. Carbon dioxide emissions during cement production are mainly due to the burning of fossil fuels to operate the rotary kiln. It is estimated that the cement industry releases 5-8% of global CO_2 emissions (Davidovits 1993).

The raw materials used in concrete are a finite resource and although the materials required are easily available in significant quantities, minimizing the quantity of these materials required for production can only be beneficial.

2.2 Geopolymer Concrete

2.2.1 Introduction and Chemistry

As noted earlier, traditional concrete relies on OPC as a binder to hold the aggregate together. Geopolymer concrete replaces traditional aggregate with alumino-silicate material and uses an alkaline solution as the binder. The alumino-silicate material may be natural or may be industrial wastes such as fly-ash or slag. The alkaline activator is usually sodium hydroxide, sodium silicate or a combination of the two. Geopolymerisation can be described as the process which occurs when the alumino-silicate powder is mixed with the alkaline solution; a paste is formed which quickly transforms into a hard geopolymer (Komnitsas & Zaharaki 2007).

The complex and not-well-understood reaction mechanisms, which occur during geopolymerisation, are outside the scope of this research; however a basic understanding of the chemistry of geopolymer concrete is relevant. In many geopolymer literary works the term 'sialate' is often used as an abbreviation for alumino-silicate oxide and the term 'polysialate' is the chemical designation preferred to describe geopolymers. Sialate networks consist of tetrahedral anions $[SiO_4]^{4-}$ and $[AlO_4]^{5-}$ which share the oxygen. These networks require positive ions (Na^+, K^+, Li^+, Ca^+, Na^+, Ba^{2+}, NH^{4+}, H_3O^+) to compensate for the electric charge of Al^{3+} which results from the tetrahedral coordination (Pacheco-Torgal et al. 2008). The polysialate has the empiric formulae:

$$M_n\{-(SiO_2)_z – AlO_2\}_n, wH_2O$$

where n is the degree of polymerization, z is 1, 2 or 3 and M is an alkali cation such as potassium. Davidovits presents some Polysialate structures diagrammatically as shown in Figure 4.

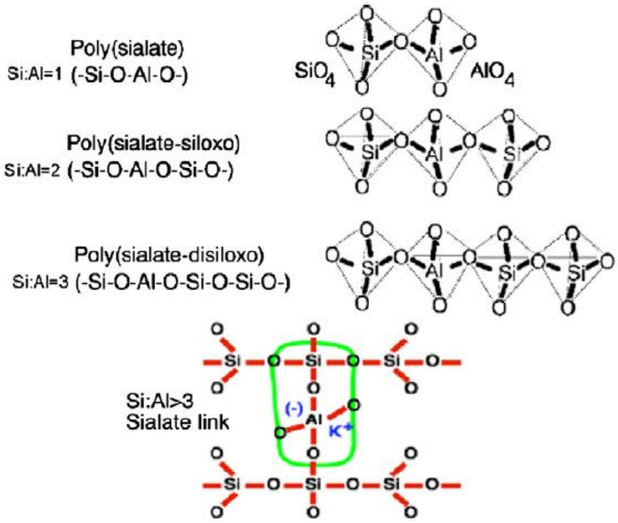

Figure 4 - Poly(sialate) Structures According to Davidovits

Much of the early research into geopolymers used kaolinite and calcined kaolinite (metakaolin) as the raw materials, while more recently the use of fly ashes and blast furnace slag has been investigated. Theoretically any material composed of silica and aluminium can be alkali activated, however fly ash and slag are recognized as attractive sources for the alumino-silicate component because they are industrial waste products.

This study will focus on geopolymer concrete using mainly fly ash as the raw material for two reasons:

1. Fly-ash is abundant in Australia
2. Fly-ash is very fine (typically 0.5μm to 100μm), which is an important property if high strength is to be achieved (Kumar et al. 2007).

2.2.2 Fluid Properties

One of the more challenging complications of this study is how to accurately model the fluid in a CFD analysis. Concrete has long been considered to behave as a Bingham fluid and research into the rheology of fly-ash based geopolymer concrete has found this geopolymer paste also conforms to the Bingham model (M. Criado 2009).

Mechanical engineers commonly deal with Newtonian fluids such as water where the shear rate (or velocity gradient) between any two adjoining layers of fluid is constant. The shear stress and the shear rate are related by a well known property called the dynamic viscosity as follows:

$$\tau = \mu \times \frac{dv}{dy}$$

Bingham fluids differ from Newtonian fluids because they possess an additional parameter; yield stress ($\boldsymbol{\tau_0}$). The yield stress represents the minimum shear stress which must be applied to the material before it will move. An excellent description of a Bingham material is provided in the *Weir Slurry Pumping Manual* as follows:

"This material behaves like a jelly when stationary and like a fluid when moving. If a shear stress below $\boldsymbol{\tau_0}$ *is applied to it, it flexes like a jelly and when the stress is removed it returns to the original shape. However, if the applied shear stress is above* $\boldsymbol{\tau_0}$ *the material begins to flow."* (Anthony Grzina 2002)

Tomato sauce is an especially good everyday example of a Bingham fluid. If a person were to shake the bottle; causing the sauce to flow, that person is imparting a shear stress on the fluid.

Rather than the dynamic viscosity, the coefficient of rigidity (sometimes termed the plastic viscosity) along with the yield stress are used to relate the shear stress and the shear rate as follows:

$$\tau = \tau_0 + \eta \times \frac{dv}{dy}$$

The difference between a Bingham fluid and a Newtonian fluid is shown in the Pseudo Shear Stress Diagram included in Figure 5.

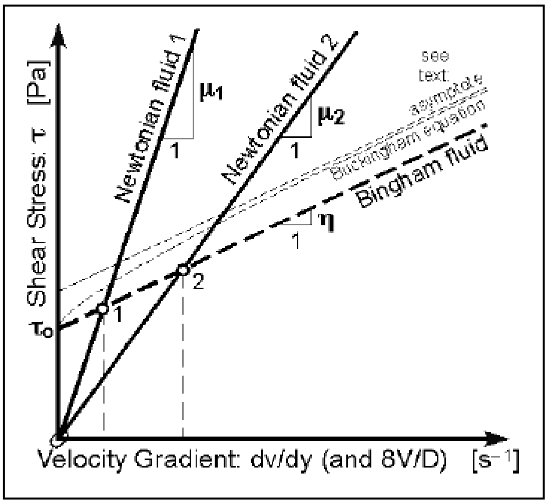

Figure 5 - Bingham Fluid - Shear Stress Diagram

To accurately assess the rheology of aerated geopolymer paste is a study in itself, therefore benchmark values for viscosity and yield stress have been taken from a previous study entitled *'Alkali Activated Fly Ash: Effects of Admixtures on Paste Rheology'* (M. Criado 2009). The results of this study are shown graphically in Figure 6. The coefficient of rigidity of fly ash is approximately five (5) times higher than that of traditional OPC based concrete, while the yield stress is approximately seven (7) times lower. This suggests that a relatively small shear stress is required before geopolymer paste will flow, but considerable effort is required to keep it flowing.

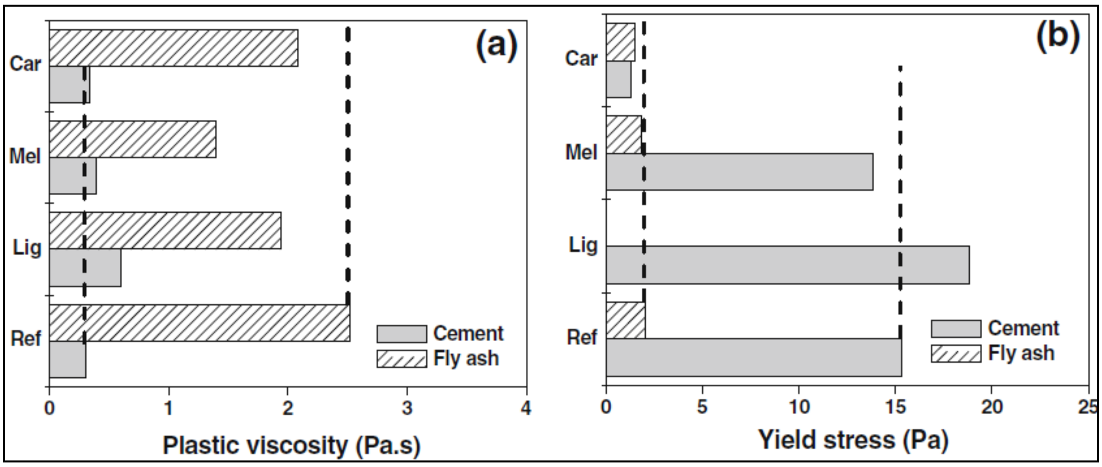

Figure 6 - Coefficient of Rigidity and Yield Stress of Alkali Activated Fly Ash

2.2.3 Factors Affecting Compressive Strength

The compressive strength of a geopolymer is generally considered to be a good indicator of the durability and stability of the product. Solid fly ash based geopolymers generally achieve compressive strengths greater than 40 MPa and given favourable curing conditions and mix designs, the compressive strength can approach 100 MPa. The compressive strength is dependent on several variables, some of which are discussed in this section.

2.2.3.1. **Fly Ash Composition**

The composition of the fly ash is thought to have a significant effect on the strength of the geopolymer produced. It is believed that there is an optimum ratio of Silicone to Aluminium; with strength increasing as the Si:Al ratio is increased from 1.375 to 1.7 (Kovalchuck et al. 2007).

More important than the Si:Al ratio is the available reactive content. A study in 2006 found specimens with similar Si and Al content differed appreciably in strength due the drastically different degree of reaction (Fernandez-Jimenez et al. 2006).

2.2.3.2. **Activators**

Studies have assessed the use of both sodium hydroxide and potassium hydroxide as activators, however no appreciable difference in strength was observed (Duxton et al. 2007). The research work performed by HALOK has concentrated on the use of NaOH activators due to the associated cost advantage. NaOH costs approximately AU$1.00/kg while KOH costs approximately AU$2.00/kg. Given that the fundamental reason for pursuing geopolymer research is to develop a commercially viable building product, any slight advantage in strength brought about through the use of KOH is far outweighed by the associated cost disadvantage.

Liquid sodium silicate (LSS) is often used in conjunction with NaOH. There is some conjecture regarding the importance of the LSS:NaOH ratio. It has been reported the 'higher the ratio of sodium silicate solution-to-sodium hydroxide solution ratio by mass, higher is the compressive strength of geopolymer concrete' (Hardjito 2005). Other published works report high strength geopolymers achieved with very low LSS:NaOH ratios (Rattanasak & Chindaprasirt).

2.2.3.3. **Fineness**

Literary works generally agree that the fineness of the raw materials used has a significant effect on the strength of the geopolymer. (Temuujin et al. 2009) milled the raw material (fly ash) for 60 minutes prior to mixing with alkali activators and reported an increase in strength of 80% compared to non-milled fly ash.

One must consider, that as the fineness of the raw material increases, so too does the surface area of the material. This often means that in order to maintain workability, more water must be added to the mixture.

2.2.3.4. **Water to Solids Ratio**

The water to solids ratio (W:S) is typically between 0.2 and 0.4 to achieve a paste with suitable workability. An increase in the W:S ratio results in higher porosity and a subsequent decrease in strength.

An investigation into the liquid alkali to ash ratio and the effect on workability and strength of lignite bottom ash geopolymer mortar found that a lower threshold of water content was required to ensure proper mixing (Sathonsaowaphak et al. 2009). There is very little published research investigating the possibility of successfully mixing geopolymer pastes at low W:S ratios.

2.2.3.5. **Curing**

Most geopolymer research has utilized curing ovens to some extent. Investigations have found that samples benefited by elevated curing temperatures with strength steeply increasing as the curing temperature was increased to 60 °C, followed by a moderate strength increase as the curing temperature was further increased toward 100 °C (Hardjito). Other authors have published similar findings related to curing temperatures.

Preliminary experiments performed by HALOK have indicated that stepped curing can be beneficial for cellular geopolymer structures. This is thought to be because high initial temperatures can cause the foam bubbles to expand, leading to excessive pore size and a decrease in strength. Comparatively good results were achieved by curing at low (40 °C) temperatures for the first 12-24 hours prior to increasing the curing temperature.

The practicality of high temperature curing for a commercially viable building product needs to be considered further. High temperature curing has many drawbacks including high capital costs associated with the construction of a large curing oven, high operating costs and high energy use. One of the major attractions of geopolymer concrete is decreased embodied energy (compared to concrete using OPC binders), therefore if the curing process requires significant energy, it somewhat defeats the purpose of the project.

2.3 Cellular Concrete and its application to Geopolymers

Cellular (lightweight) concretes were first developed in Scandinavia and have become familiar in the local building industry. It has been reported that four out of every five building erected in Sweden are built from cellular concrete (*Cellular Concrete* 1963). The main use of cellular concrete globally however, is as backfill or thermal insulation.

The results of an experiment conducted by HALOK give an indication of the thermal characteristics of aerated geopolymer. A *Hot Disk TSP2500* thermal conductivity instrument was used to measure the thermal conductivity of aerated, fly-ash-based geopolymer. The experiment yielded a thermal conductivity value of 0.2632 $\frac{W}{m.K}$. For insulation purposes, designers are seeking a low value of thermal conductively. This value compares favourably with other building materials such as brick and masonry, which have a thermal conductivity in the range of 0.38 - 0.66 $\frac{W}{m.K}$.

There are two broad categories of cellular concrete; Autoclaved Cellular Concrete is formed chemically by adding aluminium powder, whereas Physically Formed Cellular Concrete is formed either mechanically in fast rotating pug mills, or by addition a foaming agent to the mix. Chemical forming provides a higher regularity and reproducibility of pore distribution than physical forming which is why it has been the preferred method for structural applications to date (Just & Middendorf 2008). Despite the previous use of autoclaved cellular concrete for structural applications, it is thought that physically formed cellular concrete is better suited to a commercially viable pre-cast application because it is much easier to control than chemical methods and it does not require the concrete to be cured in a saturated steam atmosphere. Studies into aerated geopolymer concrete conducted by HALOK have focused on pores formed by the addition of pre-formed foam into the paste prior to mixing. This study will focus on foamed geopolymers.

The water/cement ratio significantly affects the strength of cellular concrete and cellular geopolymers. Figure 7 shows the structure of two foamed concretes where the only difference in composition is the water/cement ratio. The sample on the right hand side has lower water content; this causes a significant decrease in pore size, and an increase in strength (Just & Middendorf).

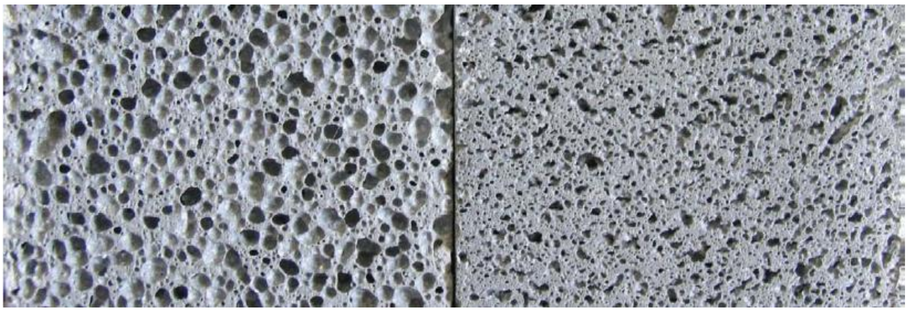

Figure 7 - Effect of Water/Cement Ratio on Cellular Concrete (Just & Middendorf)

A study into pore size found that as the pore size increased, the roundness of the pores decreased, although it is noted that the roundness is also affected by the stiffness of the fresh mortar. Regardless of the mix composition, large pores (with an area greater than 1.0mm^2) accounted for a significant percentage (18.6% - 49.6%) of the total pore area (Just & Middendorf).

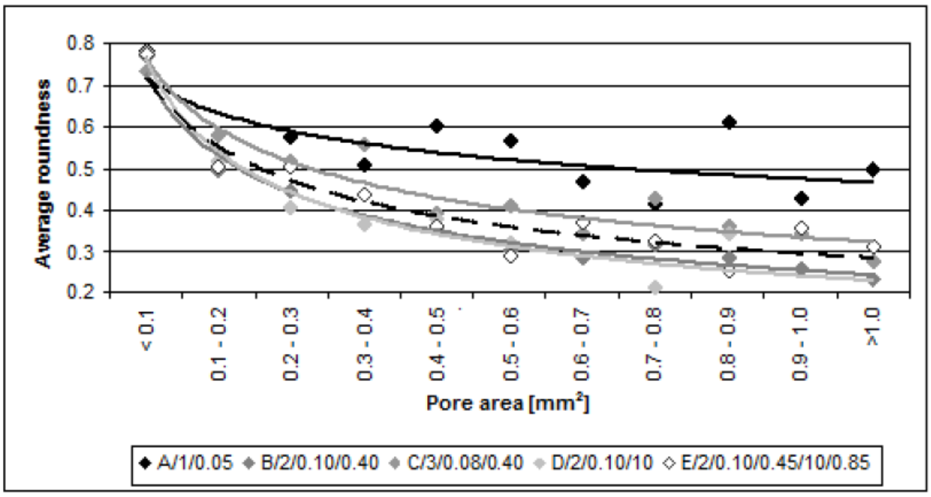

Figure 8 - Affect of Pore Size on Roundness (Just & Middendorf)

One of the main issues with cellular concrete (using OPC as a binder) is that the water/solids ratio is normally required to be between 0.4 and 0.5 to achieve a paste with suitable workability. Lower water content results in flocculation of the cement (clumping of the cement powder), a non-homogeneous stiff paste, irregular voids and ultimately low strength.

When considering the production of foamed geopolymers, it is desirable to reduce the water/solid ratio without compromising the workability of the paste. A mixture with a greater number of small void, will also improve the strength characteristics of the product.

2.4 Concrete Mixers and High Shear Mixers

The quality of concrete is heavily dependent on the homogeneity of the material after mixing and placement (Ferraris 2001). It is therefore somewhat surprising that there has been little development of concrete mixers during the last century. Any design improvements have generally targeted the energy efficiency of the mixer, rather than how effectively a mixer can produce a uniform concrete.

Traditional mixers used in the concrete industry may be divided into two broad categories; batch mixers and continuous mixers. Batch mixers are used to mix a given quantity of concrete by adding all of the required materials into a container (usually a drum or pan), mixing for a predetermined period of time, before discharging the mixture and starting the process again. In comparison, continuous mixers have raw materials continuously fed into the container at the same rate as the finished product is discharged from the mixer. For the production of precast aerated geopolymer concrete, a continuous mixing process is considered essential for cost-effective production.

While high shear mixing is not required for the production of concrete, it is common in other industries such as chemical, pharmaceutical, food and cosmetic production. IKA is a company specializing in the supply of high shear mixers utilizing a rotor-stator mixing technique as shown in Figure 9 (*IKA Industrial Mixers*). It is thought that this same technology could be applied successfully to geopolymer production because the raw material (fly ash) is a powder not dissimilar to those used in the industries noted above.

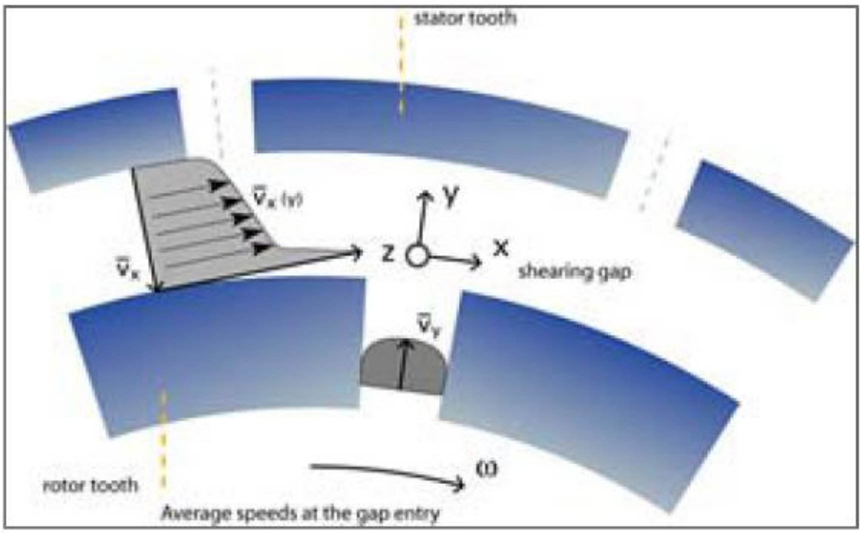

Figure 9 - Rotor-Stator High Shear Mixing (IKA Industrial Mixers)

2.5 Use of CFD in Mixer Design

As computing power improves, computational fluid dynamics (CFD) continues to become more accessible to designers and researchers alike. CFD is especially well suited to the design and optimization of turbo-machinery and is proving a useful aid in the design of agitators and hydrofoil type mixers.

2.5.1 ANSYS-CFX

HALOK currently use the commercial software package *ANSYS-CFX* for their CFD requirements. It is desirable to use this software package not only because the licence is readily available, but also so skills developed during the research project may be transferred onto other projects performed by HALOK.

ANSYS-CFX has previously been used for the analysis of various mixing components including static mixers, agitated tanks and combustion engine cylinders (*ANSYS CFD* 2010). Especially relevant to this project is the turbo-machinery design tool included in *ANSYS-CFX*. This tool is typically used to aid the design of pumps and fans, and the same design principles may be applied to a rotor-stator type high-shear mixer.

2.5.2 Modelling Considerations

Low shear hydrofoils have been successfully modeled in *ANSYS-CFX* by solving the unsteady Navier-Stokes equations and the conservation of mass equation (Spogis & Nunhex). This is the proposed technique for this study.

Typically rotating mixer analyses are run using the transient rotor-stator model (also called the frozen rotor model). A study conducted in 2006 used a rotation angle of 2° per time-step and a maximum of 10 coefficient loops at each time-step (Torre et al. 2006). The rotor analysed was a three bladed rotor, while the rotor used in a high-shear mixer is could include up to 20 blades. The high-shear mixer analysis may therefore lead to extremely long computation times.

3. CONCEPTUAL DESIGN PHASE

3.1 Primary Design Criteria

Prior to commencing any conceptual modelling or analysis a set of primary design criteria were defined as follows:

1. The mixer shall produce a geopolymer paste of a homogenous nature
2. The mixing process must preserve the voids formed in the paste
3. Reduce the water:solids ratio required for workability
4. The mixer shall be designed for use in a laboratory environment
5. The fundamental mixing technique shall be capable of being applied at an industrial scale in the future

3.2 Conceptual Modelling

The conceptual high-shear mixer has been modelled using *Solidworks*, which is a fully parametric 3D modelling package. There are several reasons for adopting a 3D modelling technique in the early stages of design:

- Model can be used to generate the fluid domains for CFD analysis
- Provides a greater understanding of the interaction between components
  - Provides a method of identifying clashes
  - Ensures that the concepts being applied in the CFD analysis can be transferred to a practical application (i.e. can be fabricated)
- Design changes are seamlessly updated through all components
- Only minor modification of the model is required to produce workshop drawings for prototype mixer

The ‘top-down’ modelling philosophy has been applied when constructing the mixer model, which means that all components are driven from a set of ‘top-level’ sketches. When a change is made to any of the ‘top-level’ sketches (such as modifying a dimension), all components which are driven off that sketch are updated automatically. This is especially useful during the conceptual design phase, where the concept undergoes continuous optimisation.

3.3 Key Design Features

The high-shear mixer concept has evolved throughout the research project according to the results of the CFD analysis. An isometric view of the most recent model is shown in Figure 10, while a partial section view is presented in Figure 11.

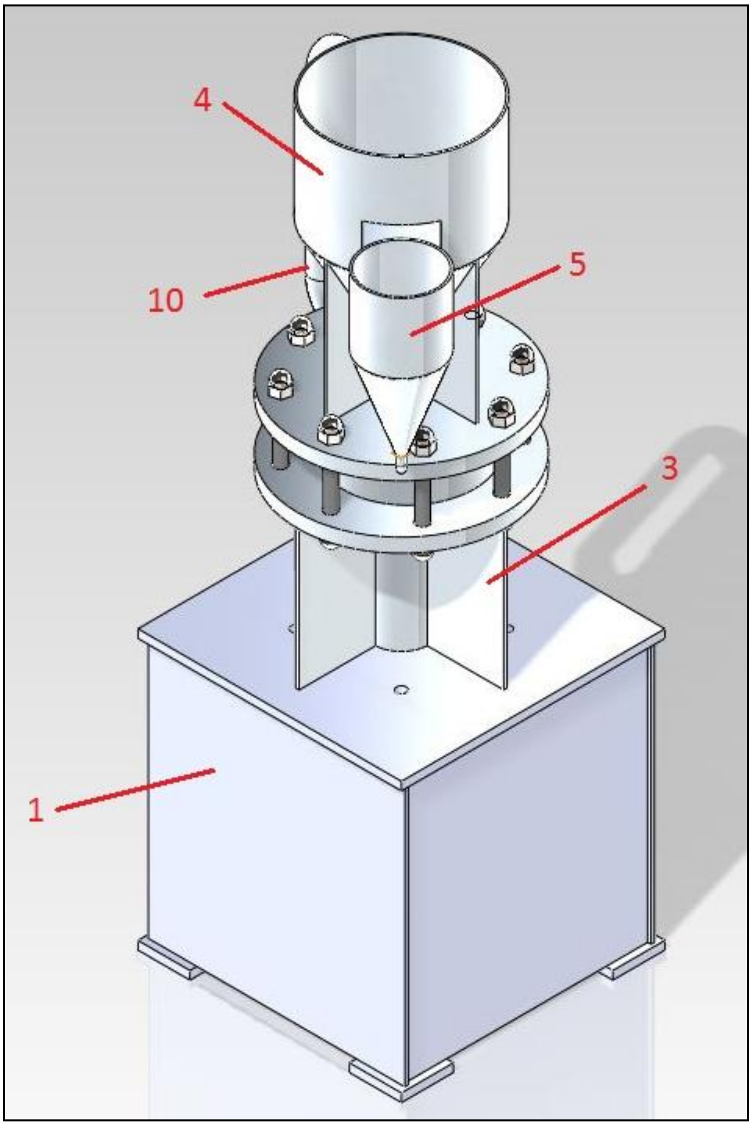

Figure 10 - High-Shear Mixer (Isometric View)

The fabricated carbon steel base frame provides a mounting location for the pedestal above and motor below (not visible). Fluid buffer capacity is provided by a hopper located above the mixer volute which allows the mixer to be gravity fed. An additional hopper stores fly-ash powder which is injected into the mixing chamber via a venturi injection system. This method of injecting the fly-ash powder into the geopolymer paste during operation is aimed reduce the water:solids ratio required for workability.

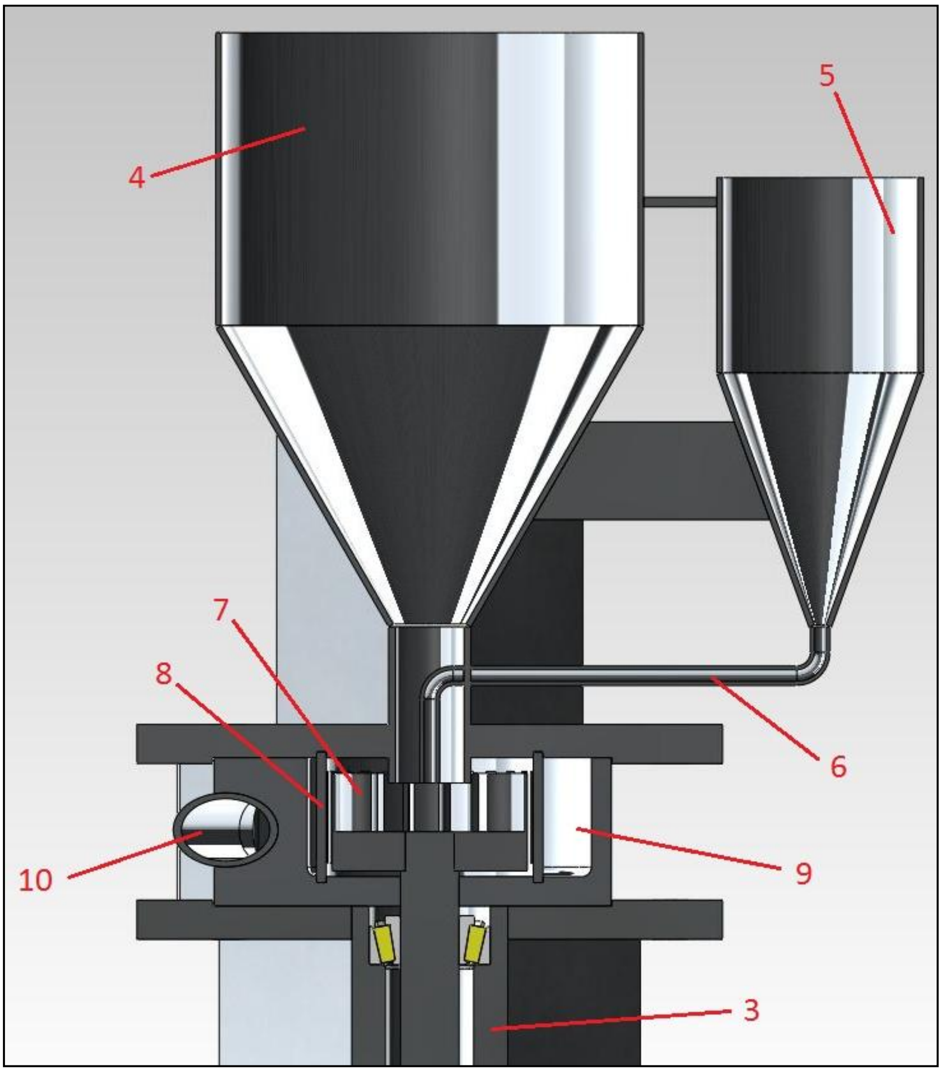

Figure 11 - High-Shear Mixer (Partial Section View)

The key concept behind the high-shear nature of the mixer is the rotor-stator arrangement shown in Figure 12. The rotor acts to accelerate the geopolymer paste, drawing it from the hopper above, and forcing it to flow through the *shear gap* (gap between the rotor and stator) and then through the passages cut into the stator. It is this process which induces significant shear stress in the fluid.

The remaining key component is a volute similar to that used in a centrifugal pump which acts to collect the geopolymer paste once it has passed through the stator, and direct it into the recirculation pipe which returns the fluid back to the buffer hopper.

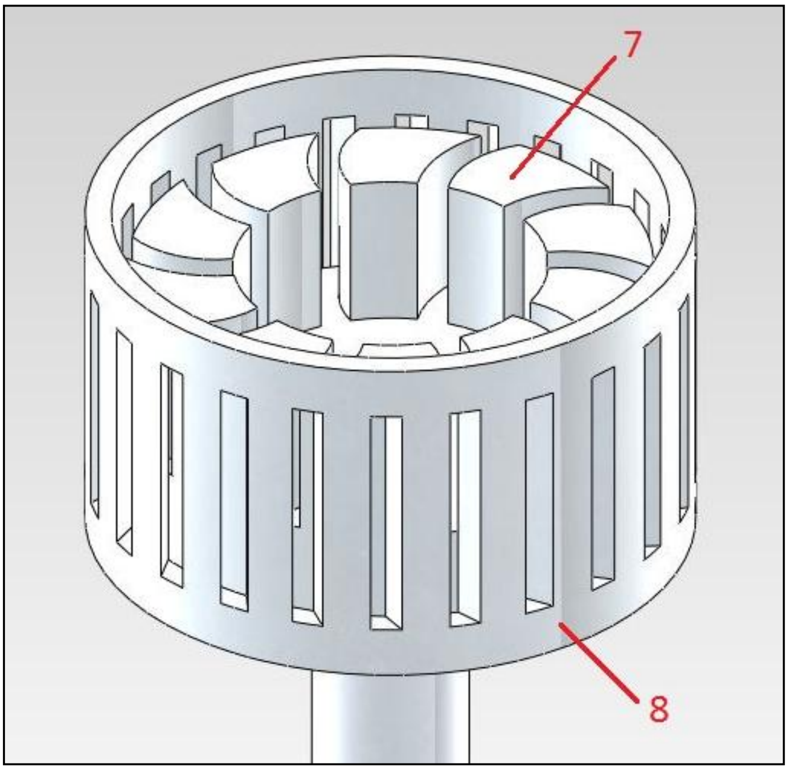

Figure 12 - High-Shear Mixer (Rotor-Stator)

3.4 Proposed Mixing Procedure

The proposed mixing procedure is aimed at reducing the water:solids ratio of the paste as well as allowing the degree-of-mixing to be varied simply by changing the mixing time. The proposed procedure involves the following steps:

1. Pre-mix the alkaline solution with approximately 80% of the fly-ash in the geopolymer paste hopper
2. Add the remaining fly-ash to the fly-ash hopper
3. Commence mixing
4. Inject approximately half the remaining fly-ash intermittently into the geopolymer paste as it recirculates through the mixer
5. Add the full quantity of foaming agent to the geopolymer hopper
6. Inject the remaining fly-ash intermittently into the foamed geopolymer paste as it recirculates through the mixer
7. Terminate mixing

The numbers in the images above are related to the key design features, which are described below:

1.	Base Frame	Lifts the mixer to a suitable working height and provides mounting location for the central pedestal and drive motor
2.	Drive Motor	Variable speed drive unit to permit the angular velocity of the rotor to be altered during prototype testing
3.	Pedestal	Provides suitable bearing housings and centralises the drive shaft
4.	Geopolymer Hopper	Provides buffer storage for the geopolymer paste and allows for recirculation
5.	Fly-ash Hopper	Stores approximately 10% of the total fly-ash required for the mix to be injected into the geopolymer paste during mixing
6.	Fly-ash Injection	Injects fly-ash powder into the mixing chamber via a tube and venturi
7.	Rotor	The angular velocity of the rotor accelerates the fluid, drawing it down from the hopper and forcing it through the stator
8.	Stator	Forces the geopolymer paste to pass through the *shear gap* (gap between the rotor and stator), essentially shearing the fluid
9.	Volute	Redirects fluid flow after it has passed through the rotor-stator arrangement
10.	Recirculation	Geopolymer paste is redirected from the volute outlet back into the hopper. This permits the fluid to be run though the mixer any number of times, depending on the required degree of mixing
11.	Modular Assembly	The modular nature of the assembly permits different rotors and stators to be trialled during prototype testing

4. DESIGN PARAMETERS

4.1 Raw Materials

As noted in Chapter 2, geopolymer concrete consists of two primary materials; an alumino-silicate and an alkaline activator. Fly-ash presents as an attractive option for the alumino-silicate because it is a waste product from coal fired power stations. Fly-ash is also relatively abundant in Queensland and throughout Australia, which is why studies conducted by HALOK have focused on its use.

4.1.1 Fly Ash

There are several potential sources of fly-ash within Queensland and many have been used in testing including Gladstone, Tarong, Swanbank and Millmerran. Tarong fly-ash has provided encouraging results in testing conducted by HALOK, and has therefore been used more than the other fly-ash samples. For this reason, the material properties of Tarong fly-ash are used in this design project.

4.1.1.1. **Chemical Composition**

Inspection of Figure 13 shows that although fly ash is composed of several elements, the two primary compounds are silicon dioxide and aluminium oxide. For design purposes, a simplified bi-component fly-ash composition is established for Tarong fly-ash as shown in Table 1.

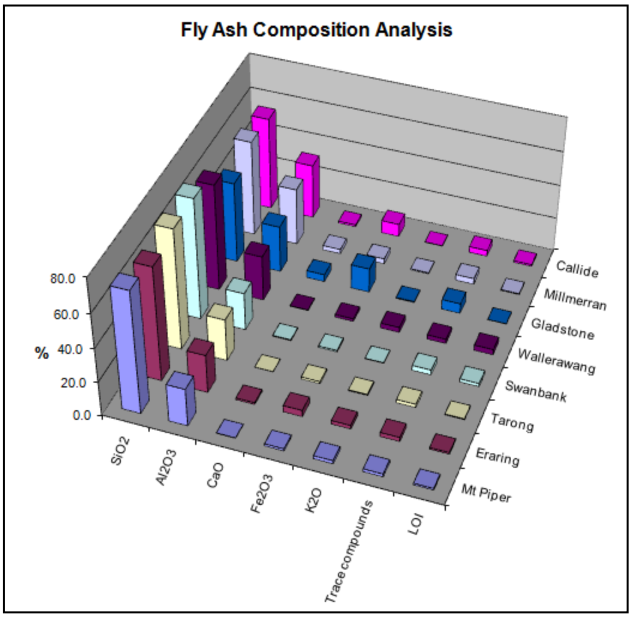

Figure 13 – Fly-ash Composition

Table 1 - Tarong Fly-ash Design Composition

Item	Description	Molecular Formula	Molar Mass	Density	Actual Mass Fraction	Assumed Mass Fraction
1	Aluminium Oxide	Al_2O_3	101.96 g/mol	3950 kg/m^3	0.247	0.258
2	Silicon Dioxide	SiO_2	60.08 g/mol	2650 kg/m^3	0.712	0.742
3	Trace elements	n/a	n/a	n/a	0.041	n/a

4.1.1.2. **Molar Mass & Density**

Based on the assumed mass fractions given in Table 1, the effective molar mass and density of fly-ash can be calculated as follows:

$$m = \left[(101.96\frac{g}{mol} \times 0.258) + (60.08\frac{g}{mol} \times 0.742) \right] = 70.89\frac{g}{mol}$$

$$\rho = \frac{1}{\left[\left(\dfrac{0.258}{3950\frac{kg}{m^3}} \right) + \left(\dfrac{0.742}{2650\frac{kg}{m^3}} \right) \right]} = 2896\frac{kg}{m^3}$$

4.1.1.3. **Particle Size**

The results of a particle size analysis of Tarong fly-ash conducted by the CSIRO are presented in Figure 14, while the full analysis report is included in Appendix B. The median particle diameter is the critical design parameter required - $d_{50} = 28.25\mu m$.

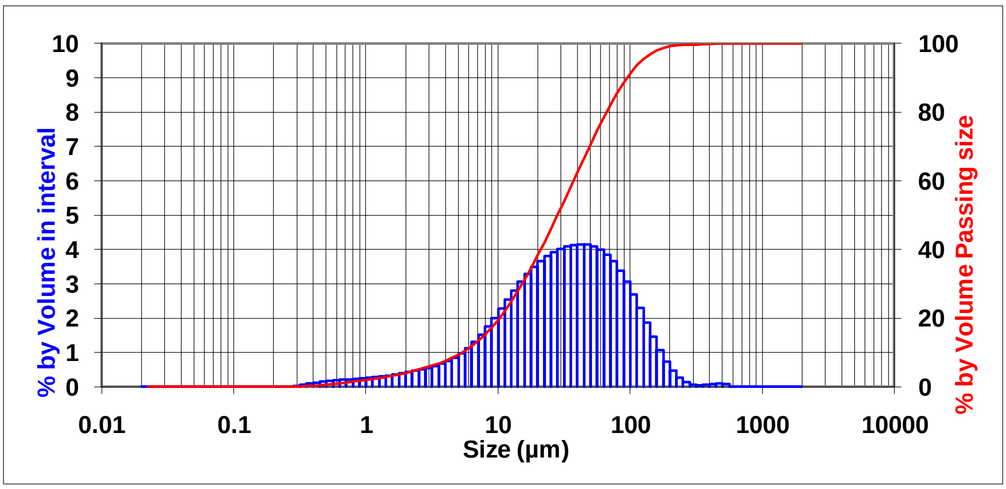

Figure 14 - Tarong Fly-ash Particle Size Distribution

4.1.2 Alkaline Solution

There are many potential combinations of NaOH and LSS which have been used in alkali activated fly-ash-based geopolymer research, but is impractical to consider all of these combinations in this design project. It is assumed that 100% NaOH is used as the alkali binder mainly due to its relatively low cost compared to LSS.

The sodium hydroxide used in trials is in the form of a pre-mixed solution containing 24.2% solids. This enables an effective mass fraction for the geopolymer paste to be calculated in Section 4.1.3.1.

4.1.3 Geopolymer Paste

Rather than run a complex multiphase CFD analysis where the fly-ash particles and alkaline solution are modelled as two separate phases, a single phase is modelled representing the geopolymer paste. In order to proceed with the analysis however, it is necessary to calculate the effective physical properties of the paste.

4.1.3.1. **Density and Molar Mass**

For the purpose of the CFD analysis, a single mix composition has been selected. This is an actual mixture prepared by HALOK using Tarong Fly-Ash, which produced a material possessing good mechanical properties. The mass fraction of the mix design used is as follows:

1. Fly-ash mass fraction = 0.612
2. Sodium hydroxide solution mass fraction = 0.269
3. Additional water mass fraction = 0.119

The effective mass fractions of the alkaline solution and water can now be calculated based on the percentage of solids present in the NaOH (described in Section 4.1.2) as follows:

$$X_{NaOH} = 0.269 \times 24.2\% = 0.065$$

$$X_{H_2O} = (0.269 \times 75.8\%) + 0.119 = 0.323$$

Table 2 - Geopolymer Paste - Mass Fractions

Item	Component	Molar Mass	Density	Mass Fraction
1	Tarong Fly Ash	70.89 g/mol	2896 kg/m^3	0.612
2	Sodium Hydroxide	40.00 g/mol	2130 kg/m^3	0.065
3	Water	18.02 g/mol	1000 kg/m^3	0.323

The effective mass fractions of the mixture are given in Table 2. These mass fractions permit the effective density and molar mass of the mixture to be calculated. Firstly the effective density of the geopolymer paste is calculated:

$$\rho_{paste} = \frac{1}{\left[\left(\frac{0.612}{2896}\right)+\left(\frac{0.065}{2130}\right)+\left(\frac{0.323}{1000}\right)\right]} = 1770\frac{kg}{m^3}$$

In a similar fashion, the effective molar mass of the paste can also be calculated:

$$m_{paste} = \left[(0.612\times 70.89)+(0.065\times 40.0)+(0.323\times 18.02)\right] = 51.81\frac{g}{mol}$$

4.1.3.2. **Rheology**

As noted in Section 2.2.2, the geopolymer paste is assumed to behave as a Bingham fluid. ANSYS-CFX, which is the software used to perform the CFD analysis, does permit Bingham fluids to be modelled, but requires the input of two variables; coefficient of rigidity and yield stress. The values used in the CFD analysis are taken from the journal entitled *'Alkali Activated Fly Ash: Effects of Admixtures on Paste Rheology'* (M. Criado 2009) and are presented in Table 3 below.

Table 3 - Adopted Geopolymer Paste Rheology Values

Item	Design Parameter	Value
1	Coefficient of rigidity	2.5 Pa.s
2	Yield stress	2.1 Pa

4.1.3.3. **Preliminary Laboratory Testing**

While a thorough analysis of the rheological properties of fly-ash-based geopolymer paste is beyond the scope of this study, an indication of the fluid characteristics can be obtained by employing a simple test using a slump plate (Anthony Grzina 2002).

A slump plate has been used successfully in the field of slurry pumping to provide an instant indication of whether a slurry is potentially pumpable with a centrifugal pump. As the adopted concept utilises a rotor-stator arrangement it behaves essentially like a centrifugal pump, hence the relevance of this test procedure. The following equipment is required for a slump plate test:

- Plate (300mm x 300mm) with concentric rings inscribed on the surface
    - Central ring diameter = 50mm
    - Remaining rings are progressively larger by 20mm
- Tube with a bore of 50mm and length of 50mm with machined ends

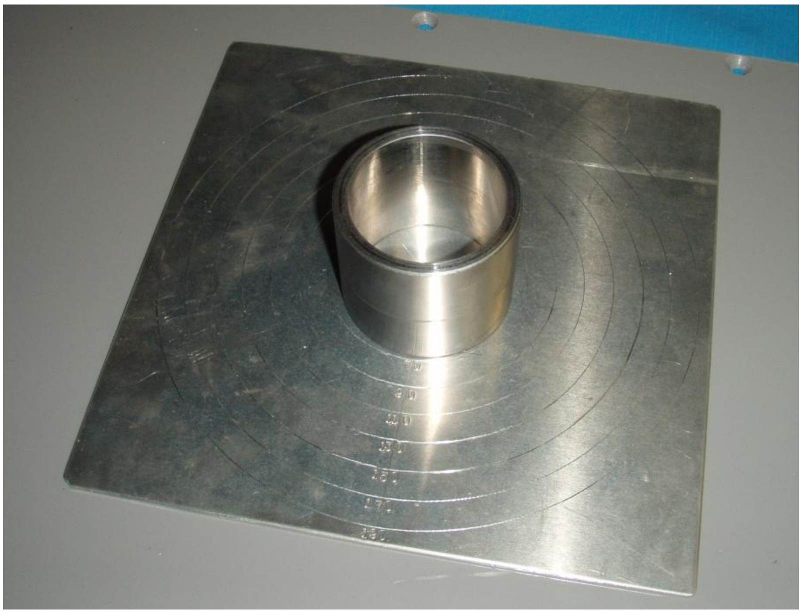

Figure 15 - Slump Plate - Equipment Set-up

The test procedure is as follows:

1. Place the tube in the centre of the plate
2. Fill the tube with a sample of the slurry to be tested
3. Gently lift the tube in the vertical direction allowing the slurry to spread
4. Measure the distance of spread

It is generally acknowledged that if the slurry fails to spread to at least the third concentric ring (110mm diameter), then it is too thick, and a centrifugal pump will not usually be able to pump it (Anthony Grzina 2002).

The results of the slump plate test performed on a typically geopolymer paste is shown in Figure 16 below. The slurry reached the seventh ring (190mm diameter), which indicates that it is pumpable with a centrifugal style pump.

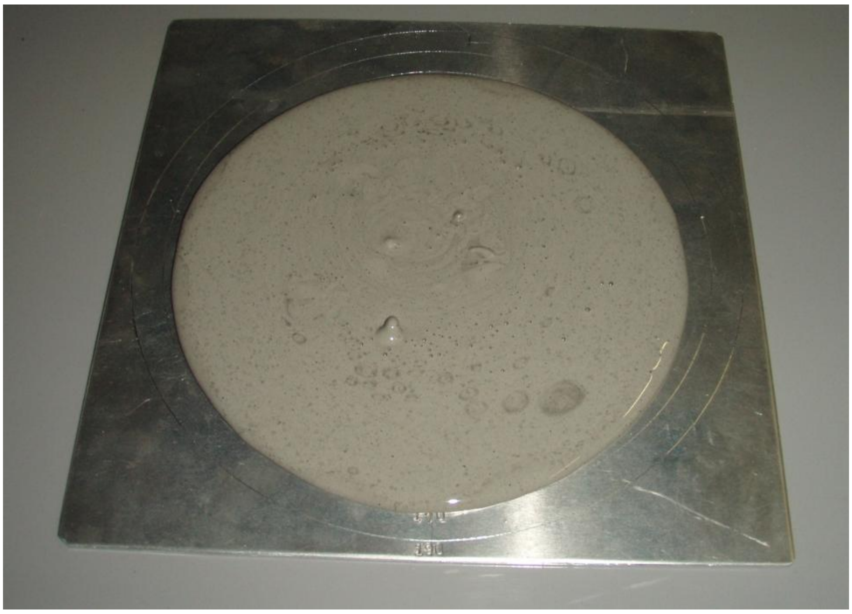

Figure 16 - Slump Plate Results - Geopolymer Paste

This type of test procedure should not be relied upon for accurate rheological data, and a comprehensive testing program will be required to confirm that the fluid can be pumped effectively. This test does provide some comfort however that the conceptual design can be implemented in practice.

4.2 Mixer Design Parameters

To ensure that the CFD analyses conducted on both the existing paddle mixer and the proposed high-shear mixer concept are good approximations real-world phenomena it is important to define appropriate design parameters. The design parameters included in Sections 4.2.1 and 4.2.2 encapsulate the key physical properties of each mixer. These same parameters are used throughout the analysis process.

4.2.1 Paddle Mixer

The paddle mixer used by HALOK in their testing regime is a common dough mixer typically used in commercial kitchens. Although the mixer has a capacity of 30 L, it is typical to prepare a 2.0 kg sample which means that there is only about 150mm of fluid in the bowl. It was therefore necessary only to model the lower section of the bowl and paddle. A site inspection of the mixer was undertaken to measure all critical dimensions and verify the operating speed. The key design parameters used in the subsequent CFD analysis are given in Table 4 below.

Table 4 - Paddle Mixer Design Parameters

Item	Design Parameter	Value	Comments
1	Bowl capacity	30 L	Maximum capacity when full
2	Fluid volume	2.0 kg	-
3	Bowl diameter	335 mm	Varies (nominal value)
4	Paddle diameter	175 mm	Varies (nominal value)
5	Shear gap	15 mm	Minimum value
6	Angular velocity (planetary)	100 rad/s	Not required for simplified analysis
7	Angular velocity (paddle)	40 rad/s	-
8	Tip velocity (paddle)	8.75 m/s	-

4.2.2 High-Shear Mixer

The conceptual model of the high-shear is detailed in Section 3 is the result of several iterations of the concept throughout the design process. Three significantly different versions of the high-shear mixer model were analysed, nominated in the remainder of the text as model A, B and C. The key design parameters are therefore broken down into two distinct categories; *fixed* or *variable*. The fixed design parameters which remain constant throughout the subsequent CFD analysis are given in Table 5.

Table 5 - High-Shear Mixer – Fixed Design Parameters

Item	Design Parameter	Adopted Value	Comments
1	Hopper capacity (paste)	5.0 kg	-
2	Hopper capacity (fly-ash)	2.0 kg	-
3	Mixer capacity	0.4 kg/s	Nominal
4	Outlet Pressure (min)	18.4 kPa	Refer Section 6.1
5	Rotor diameter	100 mm	Outside diameter
6	Number of rotor blades	12	-
7	Blade angle	25°	-
8	Cross sectional area of rotor passages	2160 mm^2	Sum of all passages
9	Angular velocity	1200 RPM	Nominal
10	Stator diameter	106 mm	Inside diameter
11	Shear gap	3.0 mm	-

The high-shear mixer analysis process involved the following steps:

1. Comprehensive preliminary analysis of 'version A' involving multiple analysis runs with varying values of *angular velocity* and *mass flow rate*
2. Identify a nominal mass flow rate and angular velocity for the remainder of the design process, based on the analysis results obtained in Step 1
3. Modify key design parameters and re-run the analysis to improve mixing characteristics

There are a number of design variables which could be varied; this research however focuses on four parameters, given in Table 6. The variable design parameters selected are as follows:

1. Stator thickness – Affects flow direction into the volute
2. Number of stator passages – Affects frequency of the rotor-stator arrangement
3. Cross sectional area of the stator passages – Restricts the flow of fluid through the stator, hence affecting *velocity* and *shear strain rate*
4. Stator angle – Affects flow direction into the volute

The fifth design parameter in Table 6 is the ratio between the cross sectional area of the stator passages to the cross sectional area of the rotor passages; therefore this ratio is directly proportional to the item 3. The area ratio can be considered to be a measure of the flow restriction in the rotor-stator arrangement.

Table 6 - High-Shear Mixer – Variable Design Parameters

Item	Design Parameter	Adopted Value		
		A	B	C
1	Stator thickness	5.0 mm	3.0 mm	5.0 mm
2	Number of stator passages	24	12	24
3	Cross sectional area of stator passages	8448 mm^2	10560 mm^2	6480 mm^2
4	Stator angle	0°	0°	30°
5	Area ratio	3.9	4.9	3

5. PADDLE MIXER ANALYSIS

5.1 Traditional Paddle Mixer

Prior to performing any analysis on the conceptual high-shear mixer, an analysis of the existing mixer was performed. There are two reasons for conducting an analysis of the existing mixer. Firstly, comparison of the analysis results with physical observations during operation serves to validate the analysis results. Secondly, it sets benchmark values for the fluid velocity and shear strain rate which are used to quantify any perceived improvements made by the high-shear mixer.

The mixer is similar to that shown in Figure 17, where the paddle rotates in a planetary motion about a vertical axis and the bowl remains stationary. It should be noted however that HALOK have modified the paddle by the addition of rubber strips, which act to reduce the gap between the mixing paddle and the bowl. This alteration is also shown in Figure 17.

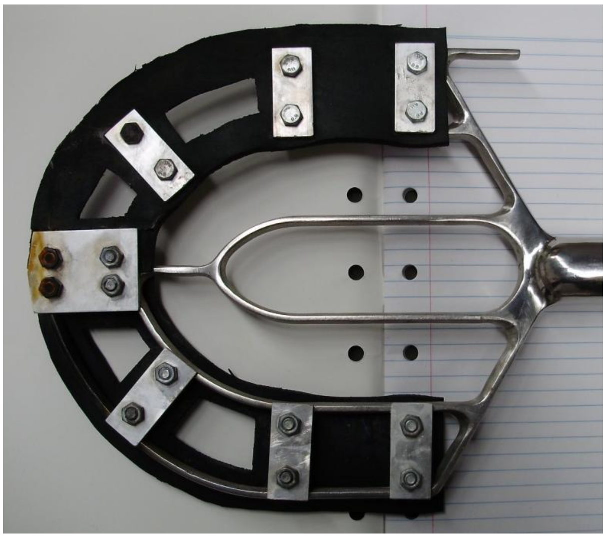

Figure 17 – Traditional Paddle Mixer and the Modified Paddle used by HALOK

The traditional method of sample preparation involves emptying all of the fly-ash and alkaline solution into the bowl, starting the mixer, and adding additional water as required while the mixer is running. An improved method is to add the alkaline solution and 90% of the fly-ash into the bowl initially, start the mixer, and then sift the remaining fly-ash into the bowl while the mixer is running. The latter method reduces the quantity of additional water required for workability, reducing the water/solids ratio of the mixture. The CFD analysis assumes that the revised mixing method is used.

5.2 CFD Analysis

The traditional paddle mixer is difficult to model accurately due to the planetary motion of the paddle, which essentially means that there are two parallel vertical axis of rotation. It must be remembered however that the purpose of this analysis is to set some benchmark values for fluid velocity and shear strain rate, therefore some assumptions can be made to simplify the modelling process.

The planetary motion of the mixer is neglected, because it is the interaction between the paddle and the bowl which is of most interest. A *steady state*, *multiple frame of reference*, *multiphase* analysis is selected, where two discrete (2) fluid domains are modelled with an interface linking the two domains together.

5.2.1 Geometry and Meshing

As noted previously the paddle mixer analysis has been conducted using the *multiple frame of reference* approach. This is a technique well suited to any turbo machinery where there are rotating blades immersed in a stationary body of fluid.

The two fluid domains defined for the paddle mixer are termed the outer and inner domains. The outer fluid domain represents the paste which is static in the bowl; hence the motion of this domain is set as stationary. The inner fluid domain represents the fluid which is rotating with the paddle; hence the motion of the domain is set to rotating (40rad/s). The paddle itself is also incorporated into this inner fluid domain which rotates about a vertical axis through the centre of the paddle.

The two fluid domains have been meshed using tetrahedral elements which is common practice for fluid dynamics simulations. Element sizing has been enforced to ensure a relatively fine mesh is obtained. Mesh statistics are provided in Table 7, while the meshed outer and inner domains are shown in Figure 18 and Figure 19 respectively.

Table 7 - Paddle Mixer Mesh Statistics

Domain	Nodes	Elements
Outer (bowl)	96,431	531,055
Inner (paddle)	42,560	232,802

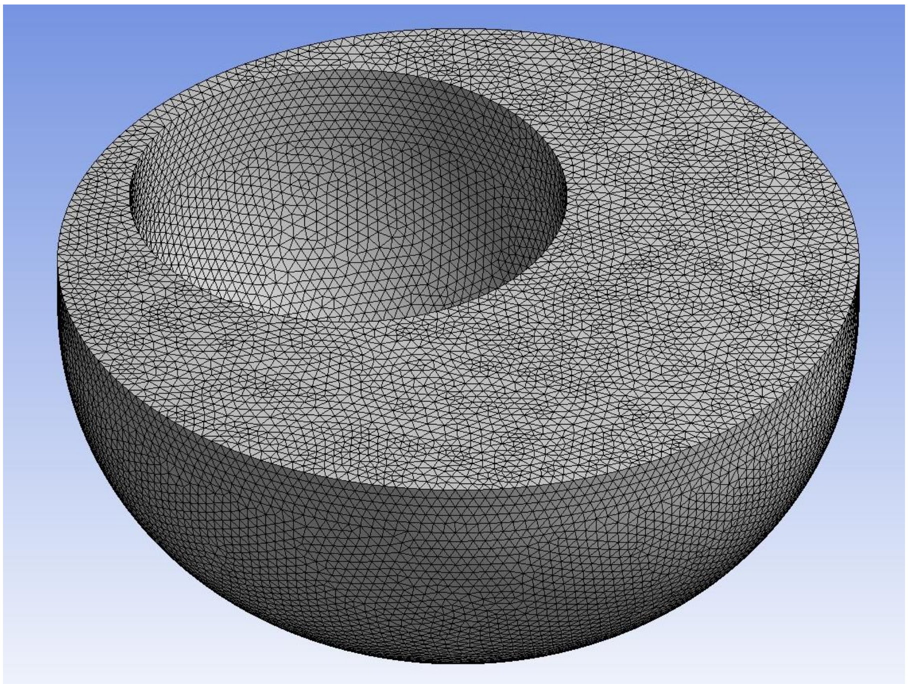

Figure 18 - Meshed Outer Fluid Domain (Bowl)

Inspection of Figure 19 reveals a strip of fluid has been modeled surrounding the paddle. This ensures that the surface areas of the respective interfaces are identical for both domains, simplifying the interface setup. This strip of fluid also defines where the interface between the stationary and rotating fluid domains is located. In this case it has been assumed that the interface occurs 4.0mm from the paddle tip. The use of the interface is described further in Section 5.2.2.

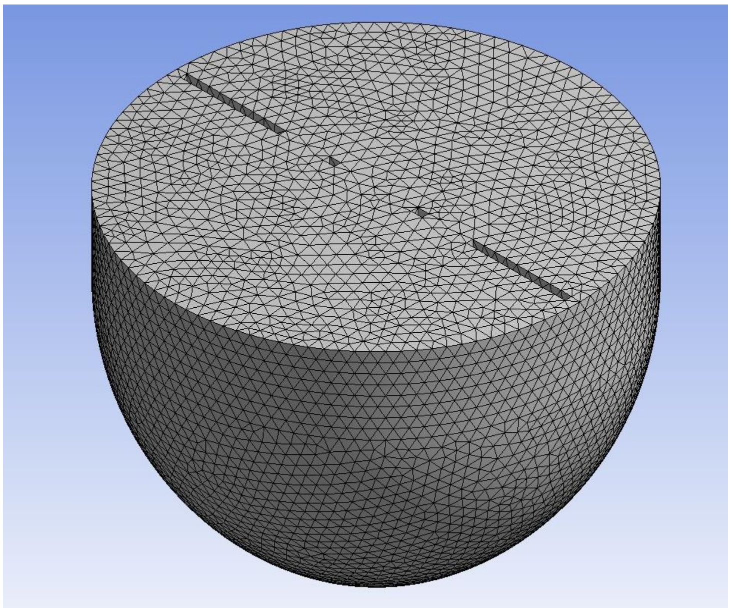

Figure 19 - Meshed Inner Fluid Domain (Paddle)

5.2.2 Boundaries and Boundary Conditions

It can be noted from the meshed fluid domains that it is only the fluid which gets included in the model. The paddle and the bowl are not required because we are only interested in the behaviour of the fluid, in this case geopolymer paste. To fully define the mixer geometry and constrain the fluid it is necessary to define several boundary conditions. Definitions for the most common boundary conditions are described as follows (*ANSYS CFX-Pre* 2010):

- Inlet – Fluid predominantly flows into the domain
- Outlet – Fluid predominantly flows out of the domain
- Opening – Fluid can simultaneously flow both into and out of the domain
- Wall – Impenetrable boundary to fluid flow
- Symmetry Plane – A plane of both geometric and flow symmetry

The following boundary conditions have been included in the paddle mixer model:

1. Outer fluid domain bowl – *Wall*
2. Outer fluid domain free surface – *Opening*
3. Inner fluid domain paddle – *Wall*
4. Inner fluid domain free surface – *Opening*

The study focussed on the fluid flow in the mixer as a whole but there are two distinct fluid domains. It is therefore necessary to establish a way to link the two domains together. This is achieved through the use of an interface between the rotating inner and stationary outer domains. The interface is represented by the green surface shown in Figure 20. The frozen rotor frame change option has been selected, and because the surface areas of the inner domain interface and the outer domain interface are identical, the pitch change option has been set to none.

As noted in Section 5.1, the improved method of sample preparation requires that a small percentage of the fly-ash is added to the paste as the mixer is running. To permit simulation of this process a Particle Injection Region has been added to the model. The region is represented by the star symbol located slightly below the origin in Figure 20.

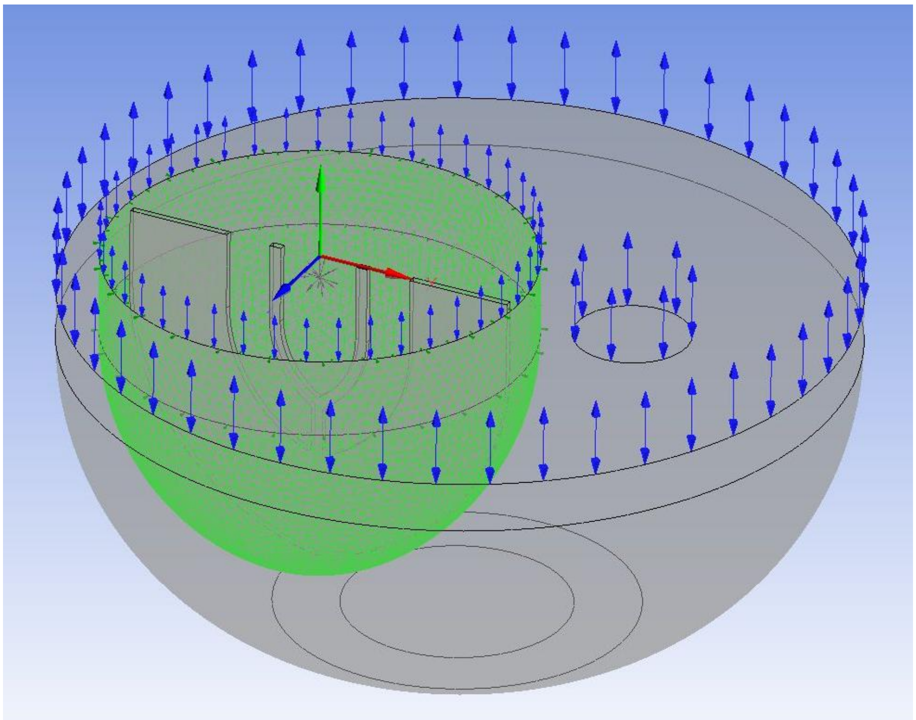

Figure 20 - Paddle Mixer Interface

5.2.3 Material Properties

ANSYS-CFX permits new materials to be defined and added to the materials library. For the paddle mixer analysis, two new materials were defined (Table 8);

1. Geopolymer paste with the properties described in Section 4.1.3
2. Tarong fly-ash with the properties described in Section 4.1.1

As noted in Section 5.2, a *multiphase* analysis technique has been used to simulate the paddle mixer. A multiphase analysis permits two different materials to co-exist in the same fluid domain, mixed at a macroscopic level. In this case, both domains (inner and outer) were assigned the two materials noted above; geopolymer paste as the continuous fluid and the fly-ash as the Particle Transport Solid.

To simulate the addition of fly-ash during the mixing process the particle transport modelling technique was used to allow solid fly-ash particles to be injected via the particle injection region at a mass flow rate of 0.01 kg/s. Particle transport modelling is very useful in mixing applications, as it allows the flow path of the particles to be tracked throughout the fluid domain.

Table 8 - Geopolymer Material Settings

Item	ANSYS-CFX Parameter	Geopolymer Paste	Tarong Fly-ash
1	Thermodynamic State	Liquid	Solid
2	Molar Mass	51.81 g/mol	70.89 g/mol
3	Density	1770 kg/m^3	2896 kg/m^3
4	Reference Temperature	25°C	-
5	Reference Pressure	0 Pa	-
6	Viscosity Model	Non-Newtonian Bingham Model (refer Table 3)	-
7	Morphology	Continuous Fluid	Particle Transport Solid

5.2.4 Analysis Settings

The general analysis settings and boundary conditions applied in ANSYS-CFX are listed in Table 9 and Table 10 respectively.

Table 9 - Paddle Mixer - Analysis Settings

Item	Category	ANSYS-CFX Parameter	Adopted Value
1	General	Analysis Type	Steady State
2		Reference Pressure	0 Pa
3		Buoyancy Model	Non Buoyant
4		Turbulence Model	None (laminar)
5		Particle Coupling	Fully Coupled
6		Drag Force	Schiller Naumann
7		Simulation Domain Motion	Outer Domain Stationary
8			Inner Domain Rotating
9		Rotational speed	100 rad/s
10	Interface	Interface Model	General Connection
11		Frame Change	Frozen Rotor
12		Pitch Change	None
13	Particle Injection	Injection Method	Sphere
14		Injection Velocity	0.1 m/s
15		Particle Diameter Distribution	Specified Diameter
16		Particle Diameter	28 µm
17		Particle Mass Flow Rate	0.01 kg/s

Table 10 – Paddle Mixer - Boundary Conditions

Item	Boundary	ANSYS-CFX Parameter	Adopted Value
1	Bowl Walls	Mass & Momentum	No Slip Wall
2	Paddle Walls	Mass & Momentum	No Slip Wall
3	Free Surface	Flow Regime	Subsonic
4		Mass & Momentum	Pressure & Direction
5		Reference Pressure	0 Pa
6		Flow Direction	Normal to Boundary

5.2.5 Results and Discussions

Quantifying the degree of mixing induced by a mixer can be somewhat subjective however there are some fluid variables which can provide a good indication of how well the fluid is mixed. The two (2) primary variables used within this study to analyse the fluid flow in detail are as follows;

1. *Velocity* – Provides an insight into the flow patterns established within the fluid domain and helps identify stagnant fluid which is vulnerable to poor mixing
2. *Shear Strain Rate* – Regions of high shear strain rate are typically also the regions where the most mixing occurs

5.2.5.1. **Velocity**

Figure 21 shows a velocity vector plot, plotted on a vertical plane through the centre of the mixing bowl. As expected, the high velocity zones occur immediately adjacent to the widest part of the rotating paddle (near the top). This is also where the tip speed is highest. Key points to note from this plot are as follows:

- At the centre of the paddle, fluid is drawn down from the free surface
- Low-velocity region present at the bottom of the mixing bowl
- Low-velocity region at top right-hand side of mixing bowl
- Majority of fluid has a velocity << 4.5 m/s

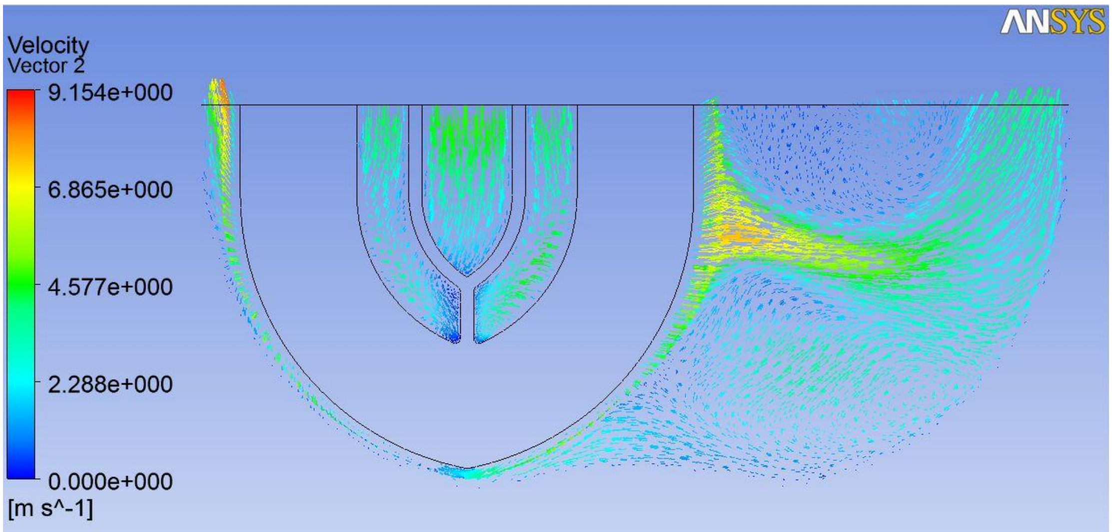

Figure 21 - Paddle Mixer - Vertical Plane Velocity Vector Plot

The fluid flow is now analysed further by plotting a second velocity vector plot on a horizontal plane 20mm below the free surface of the fluid (Figure 22). This plot emphasises the fact that the highest fluid velocities occur at the paddle tip, but closer inspection also reveals the full extent of the low-velocity region which was identified from the vertical plot.

This low-velocity region is not overly concerning however, because the paddle on the actual mixer moves about the bowl in a planetary motion. The low-velocity zone therefore only occurs instantaneously, despite the steady state analysis results.

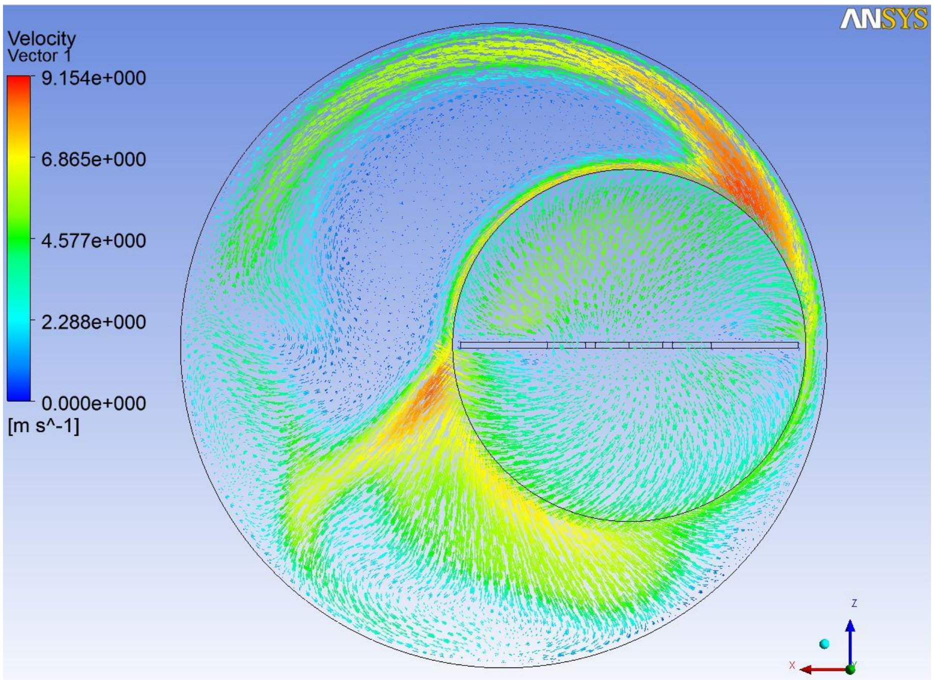

Figure 22 - Paddle Mixer - Horizontal Plane Velocity Vector Plot

5.2.5.2. **Shear Strain Rate**

While the velocity vector plots help us to understand the flow fields which are established during mixing, of far more interest is the shear strain rate. A contour plot of the shear strain rate is shown in Figure 23, once again plotted on a horizontal plane 20mm below the free surface of the fluid.

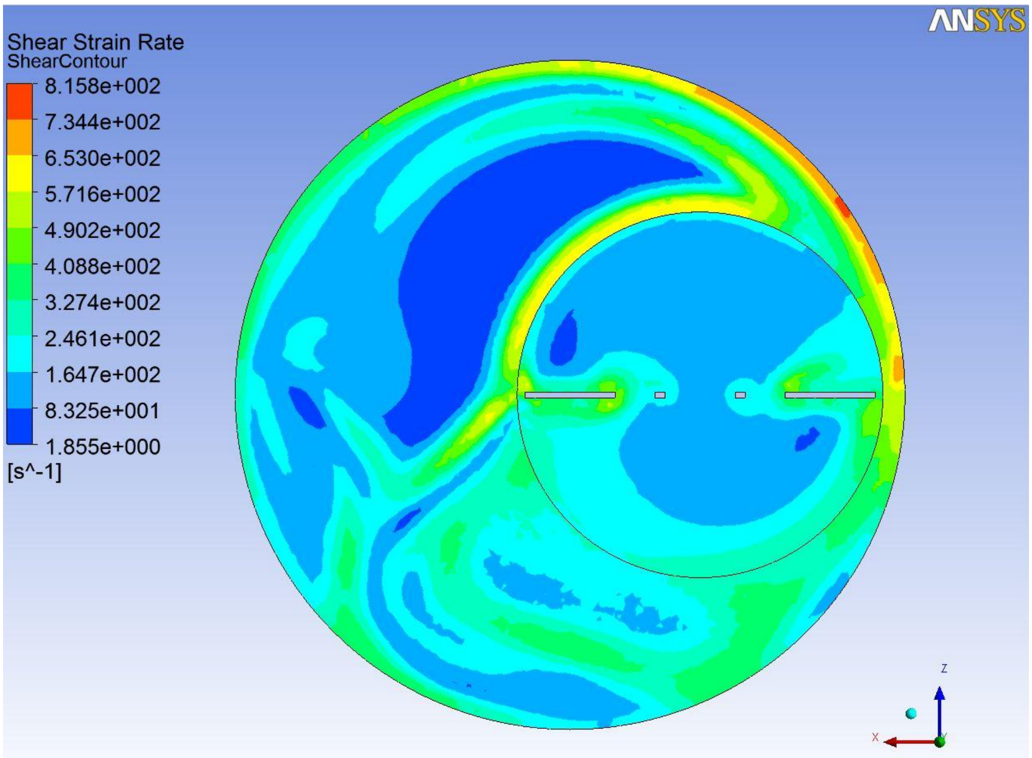

Figure 23 - Paddle Mixer - Horizontal Plane Shear Strain Rate

Comparing the shear strain rate contour plot with the velocity vector plots reveals some obvious similarities. This suggests that the regions of fluid which are subjected to high velocities are also the regions which undergo a greater degree of mixing. This relationship is best illustrated by comparing the top-left quadrant of the mixing bowl in Figure 22 with the equivalent quadrant in Figure 23.

The highest shear strain rate occurs in the region where the paddle is closest to the wall of the mixing bowl. This is to be expected due to the no-slip wall condition imposed at the boundary. The gap between the rotor and the stator (or paddle and the bowl in this case) is commonly referred to as the *shear gap*. The smaller the gap, the greater the shear imposed on the fluid.

5.2.5.3. **Particle Tracking**

As noted in Section 5.1, the last 10% of the fly-ash is added to the bowl while the mixer is operational. It is therefore important that the fly-ash is properly dispersed throughout the geopolymer paste. Figure 24 tracks five discrete fly-ash particles from the particle injection region to the fluid free surface. The analysis reveals that the particles are mixed through the paste quite well, but do remain relatively close together for the entire flow path. This is a potential problem as it can lead to agglomeration.

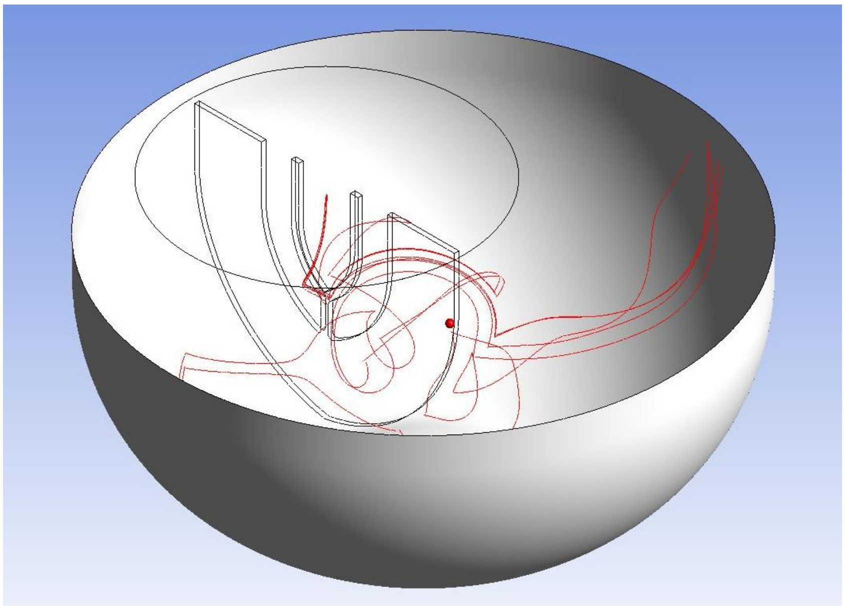

Figure 24 - Paddle Mixer - Particle Track

5.2.5.4. **Results Summary**

The key results from the analysis are summarised in Table 11. It is observed that although high maximum values are obtained for both key variables, the average values are significantly lower. These results will be used as benchmark values to compare against the proposed high-shear mixer concept in the analysis to follow.

Table 11 - Paddle Mixer Analysis - Results

Item	Variable	Minimum	Maximum	Average
1	Velocity (Bowl Fluid)	0.01 m/s	9.35 m/s	2.75 m/s
2	Shear Strain Rate (Bowl Fluid)	2 /s	964 /s	200 /s

6. HIGH-SHEAR MIXER ANALYSIS

6.1 Frictional Losses Analysis

One of the key features of the conceptual design described in Section 3 is the recirculation pipe used to transfer fluid from the mixer outlet back into the hopper. It is important that the pressure of the fluid at the outlet is high enough to overcome the static and dynamic pressure losses associated with the recirculation pipe, to ensure that the fluid can be successfully returned to the hopper.

Traditional analysis techniques are not able to be applied in this case, because we are dealing with a Bingham fluid, therefore a simplified CFD analysis has been performed to estimate the dynamic losses through the pipe.

6.1.1 Geometry and Meshing

The model geometry consists of a column of fluid with an outside diameter equal to the ID of the pipe. The length of the pipe is set to 1.8m, to allow for a flow stabilisation zone of approximately 10D (0.4m) at each end of the fluid column.

The model mesh is created from tetrahedral elements, with inflation imposed on the pipe walls to improve the accuracy of the analysis. The adopted mesh is shown in Figure 25 below.

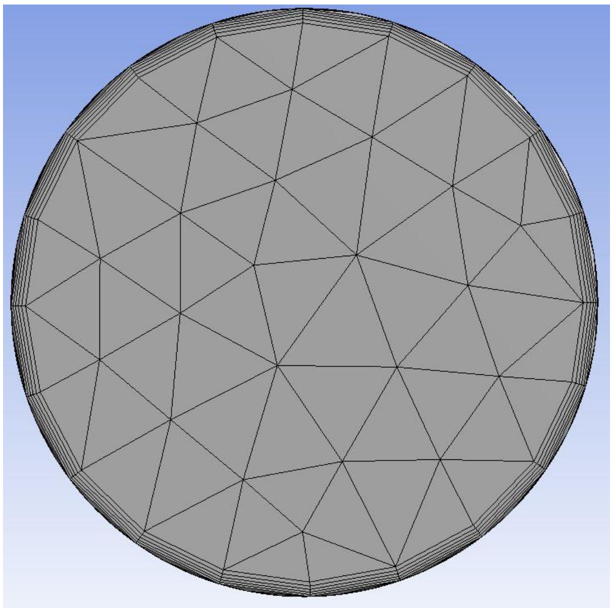

Figure 25 - Recirculation Pipe - Mesh

6.1.2 Calibration

Before progressing to the analysis of the geopolymer paste (Bingham fluid) the model must be calibrated to confirm that the modelling assumptions are reasonable. A calibration run is performed by defining the fluid as water and then comparing the results with hand calculations based on the Colebrook method of analysis.

When the calibration run confirms that the method of modelling is appropriate, then a secondary analysis is run, this time defining the fluid as geopolymer paste.

6.1.3 Analysis Settings

For both the calibration and secondary analysis, several runs were performed at various mass flow rates. The pressure was then calculated at two locations along the flow path (conveniently spaced at 1.0m centres), yielding a pressure loss per meter of pipe. The general analysis settings for the two analyses are given in Table 12, while the boundary conditions are included in Table 13.

The major difference in settings between the two analyses is that the flow is assumed to be turbulent when water is selected for the fluid, but laminar when geopolymer paste is selected. This assumption can be verified by inspection of the Reynolds number in the solutions results file.

Table 12 – Pipe Frictional Losses - Analysis Settings

Item	ANSYS-CFX Parameter	Adopted Value	
		Calibration Run	Secondary Run
1	Fluid	Water	Geopolymer Paste (refer Table 8)
2	Analysis Type	Steady State	
3	Reference Pressure	1 atm	
4	Buoyancy Model	Non Buoyant	
5	Turbulence Model	k-Epsilon	None (laminar)
6	Wall Function	Scalable	-
7	Fluid Domain Motion	Stationary	

Table 13 - Pipe Frictional Losses - Boundary Conditions

Item	Boundary	ANSYS-CFX Parameter	Adopted Value	
			Calibration Run	Secondary Run
1	Pipe Walls	Mass & Momentum	No Slip Wall	
		Wall Roughness	0.15 mm	-
2	Inlet	Flow Regime	Subsonic	
		Mass & Momentum	Static Pressure	
		Reference Pressure	0 Pa	
		Flow Direction	Zero Gradient	
		Turbulence	Zero Gradient	-
3	Outlet	Flow Regime	Subsonic	
		Mass & Momentum	Mass Flow Rate	

6.1.4 Results & Discussions

6.1.4.1. **Calibration Analysis**

A pressure contour plotted on a vertical plane through the centre of the pipe is shown in Figure 26. The fluid flows from the inlet at the LHS of the pipe to the outlet at the RHS. Clearly there is a reduction in pressure as the fluid progresses through the pipe.

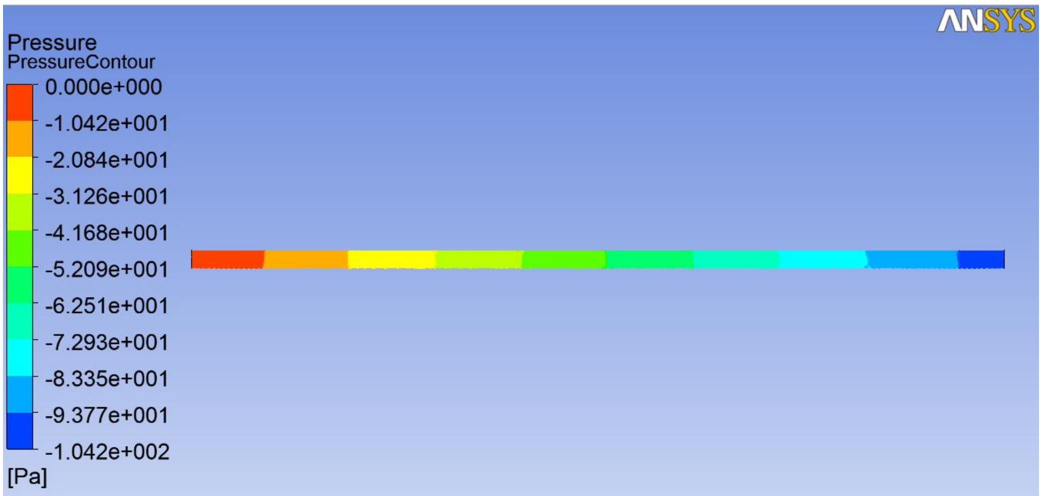

Figure 26 - Pipe Friction Losses - Pressure Contour

When a mass flow rate of 0.5 kg/s is specified as the outlet boundary condition, the analysis yields a fluid pressure at locations A and B of 101.302 kPa and 101.247 kPa respectively. The pressure drop per meter can therefore be calculated as follows:

$$\Delta P = P_1 - P_{21} = 101.302 - 101.247 = 0.055 kPa = 55 Pa$$

Inspection of the hand calculations based on the Colebrook method of analysis (Appendix C) reveals that for a nominal flow rate of 0.5 L/s (equivalent to 0.5 kg/s for water), the estimated dynamic pressure loss for water is ~60 Pa/m.

The two methods of analysis therefore vary by less than 10%, which is well within the limits of accuracy expected. This confirms that the proposed CFD analysis model is a good approximation of the flow within a pipe.

6.1.4.2. **Geopolymer Paste Analysis**

When analysing the flow of geopolymer paste through a pipe, the procedure is much the same as the calibration analysis except that instead of selecting just one flow rate, the analysis is run several times for different flow rates. The results plotted in Figure 27 reveal the high frictional losses associated with pumping geopolymer paste through a circular pipe. Such large pressure losses are expected due to the dynamic viscosity of the fluid, but serve to highlight the importance of designing a mixer capable of generating high pressures at the outlet.

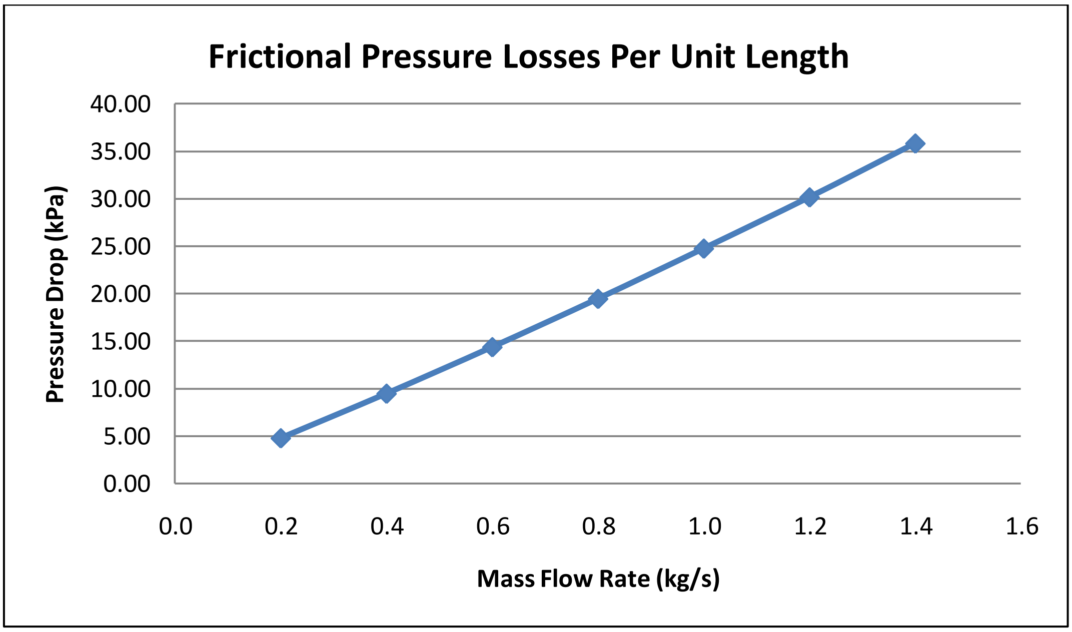

Figure 27 - Dynamic Pressure Losses - Geopolymer Paste Analysis

The total length of the recirculation pipe in the concept shown in Figure 10 is 0.5m. Assuming the *mass flow rate* ranges between 0.2 kg/s and 1.0 kg/s and neglecting minor losses, the range of the dynamic *pressure* losses can be determined using the values given in Figure 27 as follows:

$$\Delta P_{dyn\_\min} = 5\frac{kPa}{m}\times 0.5m = 2.5kPa$$

$$\Delta P_{dyn\_\max} = 25\frac{kPa}{m}\times 0.5m = 12.5kPa$$

In addition to the dynamic pressure losses, the static pressure losses must also be considered. The recirculation pipe enters the hopper 340mm above the mixer outlet; therefore the static pressure losses can be determined as follows:

$$\gamma = \rho\times g = 1170\frac{kg}{m^3}\times 9.81\frac{m}{s^2} = 17364\frac{N}{m^3}$$

$$\Delta P_{static} = \gamma\times h = 17364\times 0.34 = 5.9kPa$$

For recirculation of the geopolymer fluid to occur, the fluid pressure at the outlet of the high-shear mixer must be greater than the sum of the static and dynamic components determined above. The minimum outlet pressure of the high-shear mixer must therefore be in the following range:

$$\Delta P_{\min} = \Delta P_{static} + \Delta P_{dyn\_\min} = 5.9 + 2.5 = 8.4kPa$$

$$\Delta P_{\max} = \Delta P_{static} + \Delta P_{dyn\_\max} = 5.9 + 12.5 = 18.4kPa$$

6.2 High Shear Mixer – Version A

Having defined the remaining design parameters for the high-shear mixer and established benchmark values for the key design variable, a CFD analysis of the conceptual design can be conducted.

As noted in Section 3, the conceptual mixer is similar to a centrifugal pump; hence the outlet pressure can be expected to be related to the mass flow rate. As the flow rate is increased a subsequent reduction in outlet pressure is to be expected. It is important to quantify the relationship between the two variables to ensure that when the mixer is operating at the design capacity, the outlet pressure is sufficiently high enough to recirculate the fluid back into the hopper.

Quantifying the relationship between *pressure* and *mass flow rate* is the primary objective of this analysis, while the secondary objective is to inspect the fluid flow, and identify any potential problems with the concept which may need to be addressed.

Obtaining the relationship between flow rate and pressure involves the tedious and time consuming procedure summarised below:

1. Specify a nominal *angular velocity* for the rotor
2. Specify a nominal *mass flow rate* at the mixer outlet
3. Run the analysis
4. Calculate the fluid *pressure* at the mixer outlet from analysis results
5. Revise the *mass flow rate* at the mixer outlet and repeat steps 3 and 4
6. Repeat step 5 for several values of *mass flow rate*
7. Revise the *angular velocity* and repeat steps 2 - 6
8. Repeat step 7 for several values of *angular velocity*

6.2.1 Geometry and Meshing

The conceptual high-shear mixer described in Section 3 can be simplified to reduce computational times; the fluid inside the impellor and the volute of the mixer are the only regions required. The adopted modelling technique is similar to that used in the paddle mixer analysis (*multiple frame of reference*), with two discrete fluid domains defined. The motion of the domain representing the volute is stationary while the motion of the domain representing the impellor is rotating.

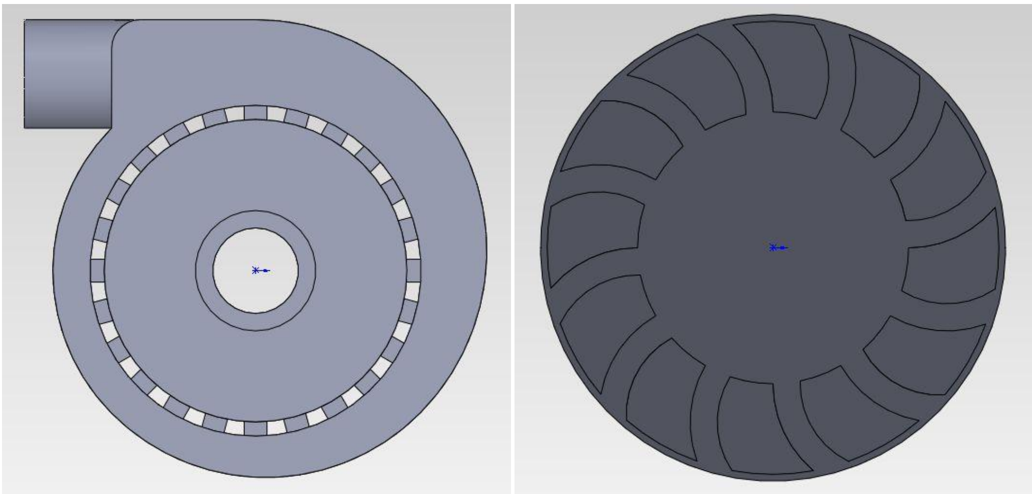

Figure 28 - High-Shear Concept - Volute & Rotor Geometry

The two fluid domains defined for the high-shear mixer concept are the volute and the rotor. The motion of the volute domain is set as stationary, while the motion of the rotor fluid domain is set as rotating. The geometry of both domains is shown in Figure 28.

The volute fluid domain represents the fluid within the volute of the mixer, therefore the outside of the faces of the model are equivalent to the inside of the actual volute shell. Closer inspection of Figure 28 shows that the rotor includes twelve backwards curved blades, while there are 24 openings included in the stator; yielding a frequency of two. Key geometric parameters are given in Table 4.

The rotor (or impellor) type selected for the high-shear mixer is termed semi-enclosed, because it consists of a plate (the web) attached to the lower side of the blades. There is no shroud on the top face of the blades, which means that fluid is free to flow in the vertical direction as it progresses through the rotor blade passages.

Tetrahedral elements have been used to mesh both fluid domains with element sizing also enforced to a maximum of 3.0mm to ensure a fine mesh is obtained. Mesh statistics are provided in Table 14, while images of the meshed volute and rotor domains are shown in Figure 29.

Table 14 - Conceptual Design - Mesh Statistics

Domain	Nodes	Elements
Volute	52,095	255,200
Rotor	12,718	56,246

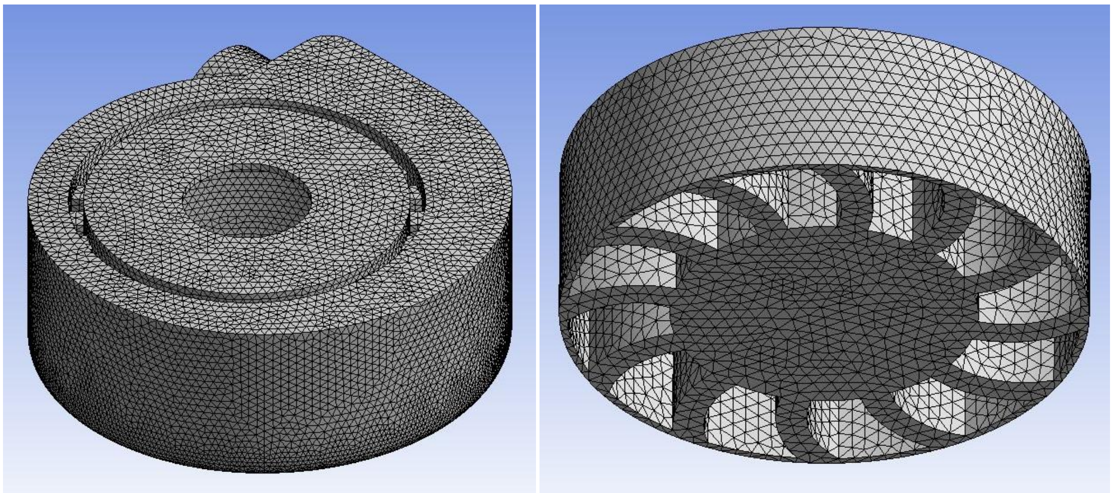

Figure 29 - High-Shear Mixer Concept – Volute & Rotor Mesh

6.2.2 Boundaries and Boundary Conditions

Just like in the paddle mixer analysis, it is necessary to define several boundary conditions to ensure the fluid flow within the domain is the same as that which would be observed in a real-world application. The following boundary conditions have been included in the conceptual high-shear mixer model:

1. Volute fluid domain (shell) – *Wall*
2. Volute fluid domain (rotor web) – *Wall*
3. Volute fluid domain (outlet) – *Outlet*
4. Rotor fluid domain (web) – *Wall*
5. Rotor fluid domain (shroud) – *Wall*
6. Rotor fluid domain (rotor blades) – *Wall*
7. Rotor fluid domain (inlet) – *Inlet*

Once again, interfaces are required between the rotor and volute fluid domains to permit fluid flow between the two. For the conceptual high-shear mixer two interfaces are defined; the first allows radial fluid flow through the rotor passages, while the second allows fluid to flow in the vertical direction. The two interfaces are represented by the green surfaces shown in Figure 30.

The frozen rotor frame change option which was selected for the paddle mixer analysis has again been adopted for the high-shear mixer analysis, and the pitch change option has been set to none.

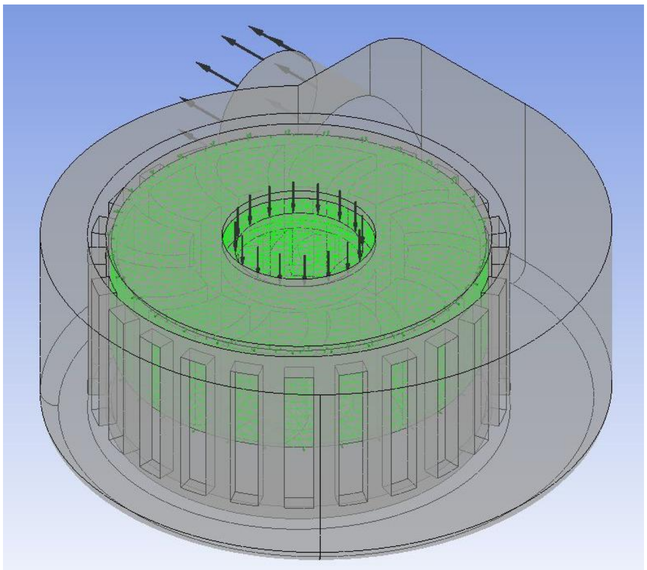

Figure 30 - Conceptual High-Shear Mixer Interfaces

6.2.3 Material Properties

No particle injection region is included in the conceptual high-shear mixer model, as this is not considered to be a primary objective of the analysis; therefore the multiphase analysis technique is not required. Only a single material (or fluid) exists in each fluid domain and it is defined as geopolymer paste. The properties of the geopolymer paste are described in Section 4.1.3, while the material analysis settings are identical to those adopted for the paddle mixer analysis (Table 8).

6.2.4 Analysis Settings

The general analysis settings and boundary conditions applied in ANSYS-CFX are listed in Table 15 and Table 16 respectively.

Table 15 – Conceptual High-Shear Mixer - Analysis Settings

<table>
<tr><th>Item</th><th>Category</th><th>ANSYS-CFX Parameter</th><th>Adopted Value</th></tr>
<tr><td>1</td><td rowspan="7">General</td><td>Analysis Type</td><td>Steady State</td></tr>
<tr><td>2</td><td>Reference Pressure</td><td>0 Pa</td></tr>
<tr><td>3</td><td>Buoyancy Model</td><td>Non Buoyant</td></tr>
<tr><td>4</td><td>Turbulence Model</td><td>None (laminar)</td></tr>
<tr><td>5</td><td rowspan="2">Simulation Domain Motion</td><td>Volute Domain Stationary</td></tr>
<tr><td>6</td><td>Rotor Domain Rotating</td></tr>
<tr><td>7</td><td>Rotational speed</td><td>Varies</td></tr>
<tr><td>8</td><td rowspan="3">Interface</td><td>Interface Model</td><td>General Connection</td></tr>
<tr><td>9</td><td>Frame Change</td><td>Frozen Rotor</td></tr>
<tr><td>10</td><td>Pitch Change</td><td>None</td></tr>
</table>

Table 16 – Conceptual High-Shear Mixer - Boundary Conditions

Item	Boundary	ANSYS-CFX Parameter	Adopted Value
1	Volute Shell Walls	Mass & Momentum	No Slip Wall
2	Volute Rotor Web Walls	Mass & Momentum	No Slip Wall
		Wall Motion	Rotating
3	Volute Outlet	Flow Regime	Subsonic
		Mass & Momentum	Mass Flow Rate
4	Rotor Web Walls	Mass & Momentum	No Slip Wall
		Frame Type	Rotating
5	Rotor Shroud Walls	Mass & Momentum	No Slip Wall
		Frame Type	Rotating
6	Rotor Blade Walls	Mass & Momentum	No Slip Wall
		Frame Type	Rotating
7	Rotor Inlet	Flow Regime	Subsonic
		Relative Pressure	0 Pa
		Flow Direction	Zero Gradient
		Frame Type	Rotating

The key settings to note from the tables above are as follows:

1. Motion of the volute fluid domain is stationary
2. Motion of the rotor fluid domain is rotating
3. Relative pressure of 0 Pa is specified the mixer inlet
4. Mass flow rate is specified at the mixer outlet
5. Rotational speed (angular velocity) of the rotor varies
6. Laminar flow has been assumed

6.3 Results and Discussions – Version A

Four values of *angular velocity* were initially selected for the analysis; 400 RPM, 800 RPM, 1200 RPM & 1600 RPM. For each of the four values of *angular velocity,* seven values of *mass flow rate* were analysed, ranging from 0.2 kg/s to 1.4 kg/s. For each run of the analysis, key variables were recorded including:

- Outlet pressure
- *Velocity* data (maximum, minimum and average)
- *Shear Strain Rate* data (maximum, minimum and average)

It is known from conservation of mass that the *mass flow rate* at the mixer inlet (included in the rotor fluid domain) must be equal to the *mass flow rate* at the mixer outlet (included in the volute fluid domain). It follows that all fluid must pass through one of the two interfaces. For convenience, it is assumed that all fluid passes through the interface set up at the outer diameter of the rotor, and because this is the location where most mixing is likely to occur, the interface has been selected as the nominal location at which to record the *velocity* and *shear strain rate* data.

6.3.1 Pressure and Mass Flow Rate Relationship

Inspection of the analysis data (included in Appendix E), revealed that for an *angular velocity* of 400 RPM the maximum outlet *pressure* obtained at a mass flow rate of 0.2 kg/s was only 1.84 kPa. So even at the lowest *mass flow rate* analysed, an *angular velocity* of 400 RPM barely produces positive pressure at the mixer outlet and therefore not a viable solution to the problem; for this reason, the 400 RPM data has been omitted from the plot provided in Figure 31.

Figure 31 reveals as expected, that the *outlet pressure* increases with increasing *angular velocity*, while the *outlet pressure* decreases as the *mass flow rate* is increased. The relationship between *outlet pressure* and *mass flow rate* is approximately linear over the range of values analysed. Despite this fact, interpolation of the results outside of the range of flow rates analysed should be performed with caution.

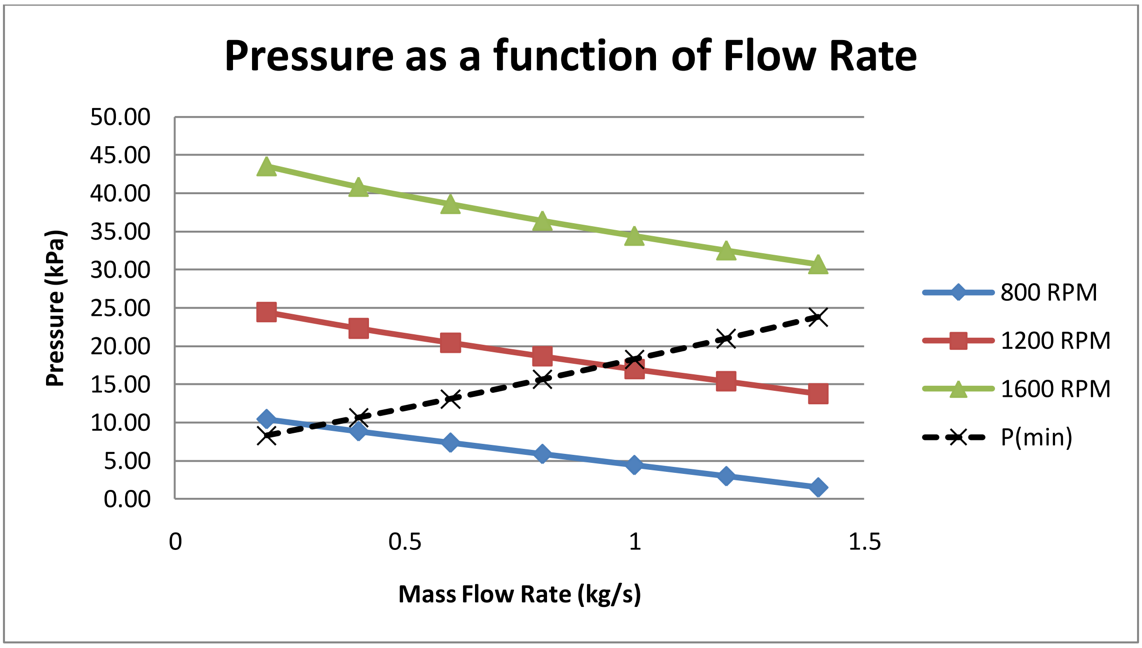

Figure 31 - High-Shear Mixer (Version A) - Pressure v Flow Rate

In addition to plotting the mixer *outlet pressure* determined by the CFD analysis, the minimum pressure required at the mixer outlet is represented by the dashed line. Inspecting where the minimum pressure line intersects the respective outlet pressure line allows the following observations to be drawn from this plot:

- Angular velocity of 800 RPM is acceptable for mass flow < 0.3 kg/s
- Angular velocity of 1200 RPM is acceptable for mass flow < 0.9 kg/s
- Angular velocity of 1600 RPM is acceptable over full range of flow rates

It is not expected that a mass flow rate greater than 0.5 kg/s would be required for a laboratory mixer, so a nominal angular velocity of 1200 RPM would be acceptable.

6.3.2 Velocity Observations

A velocity contour plot for *a mass flow rate* of 0.4 kg/s and an *angular velocity* of 1200 RPM is presented in Figure 32. As expected, the high velocity zone is limited to the void between the rotor and the stator. The analysis has identified a maximum velocity of 3.75 m/s at the *shear gap*; however the velocity in the volute does not exceed 0.4 m/s.

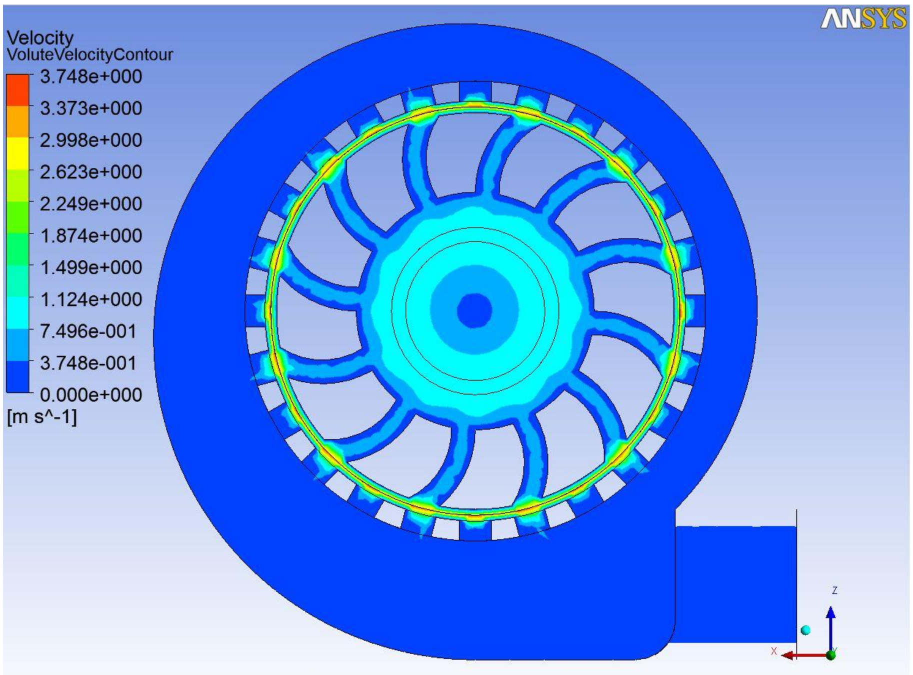

Figure 32 - High-Shear Mixer (Version A) - Velocity Contour Plot

A velocity vector plot for the same boundary conditions is shown in Figure 33. Although not immediately apparent from the image below, closer inspection reveals that rather than flowing in the same direction as the rotor (anti-clockwise), some of the fluid flows in a clockwise direction as indicated by the arrow. This is an undesirable flow characteristic because the flow is following an inefficient flow path.

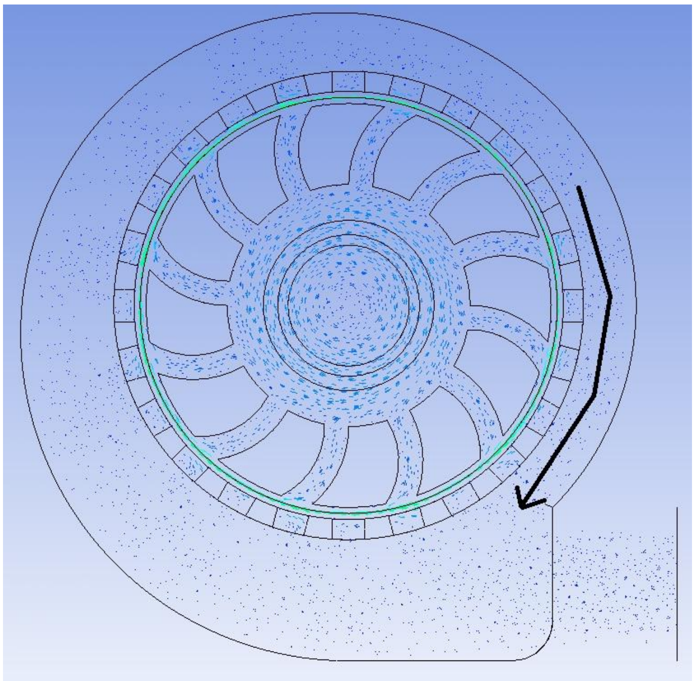

Figure 33 - High-Shear Mixer (Version A) - Velocity Vector Plot

6.3.3 Shear Strain Rate Observations

The *shear strain rate* at the interface (i.e. at the *shear gap*) has been plotted against the *mass flow rate* for several values of *angular velocity* in Figure 34. Inspection of the graph reveals two interesting trends.

Firstly, the shear strain rate increases with increasing angular velocity. This is to be expected because the velocity of the fluid is also directly proportional to the angular velocity of the rotor.

Secondly, it is observed that although the *shear strain rate* does decrease as the *mass flow rate* increases, the decrease is not substantial for the range of flow rates analysed. This result is somewhat surprising, but can be explained in part because the geometry of the rotor-stator arrangement has a significant influence on the shear imparted on the fluid. This suggests that even at relatively *high mass flow rates*, the mixer will be capable of imparted a high *shear stress* on the fluid.

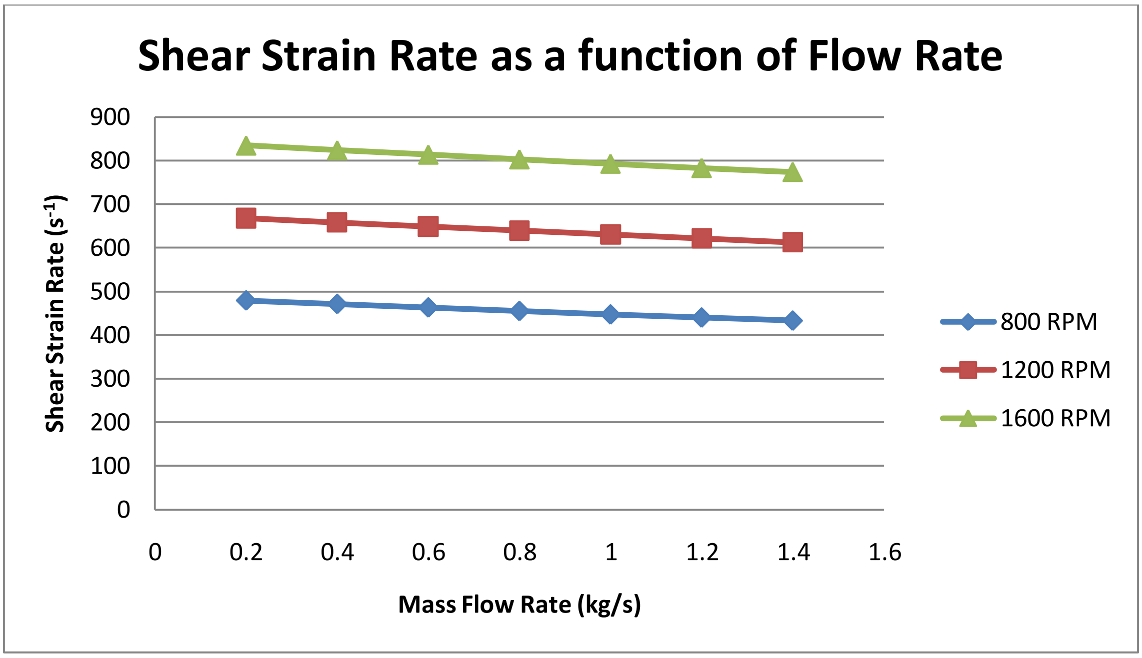

Figure 34 - High-Shear Mixer (Version A) - Shear Strain Rate v Flow Rate

A contour plot of the *shear strain rate* through the rotor-stator arrangement is provided in Figure 35, for a *mass flow rate* of 0.4 kg/s and an *angular velocity* of 1200 ROM. Comparing Figure 33 against Figure 35 reveals the strong relationship between the velocity and the shear strain rate.

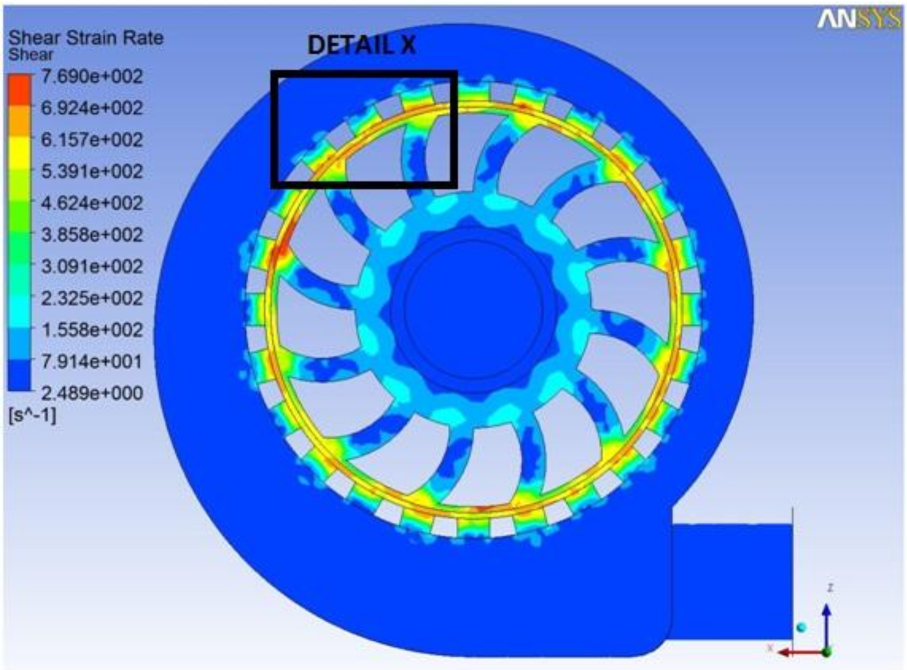

Figure 35 - High-Shear Mixer (Version A) - Shear Strain Rate

A detailed view of the shear strain rate plot is provided in Figure 36 below. As expected, the highest value of shear strain rate occurs as the fluid passes through the *shear gap*.

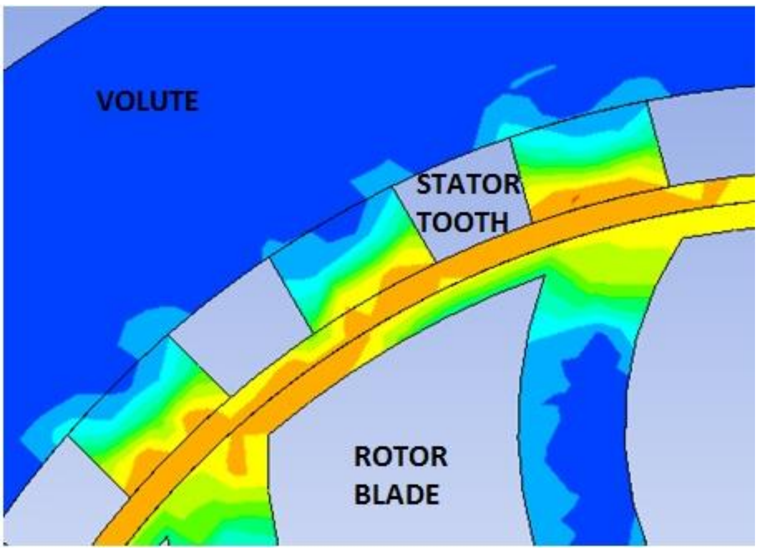

Figure 36 - High-Shear Mixer (Version A) - Detail X

6.3.4 Areas Indentified for Optimisation

The results obtained from the preliminary ‘Version A’ CFD analysis of the high-shear mixer were better than expected. The *shear strain rates* at the rotor-stator interface were significantly higher than the results obtained from the paddle mixer analysis, and this was achieved without a significant increase in *velocity*.

The main issue identified while reviewing the CFD results concerned the flow of fluid from through the stator, and around the volute to the mixer outlet. The inefficiencies observed in this area are thought to reduce the fluid pressure at the fluid outlet therefore improving the flow characteristics through the volute would improve the overall performance of the mixer.

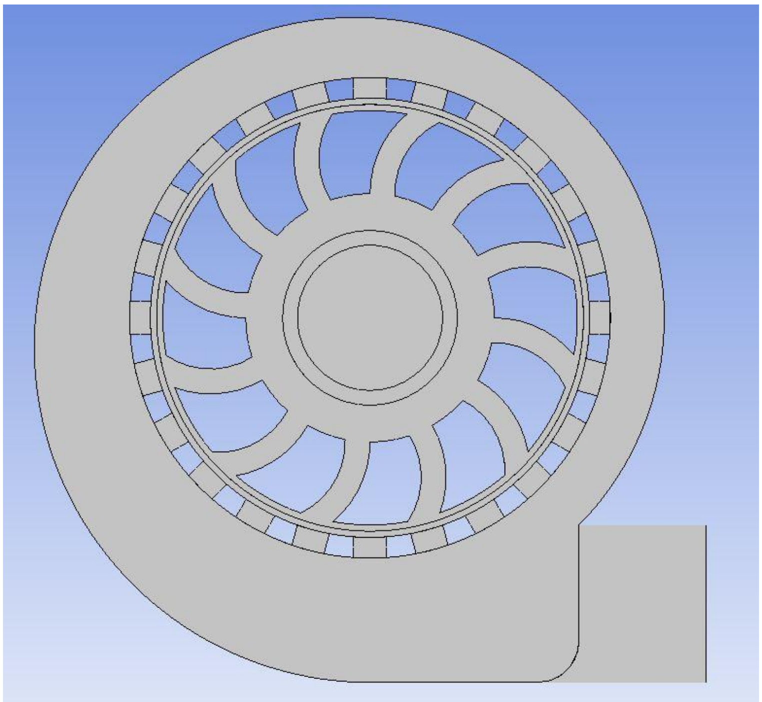

Figure 37 - High-Shear Mixer Geometry (Version A)

The model used in ‘Version A’ of the high-shear mixer analysis is shown in Figure 37 above. There are two variables identified for optimisation with the objective being to improve the fluid flow through the volute, the volute geometry and the stator geometry. Alterations to the stator and volute geometry include the following:

- Exaggerate the increase in radius in the direction of fluid flow
- Reduce cut-off distance between the stator and the volute
- Vary the stator tooth geometry (thickness, angle & passage area)

6.4 Concept Optimisation

During the optimisation phase of the CFD analysis, it is desirable to consider the flow path of the fly-ash particles as they are injected into the mixing chamber. The high-shear mixer optimisation analysis is therefore defined as *multiphase,* with each fluid domain containing the geopolymer paste and the fly-ash particles mixed at a macroscopic level. The flow path of the fly-ash particles will be tracked through the fluid domain using the same technique as that applied in the paddle mixer analysis.

6.4.1 Analysis Settings

The majority of the analysis settings are exactly the same as those employed during the analysis of the 'Version A' high-shear mixer with one exception. To simulate the addition of fly-ash during the mixing process the particle transport modelling technique is used, with solid fly-ash particles being injected via the particle injection region at a mass flow rate of 0.01 kg/s. Additional analysis settings related to particle injection and tracking are listed in Table 17.

Unlike the 'Version A' high-shear mixer analysis where the analysis was run several times at varying mass flow rates and angular velocities, analysis performed during the optimisation phase of the high-shear mixer concept has been performed at a nominal mass flow rate and angular velocity of 0.4 kg/s and 1200 RPM respectively.

Table 17 - High-Shear Mixer Optimisation - Analysis Settings

Item	ANSYS-CFX Parameter	Adopted Value
1	Particle Coupling	Fully Coupled
2	Drag Force	Schiller Naumann
3	Injection Method	Sphere
4	Injection Velocity	0.1 m/s
5	Particle Diameter Distribution	Specified Diameter
6	Particle Diameter	28 μm
7	Particle Mass Flow Rate	0.01 kg/s

6.4.2 Geometry Modifications – Version B

The geometry for 'Version B' of the high-shear mixer is shown in Figure 38. There are two substantial modifications from 'Version A'; the first involves the volute and the second, the stator.

The original high-shear mixer volute was modelled as a series of tangential arcs, with the radius of each arc increasing in an anti-clockwise direction around the volute. It is more common in the design of pumps to use a spiral; and this spiral design has subsequently been adopted for the 'Version B' volute geometry. The advantage of a spiral is that the cross-sectional area of the volute increases evenly as the fluid progresses around the volute. The cut-off distance between the stator and the volute has also been reduced, to prevent fluid flowing in a clockwise direction through the volute.

The objective with the geometry changes to the stator was to promote a more direct fluid path through the open passages. To achieve this, the stator thickness was reduced from 5.0mm to 3.0mm and the cross-sectional area of the openings in the stator increased. The *opening ratio* is defined as the ratio between the fluid passages in the stator to the fluid passages in the rotor. For the 'Version B' analysis, the *opening ratio* has been increased by approximately 25% from 3.9 to 4.9.

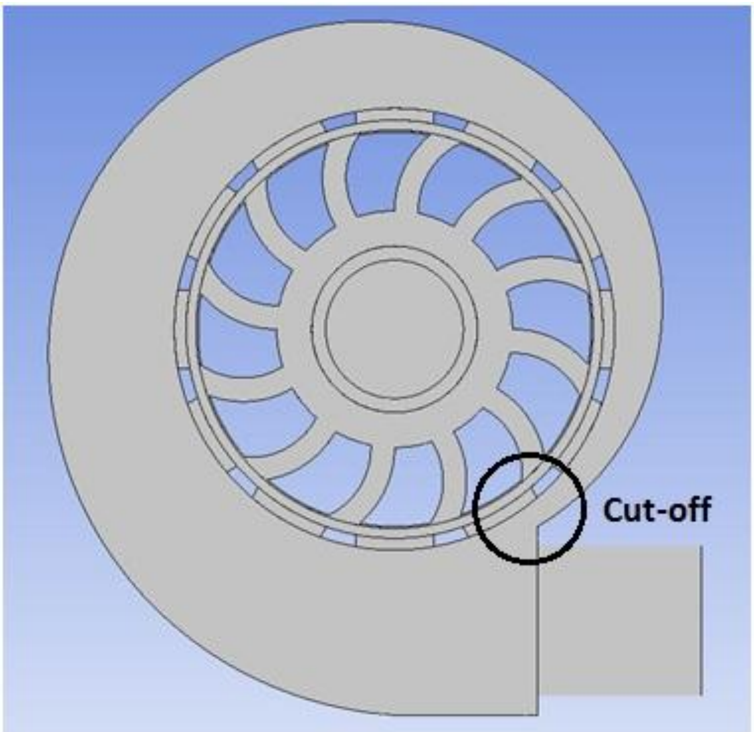

Figure 38 - High-Shear Mixer Geometry (Version B)

6.4.3 Results and Discussions – Version B

The shear strain rate for the 'Version B' analysis is presented on the contour plot in Figure 40. Although some extremely high values of shear stress are indentified, these are restricted to localised areas at the stator teeth, and are not considered to be good representation of the shear stress. The average *shear strain rate* calculated at the rotor-stator interface provides a better comparison with the original mixer, and at 661/s, it was almost identical to the results obtained in the 'Version A' analysis. This suggests that the *shear gap* has a greater effect on the *shear strain rate* than the stator geometry. The stator geometry can therefore be modified as required to improve the fluid flow profile in the volute, without sacrificing the high-shear characteristics of the mixer.

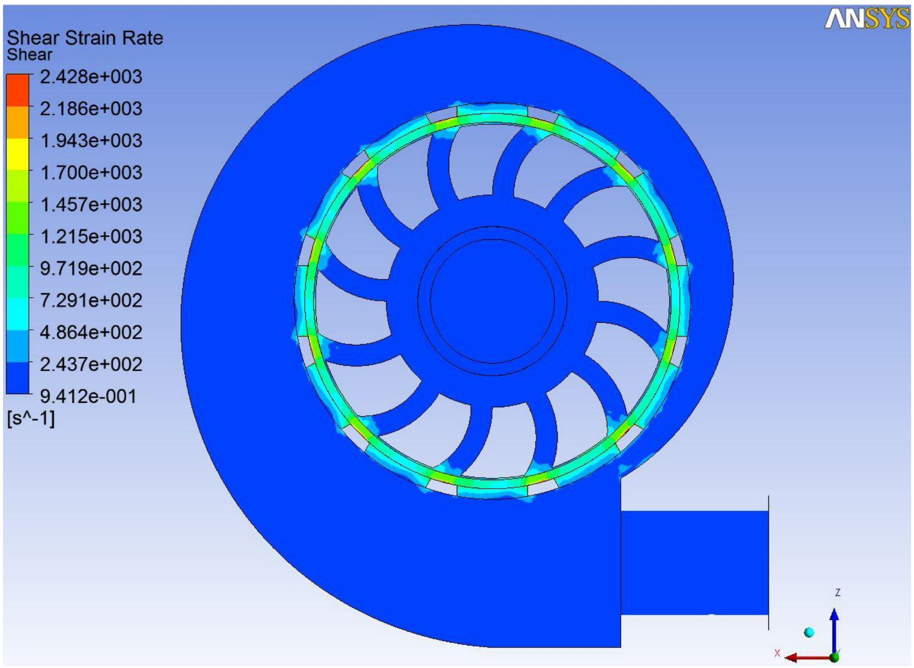

Figure 39 - High-Shear Mixer (Version B) - Shear Strain Rate

To check whether the fluid flow through the volute has been improved, particle tracking is used to track the flow path of a particle injected into the mixing chamber at the centre of the rotor (Figure 40). The flow path shows a significant improvement over the 'Version A' geometry because there is no counter-current flow present.

As expected, the fluid flows from the centre of the rotor towards the tip, before flowing between the rotor and stator in an anti-clockwise direction for about 90°. When the fluid passes through the stator, it continues flowing in an anti-clockwise direction around the volute until it reaches the mixer outlet.

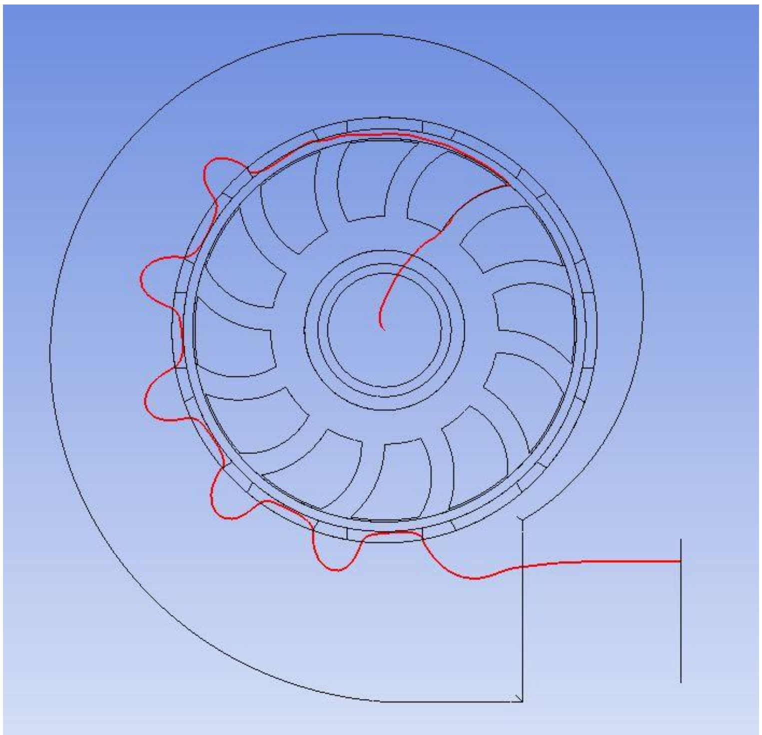

Figure 40 - High-Shear Mixer (Version B) - Particle Track

The flow path described above indicates that the modified volute geometry has solved the problem associated with counter-current flow; however the modified stator has caused a secondary issue. The reduced stator thickness and increased *opening ratio* does not direct the fluid far enough away from the stator therefore the fluid continually gets drawn back towards the stator as it progresses around the volute.

6.4.4 Geometry Modifications – Version C

'Version C' of the high-shear mixer geometry involves no changes to the volute, but the stator geometry is further refined with the objective being to direct the fluid further towards the outside shell of the volute as it passes through the stator.

To achieve this, the stator thickness was returned to the original value of 5.0mm, and the stator teeth were modelled at an angle of the 30°. The *opening ratio* for the 'Version C' analysis was also reduced to a value of 3.0, which represents a reduction of approximately 25% on the original geometry. The reason for the reduction in the *opening ratio* was not to increase the shear, but to increase the velocity of the fluid as it passes through the stator. The refined geometry is presented in Figure 41.

The final geometric modification to the stator was to increase the number of teeth from 12 to 24, which was the same number as the initial concept. The reason for this modification was to promote a more uniform shear strain rate around the rotor-stator interface.

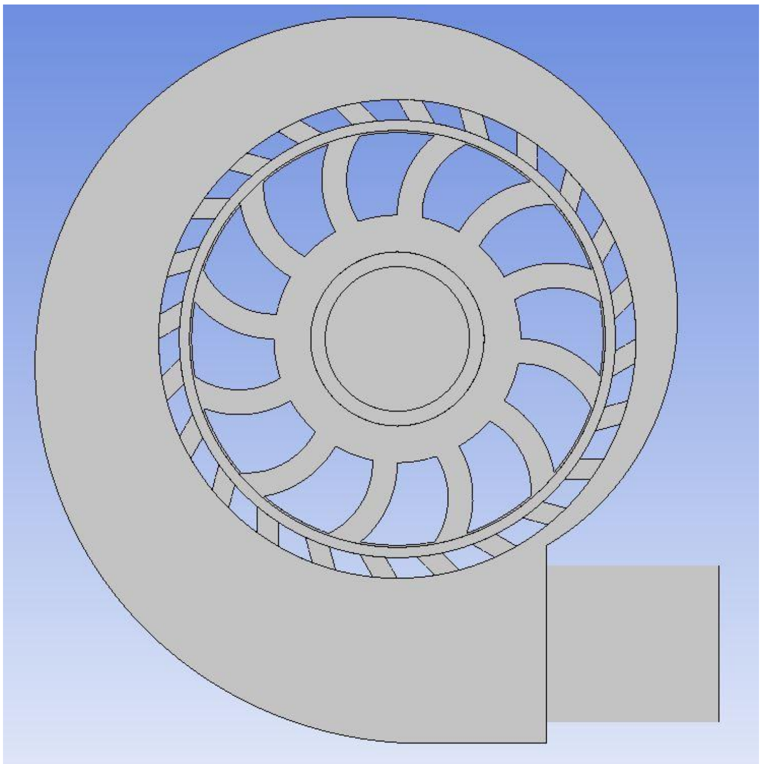

Figure 41 - High-Shear Mixer Geometry (Version C)

6.4.5 Results and Discussions – Version C

The shear strain rate contour plot for the 'Version C' mixer geometry is presented in Figure 42. Comparison with Figure 39 reveals that the results are similar to those obtained for the 'Version B' geometry. The exception is that the *shear strain rate* is consistently in the region between 900/s and 1400/s throughout the *shear gap*, whereas for 'Version B' the shear strain rate dropped as low as 500/s between the stator teeth.

Figure 43 plots the particle tracks for ten (10) discrete fly-ash particles. The results are a significant improvement on the 'Version B' results, with the stator geometry modifications working precisely as intended.

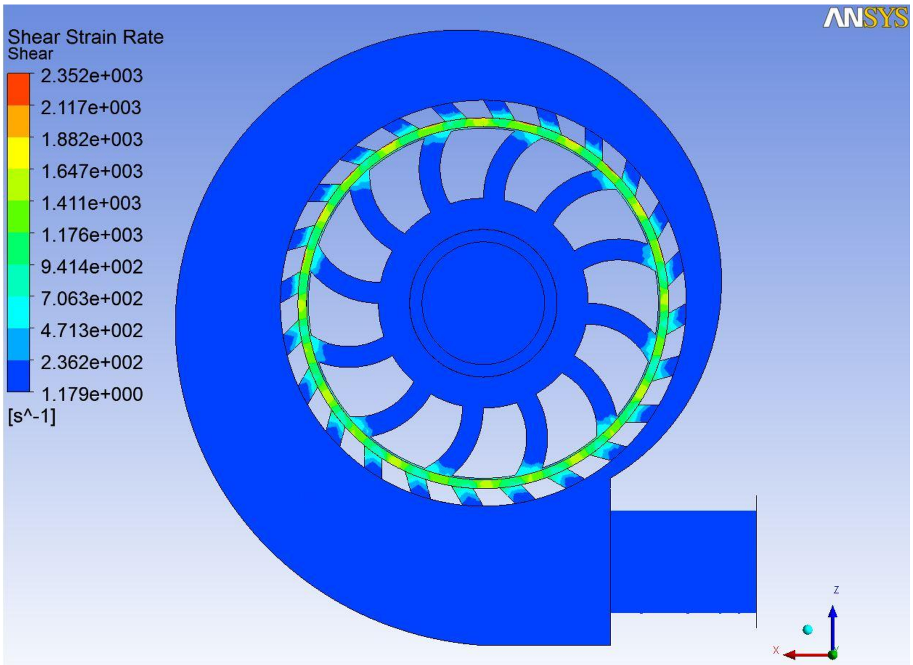

Figure 42 - High-Shear Mixer (Version C) - Shear Strain Rate

It is observed from Figure 43 that as the fluid passes through the stator, it initially flows in a clockwise direction before being corrected by the fluid already flowing though the volute. This suggests that several more iterations of the rotor-stator configuration could be performed to further optimise the fluid flow.

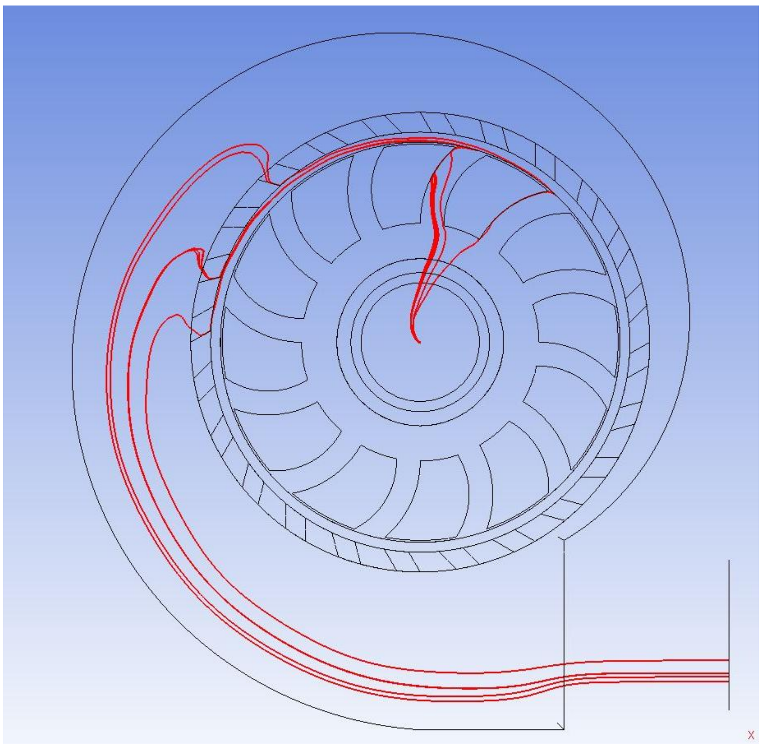

Figure 43 - High-Shear Mixer (Version C) - Particle Track

6.5 Optimised Analysis – Results Summary

The results from the mixer optimisation phase of analysis are provided in Table 18. These values have been obtained at the rotor-stator interface using the boundary conditions prescribed in Section 6.4.1. The most relevant variables are the average *velocity*, average *shear strain rate* and *outlet pressure*.

Inspection of the results summary table shows that the *shear strain rate* has been increased with consecutive design iterations. The average velocity for 'Version B & C' are very similar, yet there is a significant difference for 'Version A'. This is believed to be due to the location of the interface, which was relocated from 1.5mm from the rotor during the preliminary analysis, to 0.5mm from the rotor for the subsequent analyses. The outlet pressure has also been increased with subsequent design iterations due to the improvements made to the fluid flow path through the volute.

Table 18 - High-Shear Mixer - Optimisation Results Summary

Version	Velocity (m/s)			Shear Strain Rate (/s)			Outlet Pressure (kPa)
	Min	Max	Ave	Min	Max	Ave	
A	1.54	5.07	2.81	377	1419	658	22.32
B	0.48	4.69	1.37	160	1526	661	24.30
C	0.50	4.79	1.51	140	1486	721	26.03

The results summary presented in Table 18 provides a good comparison between the various geometries analysed, but because the values have been obtained at the rotor-stator interface, they cannot be directly compared with the benchmark results from the paddle mixer analysis which were obtained by averaging the fluid properties throughout the bowl fluid domain. Table 19 provides the equivalent results from the 'Version C' analysis, obtained by averaging the fluid properties throughout the volute.

Table 19 - High-Shear Mixer (Version C) - Volute Fluid Domain Results

Item	Variable	Minimum	Maximum	Average
1	Velocity	0 m/s	7.96 m/s	0.47 m/s
2	Shear Strain Rate	0 /s	8350 /s	451 /s

7. CONCLUSIONS

7.1 Introduction

The purpose of this study was to investigate the existing mixing methodology used in the production of aerated geopolymer concrete, and look to refine the process through the use of a high-shear mixing device.

The original scope for the project was to include the fabrication and testing of a prototype mixer in addition to the detailed design of the mixer, however the scope has since been revised to focus on the conceptual design and analysis only.

The initial concept has been modified significantly throughout the design phase to reflect the results obtained from thorough CFD analysis. The latest version of the 3D model therefore provides a base point from which the detailed design phase can commence.

7.2 Conclusions

A conceptual high-shear mixer has been designed to improve the mixture quality of aerated geopolymer paste. The conceptual design utilises a rotor-stator arrangement which imparts significant shear stress on the fluid, and increases the fluid pressure; promoting recirculation of the fluid back into the mixer hopper.

A preliminary CFD analysis of the paddle mixer currently used for preparing geopolymer samples identified an average value of average *shear strain rate* of 200/s for the fluid in the mixing bowl. The average *shear strain rate* for the fluid in the volute of the high-shear mixer was identified as 451/s, which represents an increase of 125%.

After performing a preliminary analysis of the high-shear mixer to confirm the validity of the concept, further iterations of the mixer geometry have been made, and subsequent analyses conducted. The result is an optimised concept, including streamlined volute and stator geometry.

On the basis of the work conducted for this study, the proposed conceptual design looks to be a significant improvement on the ‘paddle mixer’ used previously to prepare geopolymer concrete samples.

7.3 Further Work and Recommendations

Despite the large amount of analysis conducted to date, much more work is required before a prototype mixer can be fabricated.

1. It is recommended that a specific study is conducted to investigate the rheology properties of the aerated geopolymer paste further before proceeding with any additional mixer analysis. The primary objective of this study shall be to obtain more reliable viscosity values, for use in the analysis.
2. The 'Version C' analysis shall be re-run based on revised fluid properties ascertained in Step 1 above
3. Further refinement of the rotor-stator geometry is required to maximise the outlet pressure at the mixer outlet
4. Detailed design phase is required to refine the existing 3D model and 2D workshop drawings are then required
5. Prototype mixer to be fabricated and assembled for testing
6. Test program required to verify the operation of the conceptual design and optimise the mixing procedure including mix ratios and total duration of mixing

8. REFERENCES

ANSYS CFD, 2010.

ANSYS CFX-Pre, 2010, 13.0 edn.

Anthony Grzina, AR, Kevin Burgess 2002, *Weir Slurry Pumping Manual*.

BuildingGreen.com 1993, *Cement and Concrete: Environmental Considerations*.

Cellular Concrete, 1963, C630005.

Davidovits, J 1993, 'Geopolymer Cements To Minimise Carbon-Dioxide Greenhouse-Warming', *Ceramic Transactions, Cement Based Materials: Present, Future and Environmental Aspects*, vol. 37,

Duxton, P, Mallicoat, SW, Lukey, GC, Kriven, WM & Deventer, JSJ 2007, 'The effect of alkali and SI/AL ratio on the development of mechanical properties of metakaolin-based geopolymers', *Colloids and Surfaces*, pp. 8-20,

Fernandez-Jimenez, A, Palmolo, A, Sobrados, I & Sanz, J 2006, 'The role played by the reactive alumina content in the alkaline activation of fly ashes', *Microporous and Mesoporous Materials*, no. 91, pp. 111-9,

Ferraris, CF 2001, 'Concrete Mixing Methods and Concrete Mixers: State of the Art', *Journal of Research of the National Institute of Standards and Technology*, vol. 106, no. 2, pp. 391-9,

Hardjito, D 2005, 'Studies on Fly Ash-Based Geopolymer Concrete', Curtin University of Technology.

IKA Industrial Mixers, viewed 10/05/2011, <http://www.ikausa.com/index.htm>.

Just, A & Middendorf, B 2008, 'Microstructure of High-Strength Foam Concrete', *Materials Characterization*,

Komnitsas, K & Zaharaki, D 2007, 'Geopolymerisation: A review and prospects for the minerals industry', *Minerals Engineering*, vol. 20, pp. 1261-77,

Kovalchuck, G, Fernandez-Jimenez, A & Palmolo, A 2007, 'Alkali-activated fly ash: Effect of thermal curing conditions on the mechanical and microstructural development - Part II', *Fuel*, vol. 86, no. 3, pp. 315-22,

Kumar, R, Kumar, S & Mehrotra, SP 2007, 'Towards sustainable solutions for fly ash through mechanical activation', *Resources Conservation and Recycling*, vol. 52, pp. 157-79,

M. Criado, AP, A. Fernandez-Jimenez 2009, 'Alkali Activated Fly Ash: Effect of Admixtures on Paste Rheology', *Rheol Acta*,

Pacheco-Torgal, F, Castro-Gomes, J & Jalali, S 2008, 'Alkali-activated binders: A review', *Construction and Building Materials*, vol. 22, pp. 1305-14, Pulselli, R, Simoncini, E, Ridolfi, R & Bastianoni, S 2008, 'Specific emergy of cement and concrete: An energy-based appraisal of building materials and their transport', *Ecological Indicators*, pp. 647-56,

Rattanasak, U & Chindaprasirt, P 'Influence of NaOH solution on the synthesis of fly ash geopolymer', *Minerals Engineering*, vol. In Press, no. Corrected Proof,

Sathonsaowaphak, A, Chindaprasirt, P & Pimraksa, K 2009, 'Workability and strength of lignite bottom ash geopolymer mortar', *Journal of Hazardous Materials*,

Spogis, N & Nunhex, JR 'Design of a Low Shear Hydrofoil through the use of Computational Fluid Dynamics and Multi-Objective Design Optimization'.

Temuujin, J, Williams, RP & van Riessen, A 2009, 'Effect of mechanical activation of fly ash on the properties of geopolymer cured at ambient temperature', *Journal of Materials Processing Technology*,

Torre, J-P, Fletcher, DF, Lasuye, T & Xuereb, C 2006, *CFD Modelling of Partially Baffled Agitated Vessels with Free Surfaces*, CSIRO, Melbourne, Australia.

Appendix A – Project Specification

University of Southern Queensland

FACULTY OF ENGINEERING & SURVEYING

ENG4111/4112 Research Project

Project Specification

FOR: Steven Jon BROWN

TOPIC: HIGH SHEAR MIXING OF AERATED GEOPOLYMER CONCRETE

SUPERVISOR: Hao Wang – Senior Lecturer (Manufacturing & Materials Engineering)
Andrew Reid – Managing Director (Haald Engineering)

SPONSOR: Haald Engineering

PROJECT AIM: Design a high shear mixer capable of mixing aerated geopolymer concrete of a homogeneous nature

REVISION: Issue A – 22nd March 2011 – for supervisor review

PROGRAMME:

1) Research OPC concrete and geopolymer concrete fundamentals
2) Research high shear mixers used in other industries
3) Conceptual design of high shear mixer – key objective are to develop a concept which may be applied in a commercial environment in the future, and which will be adequate for short-term lab testing
4) Detailed design – CFD analysis required to confirm high velocities and agitation the concrete slurry is being achieved
5) Fabrication – Project management will be required, but the actual fabrication is likely to be performed by a machine shop
6) Testing – Comparison of sample properties between those produced by ordinary mixing and high shear mixing (SOME TESTING MAY BE PERFORMED BY ZUHUA ZHANG)
7) Submit an academic dissertation summarising the research

NOTE: Refer Figure 1 – Preliminary Project Workflow and Figure 2 - Preliminary Schedule for further details including key dates and milestones.

Andrew Reid

AGREED: ______________ (student) DATE: 6/04/2011

HAO WANG

AGREED: ______________ (supervisors) DATE: 5/04/2011

AGREED: ______________ (examiner) DATE: __________


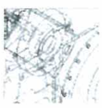
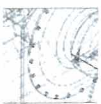

Halok Pty Ltd
ABN 84133183561
Level 1, 162 Boundary Street West End QLD 4101
PO Box 5154 West End QLD 4101
Ph +61 7 3844 0422 Fx +61 7 3844 0433
web www.haald.com.au email info@haald.com.au

Appendix B – Particle Size Analysis Report

Analysis Report

CSIRO
Division of Minerals
Particle Analysis Service

Sample Name: 14A Tarong
Batch No: R0911343
PAS ID No: P62324

Dispersant:	Water	**RI/ABS:**	2.74 / 1
Additives:	10 ml Sodium hexametaphosphate	**Analysis Model:**	General purpose
Sonication:	10 minutes in ultrasonic bath	**Result units:**	Volume

---

Concentration:	0.012 % vol	**Vol. Weighted Mean D[4,3]:**	41.873 µm	**d(0.1):**	5.335	µm
Obscuration:	10.24 %	**Surface Weighted Mean D[3,2]:**	9.327 µm	**d(0.5):**	28.245	µm
Weighted Residual:	0.519 %	**Specific Surface Area:**	0.643 m^2/cc	**P80:**	66.338	µm
				d(0.9):	94.78	µm

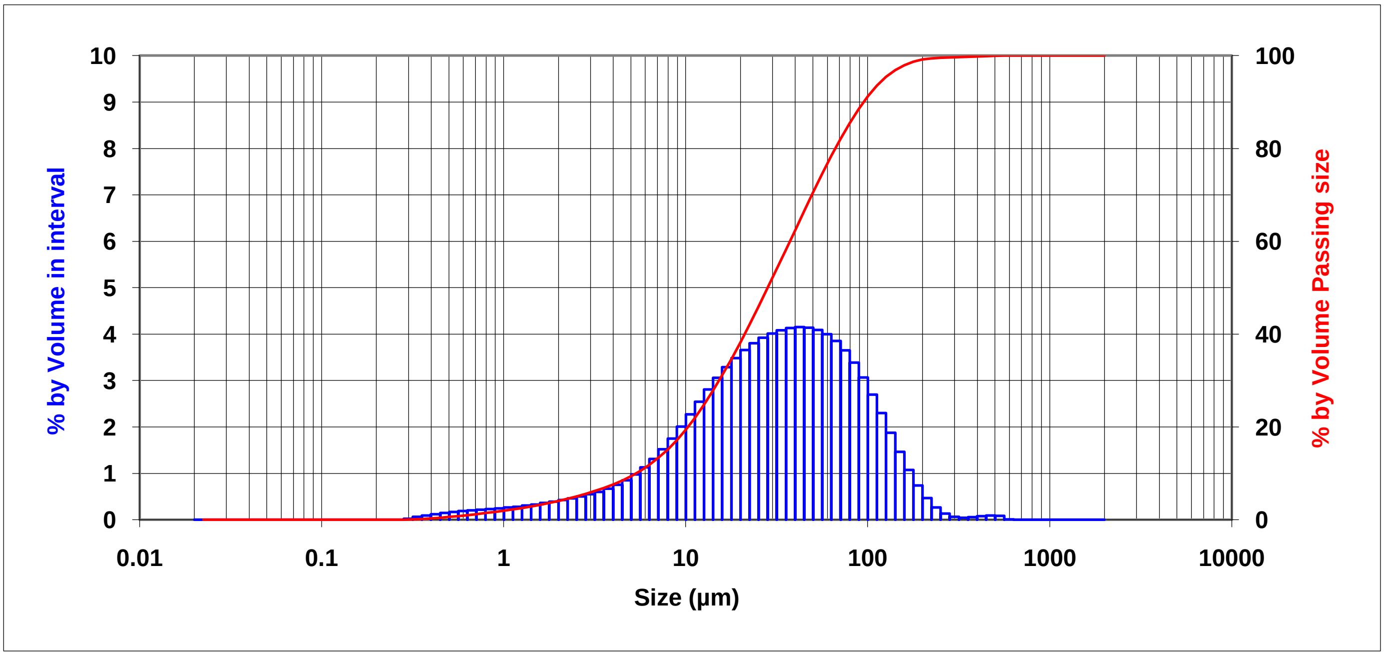

Size (µm)	Vol Under %	Size (µm)	Vol Under %	Size (µm)	Vol Under %	Size (µm)	Vol Under %	Size (µm)	Vol Under %	Size (µm)	Vol Under %
0.020	0.00	0.142	0.00	1.002	1.96	7.096	13.39	50.238	70.61	355.656	99.74
0.022	0.00	0.159	0.00	1.125	2.24	7.962	15.15	56.368	74.60	399.052	99.82
0.025	0.00	0.178	0.00	1.262	2.55	8.934	17.15	63.246	78.46	447.744	99.91
0.028	0.00	0.200	0.00	1.416	2.88	10.024	19.43	70.963	82.11	502.377	99.99
0.032	0.00	0.224	0.00	1.589	3.24	11.247	21.97	79.621	85.50	563.677	100.00
0.036	0.00	0.252	0.00	1.783	3.63	12.619	24.78	89.337	88.56	632.456	100.00
0.040	0.00	0.283	0.02	2.000	4.06	14.159	27.84	100.237	91.26	709.627	100.00
0.045	0.00	0.317	0.09	2.244	4.52	15.887	31.12	112.468	93.56	796.214	100.00
0.050	0.00	0.356	0.18	2.518	5.03	17.825	34.61	126.191	95.43	893.367	100.00
0.056	0.00	0.399	0.30	2.825	5.58	20.000	38.27	141.589	96.89	1002.374	100.00
0.063	0.00	0.448	0.45	3.170	6.18	22.440	42.07	158.866	97.97	1124.683	100.00
0.071	0.00	0.502	0.62	3.557	6.85	25.179	45.99	178.250	98.70	1261.915	100.00
0.080	0.00	0.564	0.80	3.991	7.60	28.251	50.01	200.000	99.17	1415.892	100.00
0.089	0.00	0.632	1.01	4.477	8.45	31.698	54.09	224.404	99.44	1588.656	100.00
0.100	0.00	0.710	1.22	5.024	9.43	35.566	58.22	251.785	99.57	1782.502	100.00
0.112	0.00	0.796	1.45	5.637	10.56	39.905	62.37	282.508	99.64	2000.000	100.00
0.126	0.00	0.893	1.70	6.325	11.87	44.774	66.51	316.979	99.69		

Appendix C – Calculations

HAALD Engineering
PO Box 5154
WEST END Q 4101

Ph 61 7 3844 0422
Fx 61 7 3844 0433
haald@haald.com.au

CLIENT:	USQ	EQUIP No:	High-shear Mixer
PROJECT:	Final Year Project	AUTHOR:	SJB
LOCATION:	n/a	PROJECTNo:	n/a
CALC No:	ENG4111-01	CALC TITLE:	Pipe frictional losses

This document calculates the unit pressure losses due to friction through the mixer outlet pipe for water. This is used to calibrate the CFD model which estimates the pressure losses for geopolymer paste (assumed to behave as a bingham fluid).

SYSTEM PROPERTIES:

Pipe Properties:

Material: Steel

Absolute roughness factor for steel pipe: $\varepsilon_{steel} := 0.15\text{mm}$

Pipe outside diameter: $D_o := 48.2\text{mm}$

Wall thickness: $t := 3.68\text{mm}$

Pipe inside diameter: $D_i := \left[D_o - (2t)\right] = 40.84\cdot\text{mm}$

Area of pipe: $A_p := \left(D_i^{\,2}\right)\frac{\pi}{4} = 0.001\ \text{m}^2$

Length of pipe: $L_p := 1\text{m}$

Fluid Properties:

Fluid: Water

Density: $\rho_{h2o} \equiv 998\,\frac{\text{kg}}{\text{m}^3}$

Specific weight: $\gamma_{h2o} \equiv 9790\,\frac{\text{N}}{\text{m}^3}$

Flow rate: $Q := 0.5\,\frac{\text{l}}{\text{s}}$

FRICTIONAL HEAD LOSS:

Velocity in pipe:

$$v_p := \frac{Q}{A_p} = 0.382\,\frac{m}{s}$$

Reynolds number:

$$Re_p := \frac{\rho_{h2o} \cdot v_p \cdot D_i}{\mu_{h2o}} = 15556.967$$

Guess value for friction factor:

$$f := 0.02$$

Darcy friction factor (Colebrook equation):

$$\text{Friction}(f) := -2 \cdot \log\left(\frac{\varepsilon_{steel}}{3.7 \cdot D_i} + \frac{2.51}{Re_p \cdot \sqrt{f}}\right) - \frac{1}{\sqrt{f}}$$

$$f := \text{root}(\text{Friction}(f), f) = 0.034$$

Head loss due to friction:

$$h_f := \frac{L_p \cdot f \cdot v_p^{\,2}}{D_i \cdot 2 \cdot g} = 0.006\,m$$

Pressure drop per metre of pipe:

$$\Delta p := h_f \cdot \gamma_{h2o} = 59.837 \cdot Pa$$

Appendix D – High-Shear Mixer (Version A) CFD Results

Conceptual High-Shear Mixer Analysis Data

	Mass Flow Rate (kg/s)	0.2	0.4	0.6	0.8	1	1.2	1.4
400 RPM	Pressure (out)	1.84	0.52	-0.78	-2.09	-3.35	-4.75	-6.11
	Velocity (min)	0.16	0.16	0.16	0.16	1.60	0.16	0.16
	Velocity (max)	2.08	2.08	2.08	2.08	2.09	2.07	2.07
	Velocity (ave)	1.01	1.00	1.00	1.00	1.00	1.00	1.00
	Shear Strain Rate (min)	149	143	136	129	120	117	111
	Shear Strain Rate (max)	498	496	494	493	499	489	488
	Shear Strain Rate (ave)	258	252	246	240	237	230	225
800 RPM	Pressure (out)	10.42	8.83	7.34	5.86	4.41	2.96	1.49
	Velocity (min)	0.86	0.86	0.86	0.85	0.84	0.84	0.83
	Velocity (max)	3.69	3.68	3.68	3.68	3.68	3.67	3.67
	Velocity (ave)	1.95	1.94	1.93	1.92	1.92	1.91	1.91
	Shear Strain Rate (min)	274	270	262	254	246	239	232
	Shear Strain Rate (max)	983	980	977	974	971	969	967
	Shear Strain Rate (ave)	479	471	463	455	447	440	433
1200 RPM	Pressure (out)	24.43	22.32	20.45	18.66	16.97	15.38	13.77
	Velocity (min)	1.55	1.54	1.53	1.52	1.50	1.49	1.48
	Velocity (max)	5.08	5.08	5.07	5.07	5.06	5.06	5.06
	Velocity (ave)	2.82	2.81	2.79	2.78	2.77	2.76	2.75
	Shear Strain Rate (min)	382	377	370	361	352	344	336
	Shear Strain Rate (max)	1422	1419	1415	1412	1411	1409	1407
	Shear Strain Rate (ave)	668	658	649	640	631	622	613
1600 RPM	Pressure (out)	43.55	40.85	38.60	36.41	34.43	32.52	30.71
	Velocity (min)	2.11	2.11	2.10	2.10	2.10	2.09	2.09
	Velocity (max)	6.45	6.44	6.43	6.42	6.41	6.40	6.39
	Velocity (ave)	3.65	3.63	3.61	3.60	3.58	3.57	3.56
	Shear Strain Rate (min)	475	469	464	456	447	438	429
	Shear Strain Rate (max)	1829	1825	1822	1820	1817	1815	1812
	Shear Strain Rate (ave)	835	824	814	803	793	783	774

Appendix E – High-Shear Mixer (Version A) CFD Images

<table>
<tr><th colspan="2">Mass Flow Rate = 0.2 kg/s</th></tr>
<tr><th colspan="2">400 RPM</th></tr>
<tr><th>Velocity</th><th>Shear Strain Rate</th></tr>
<tr><td>

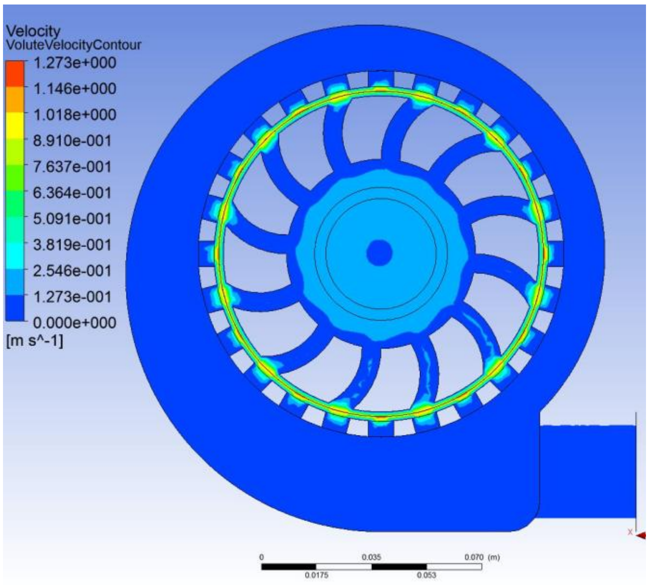

</td><td>

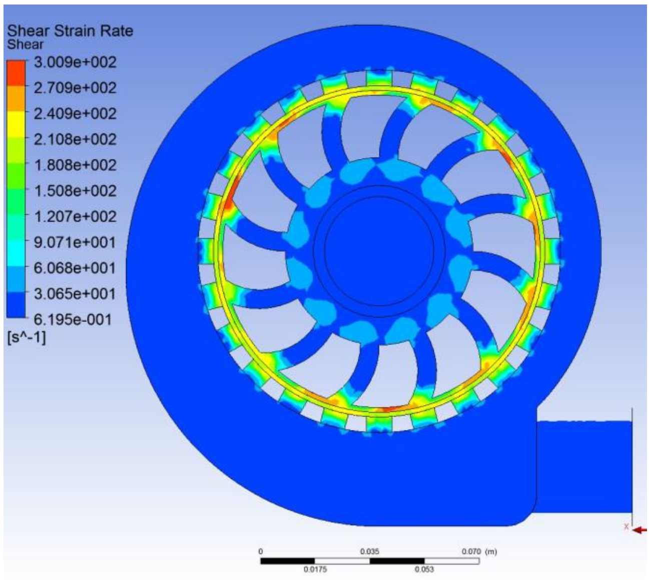

</td></tr>
<tr><th colspan="2">800 RPM</th></tr>
<tr><th>Velocity</th><th>Shear Strain Rate</th></tr>
<tr><td>

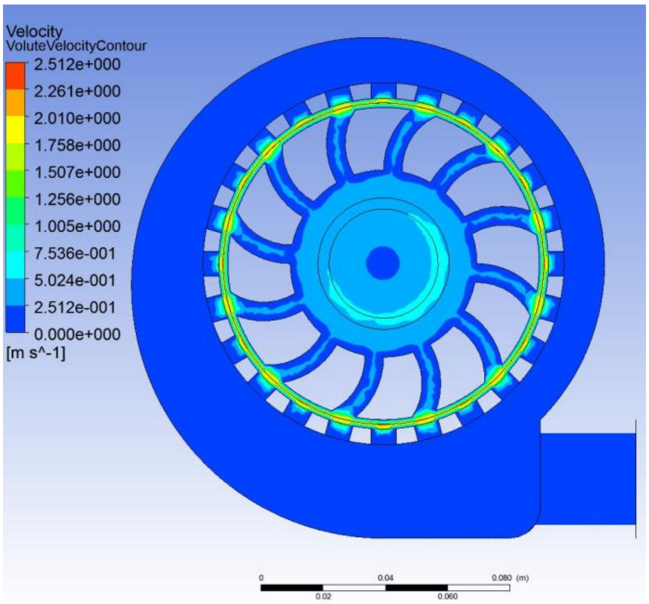

</td><td>

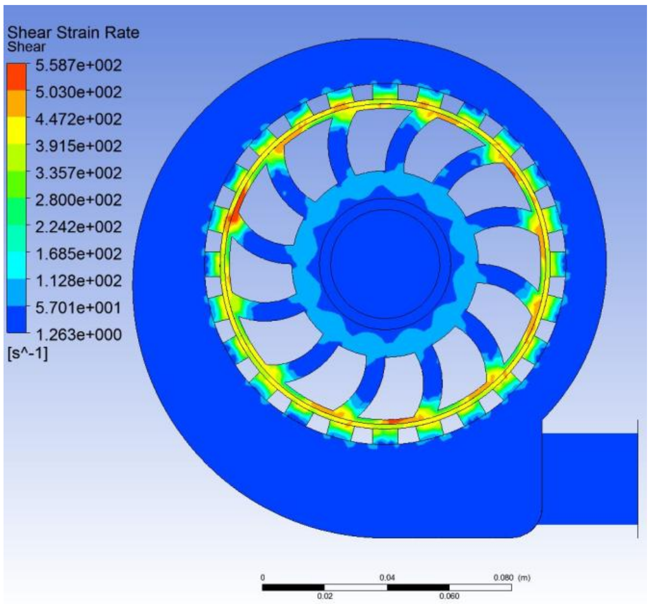

</td></tr>
</table>

<table>
<tr><th colspan="2">Mass Flow Rate = 0.2 kg/s</th></tr>
<tr><th colspan="2">1200 RPM</th></tr>
<tr><th>Velocity</th><th>Shear Strain Rate</th></tr>
<tr><td>

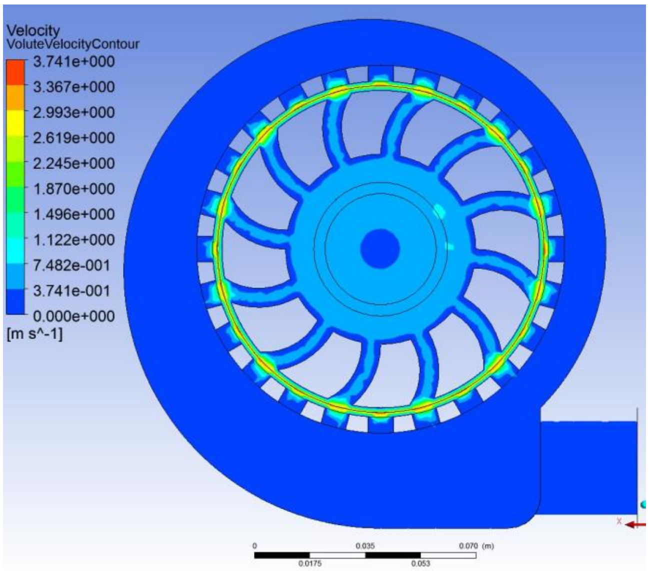

</td><td>

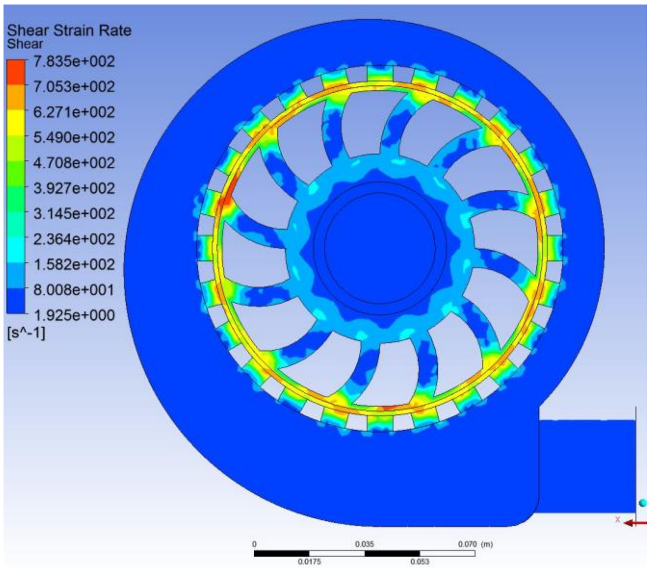

</td></tr>
<tr><th colspan="2">1600 RPM</th></tr>
<tr><th>Velocity</th><th>Shear Strain Rate</th></tr>
<tr><td>

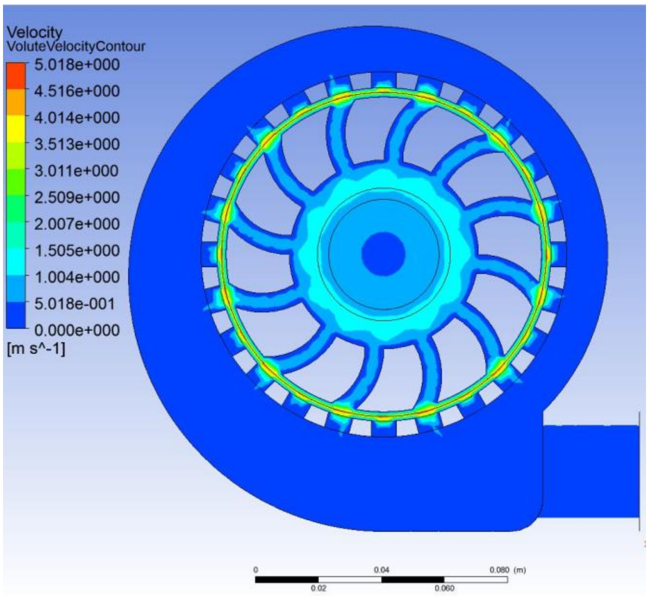

</td><td>

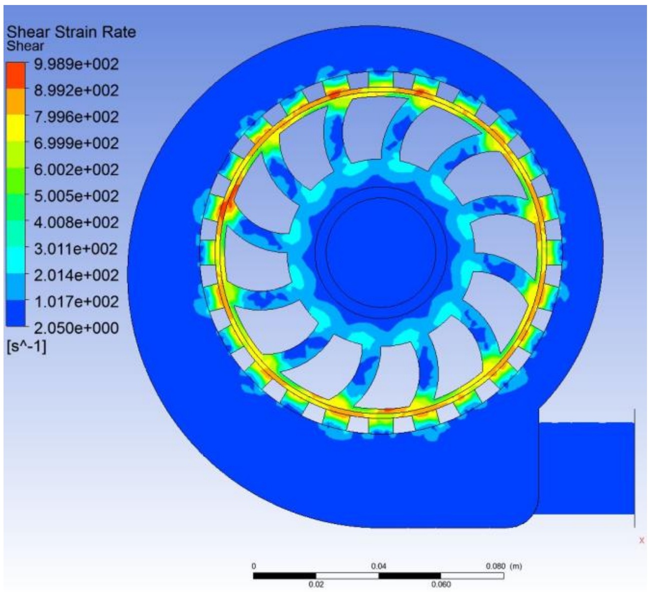

</td></tr>
</table>

Mass Flow Rate = 0.4 kg/s	
400 RPM	
Velocity	**Shear Strain Rate**

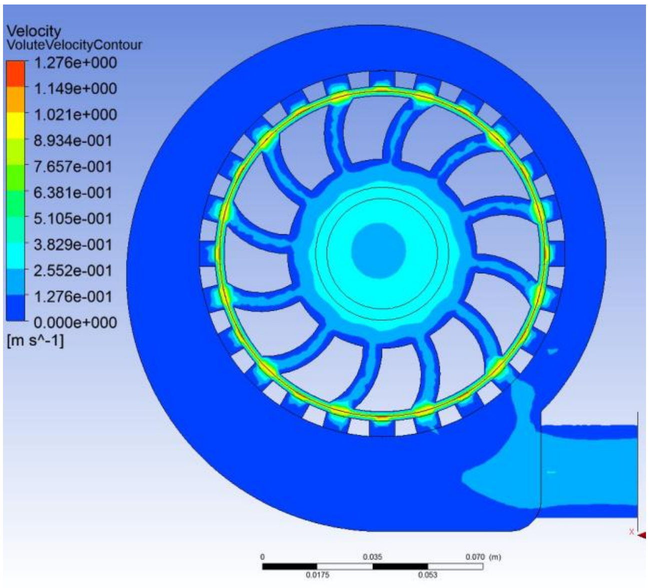

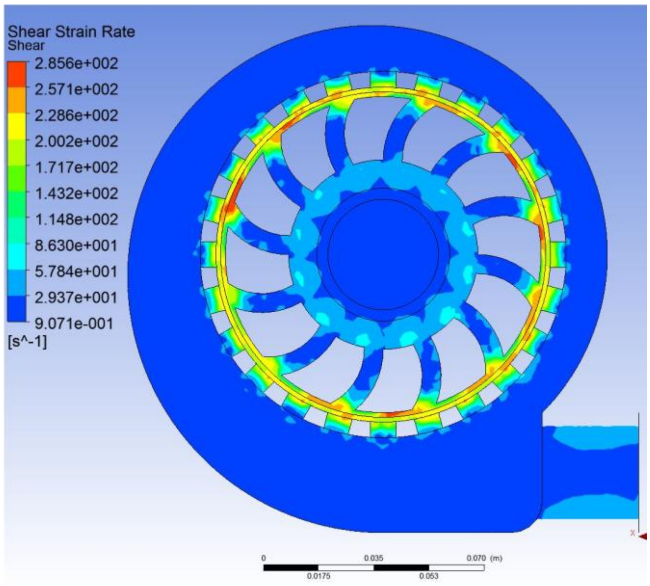

800 RPM	
Velocity	**Shear Strain Rate**

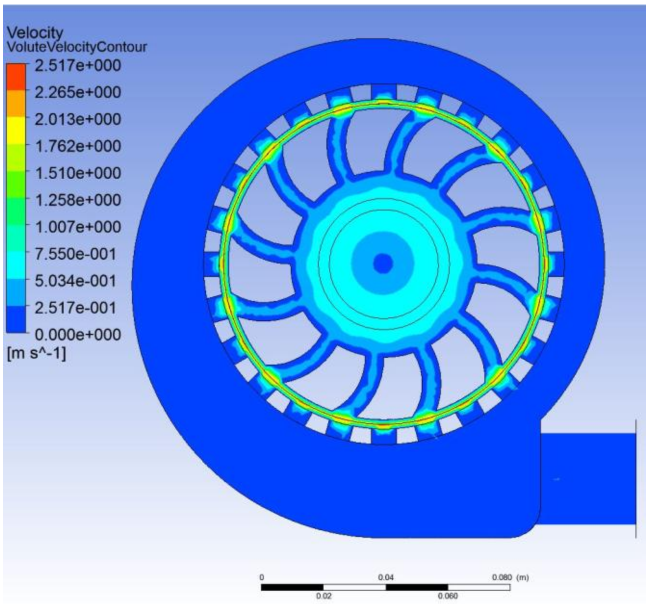

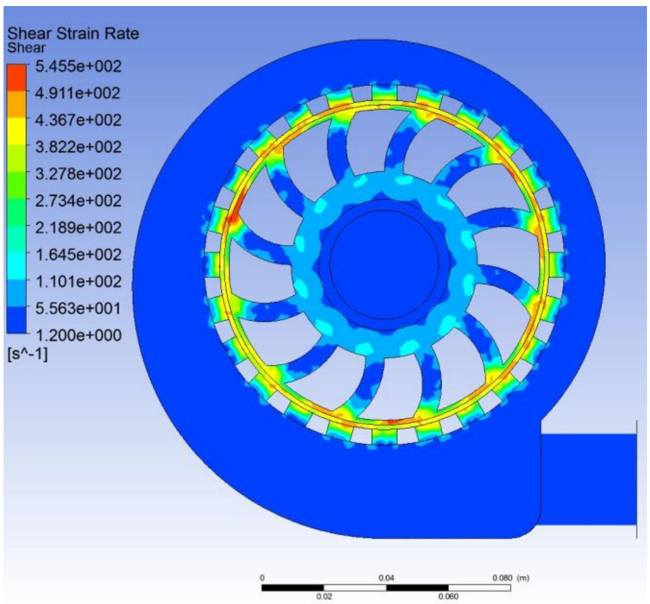

<table>
<tr><th colspan="2">Mass Flow Rate = 0.4 kg/s</th></tr>
<tr><th colspan="2">1200 RPM</th></tr>
<tr><th>Velocity</th><th>Shear Strain Rate</th></tr>
<tr><td>

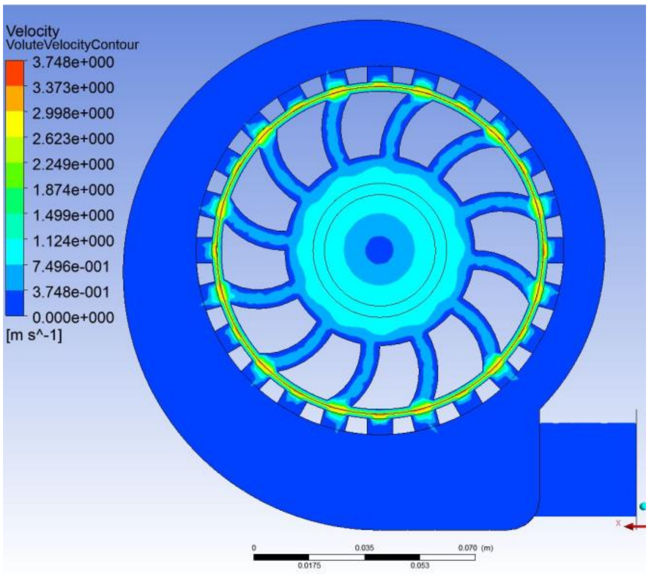

</td><td>

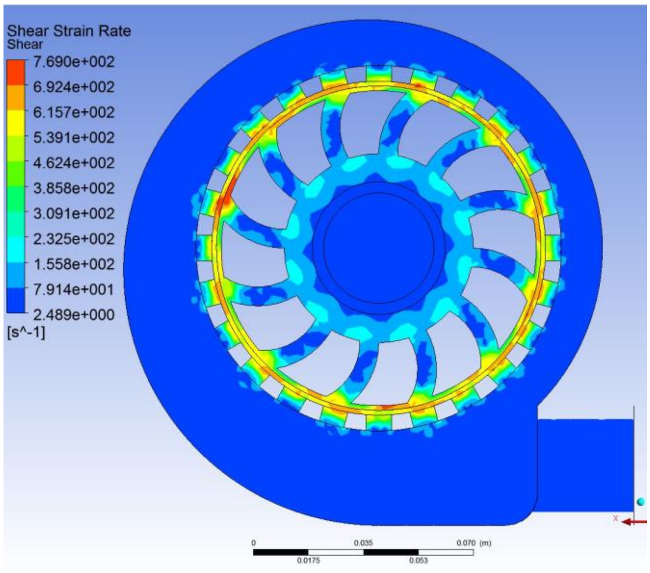

</td></tr>
<tr><th colspan="2">1600 RPM</th></tr>
<tr><th>Velocity</th><th>Shear Strain Rate</th></tr>
<tr><td>

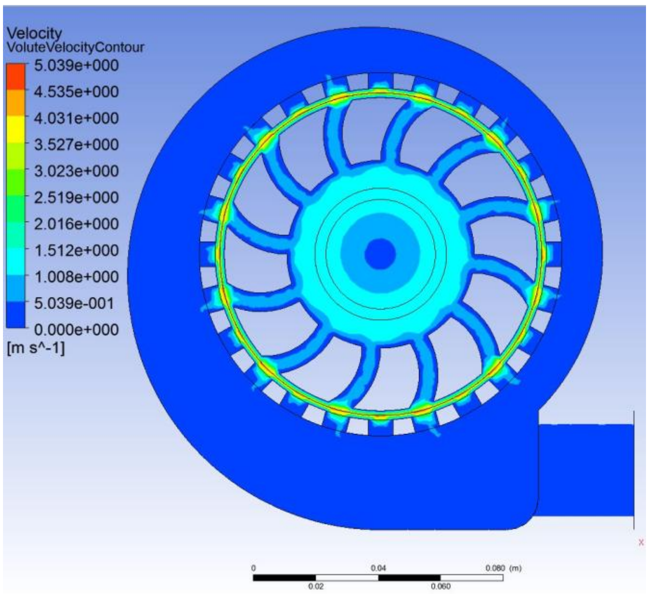

</td><td>

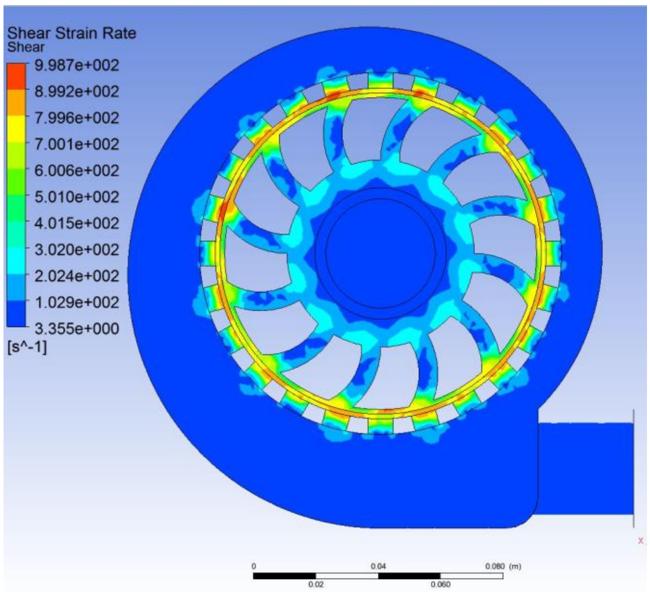

</td></tr>
</table>

Mass Flow Rate = 0.6 kg/s	
400 RPM	
Velocity	**Shear Strain Rate**
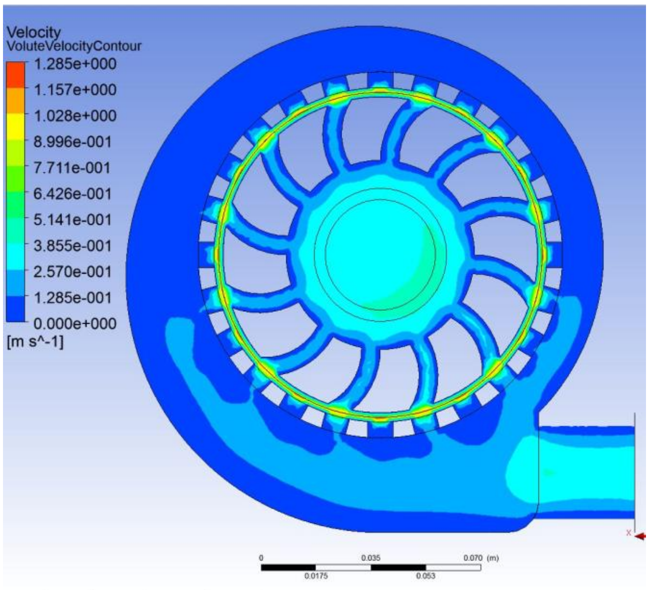	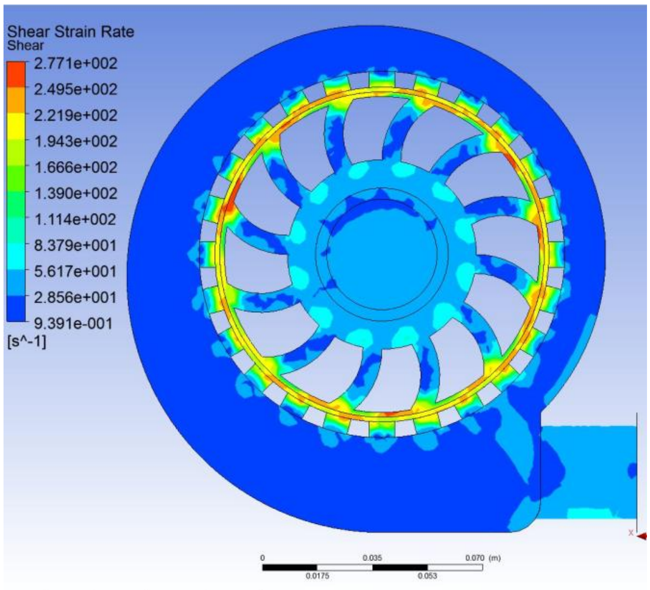
800 RPM	
Velocity	**Shear Strain Rate**
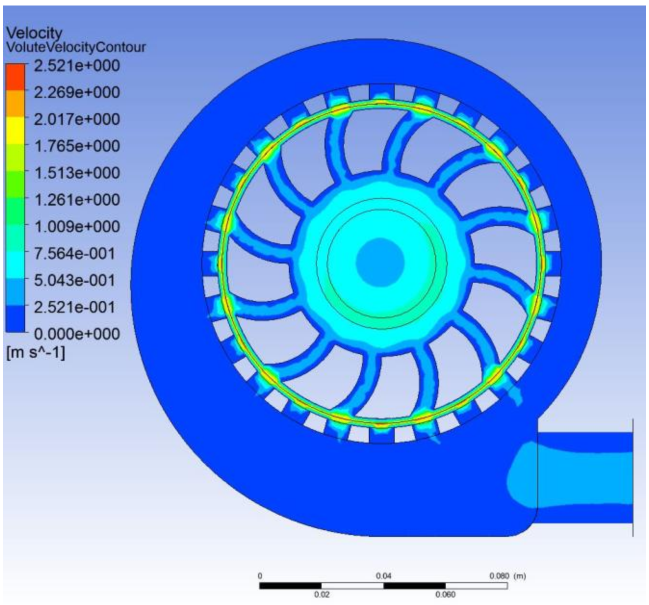	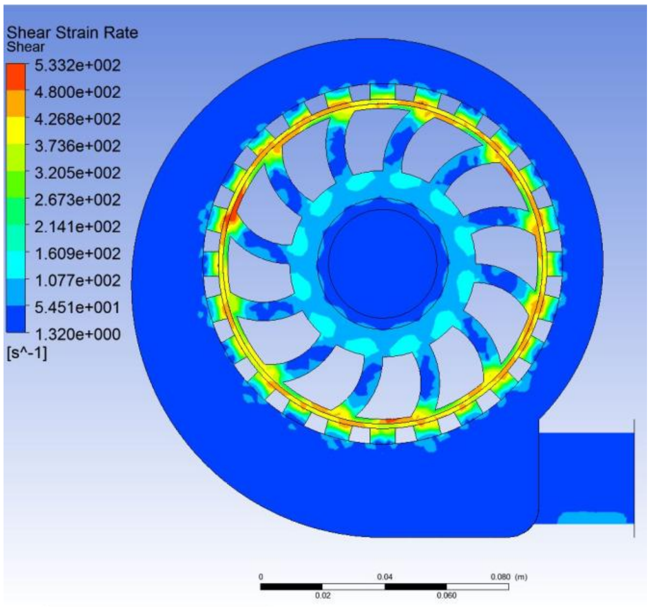

Mass Flow Rate = 0.6 kg/s

1200 RPM

Velocity	**Shear Strain Rate**

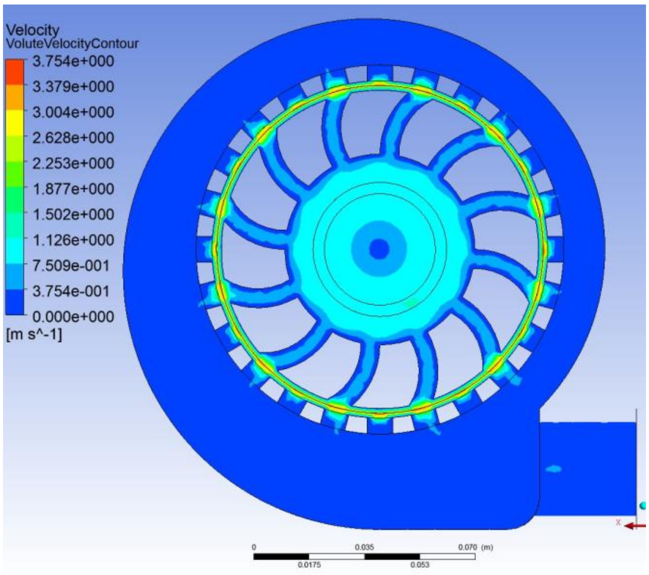

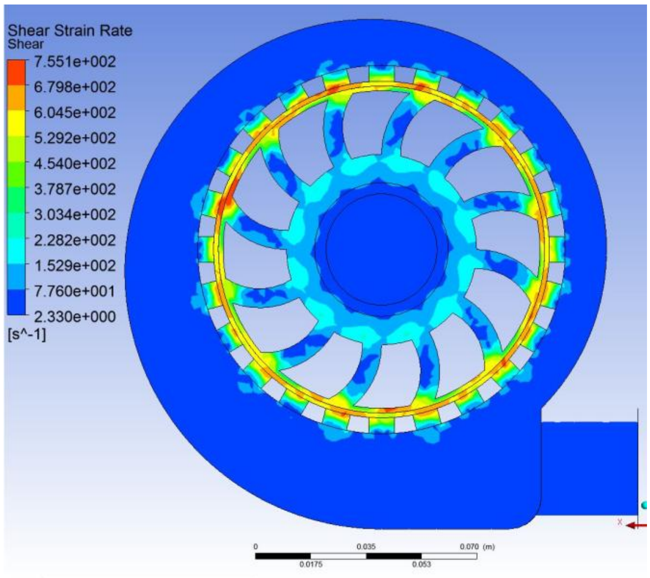

1600 RPM

Velocity	**Shear Strain Rate**

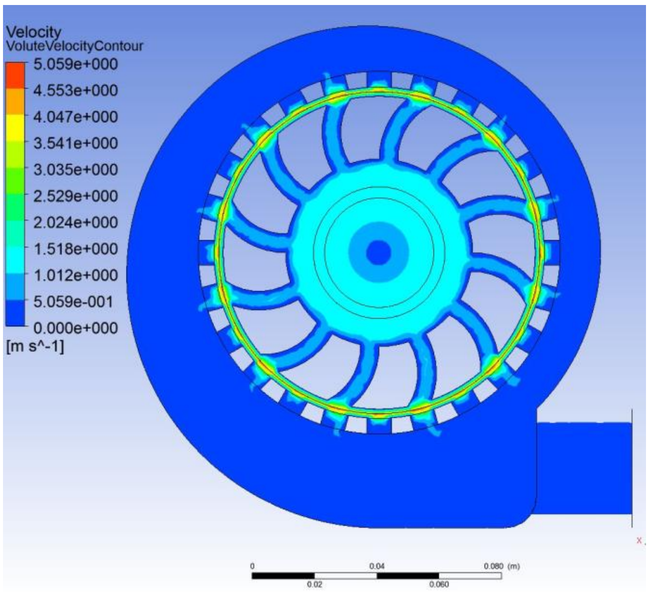

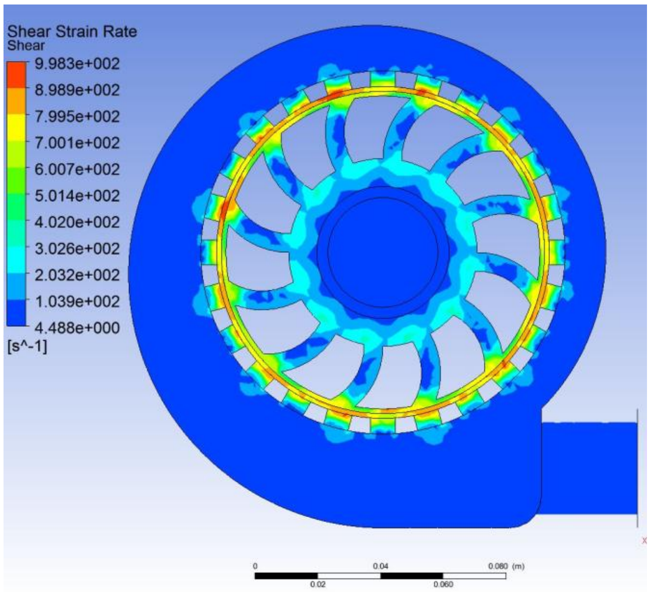

<table>
<tr><th colspan="2">Mass Flow Rate = 0.8 kg/s</th></tr>
<tr><th colspan="2">400 RPM</th></tr>
<tr><th>Velocity</th><th>Shear Strain Rate</th></tr>
<tr><td>

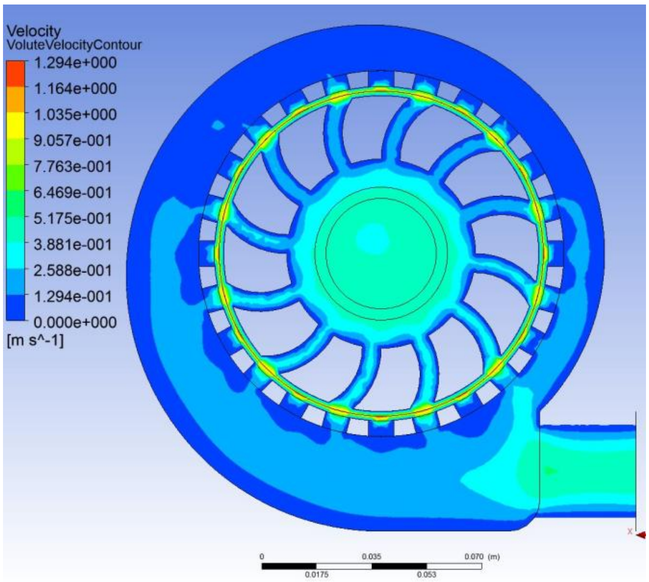

</td><td>

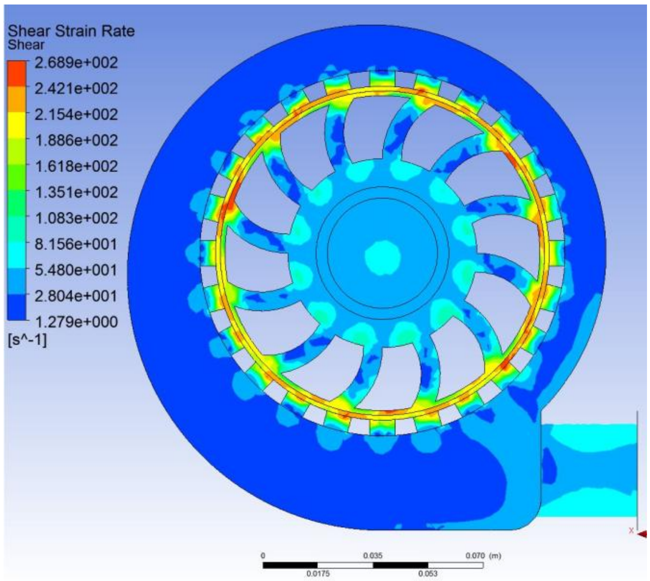

</td></tr>
<tr><th colspan="2">800 RPM</th></tr>
<tr><th>Velocity</th><th>Shear Strain Rate</th></tr>
<tr><td>

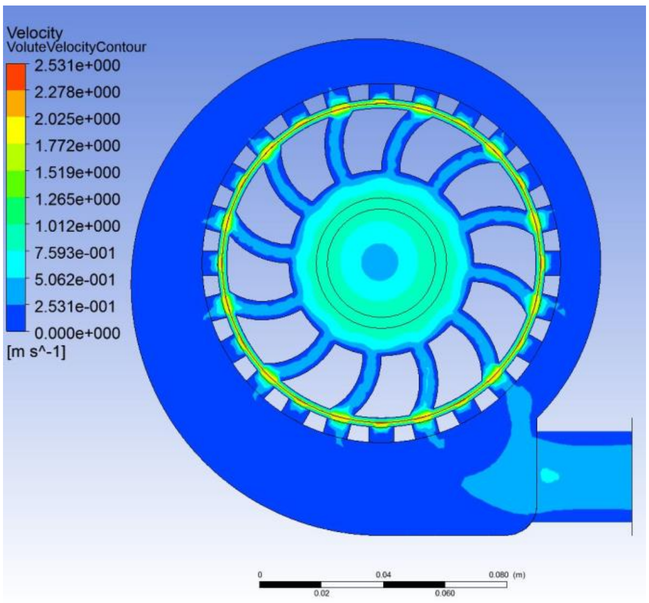

</td><td>

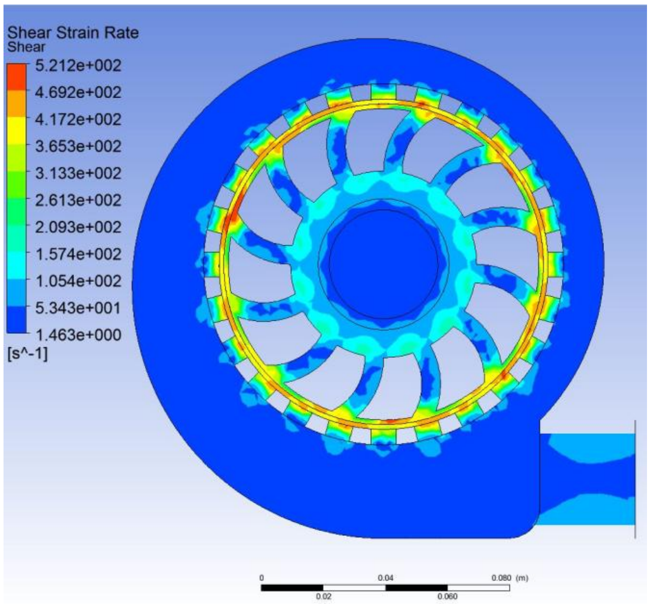

</td></tr>
</table>

<table>
<tr><th colspan="2">Mass Flow Rate = 0.8 kg/s</th></tr>
<tr><th colspan="2">1200 RPM</th></tr>
<tr><th>Velocity</th><th>Shear Strain Rate</th></tr>
<tr><td>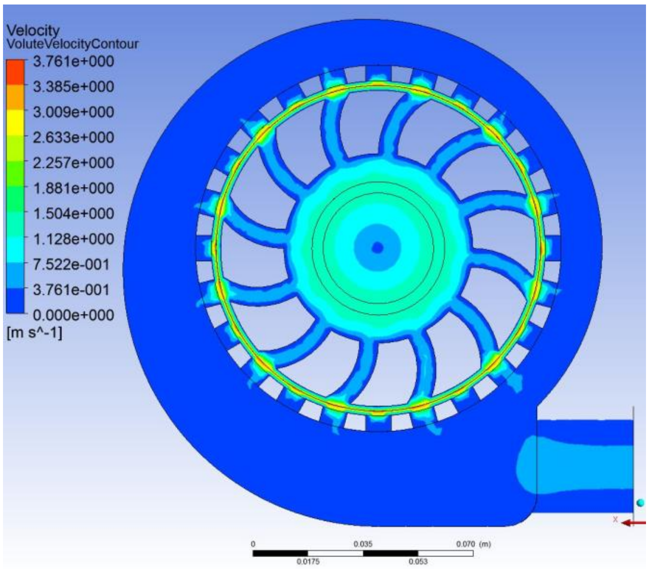
</td><td>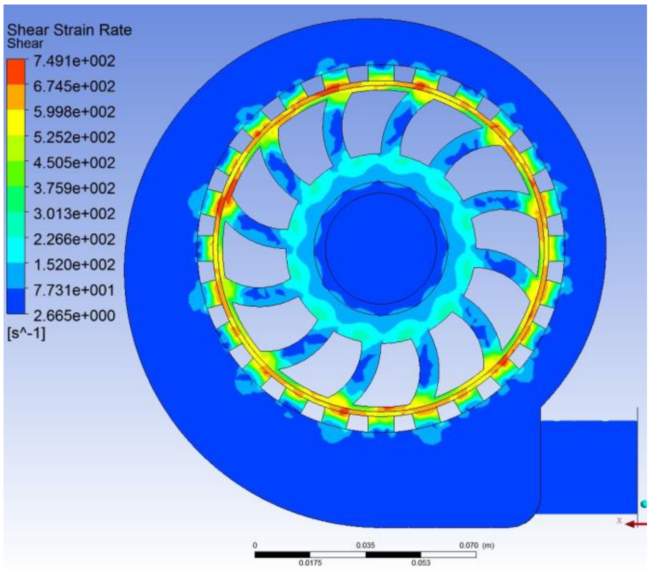
</td></tr>
<tr><th colspan="2">1600 RPM</th></tr>
<tr><th>Velocity</th><th>Shear Strain Rate</th></tr>
<tr><td>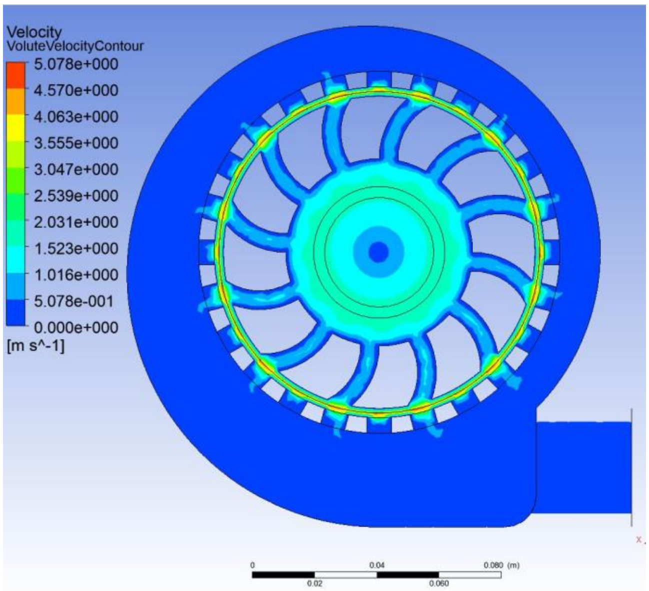
</td><td>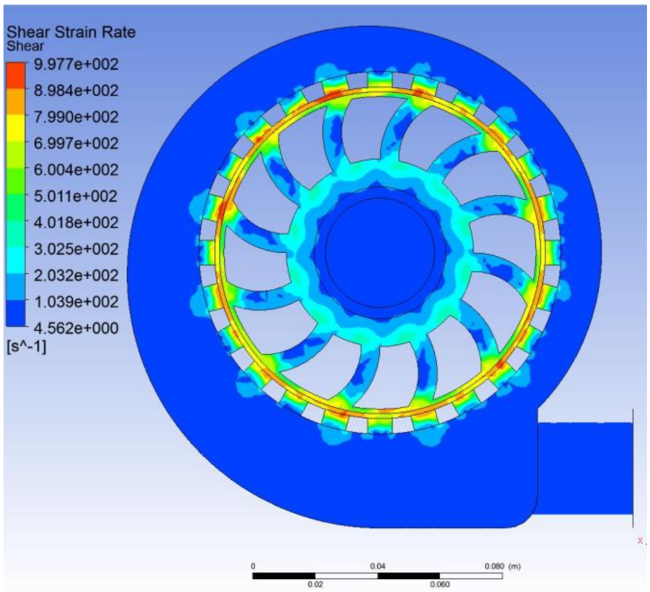
</td></tr>
</table>

<table>
<tr><th colspan="2">Mass Flow Rate = 1.0 kg/s</th></tr>
<tr><th colspan="2">400 RPM</th></tr>
<tr><th>Velocity</th><th>Shear Strain Rate</th></tr>
<tr><td>
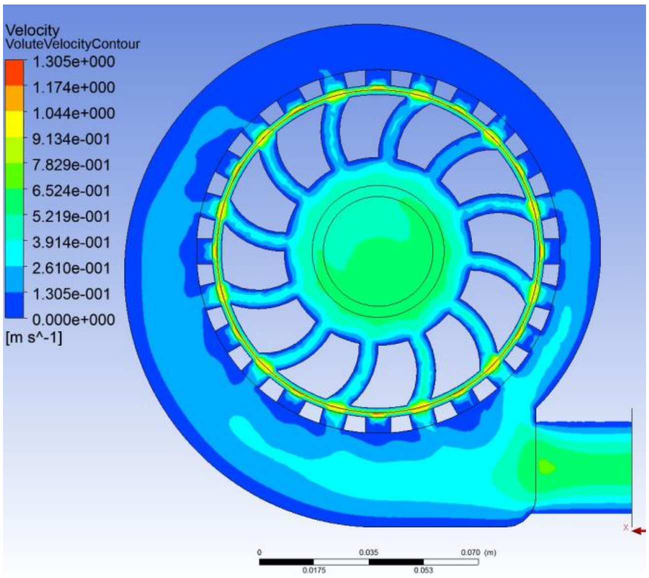

</td><td>
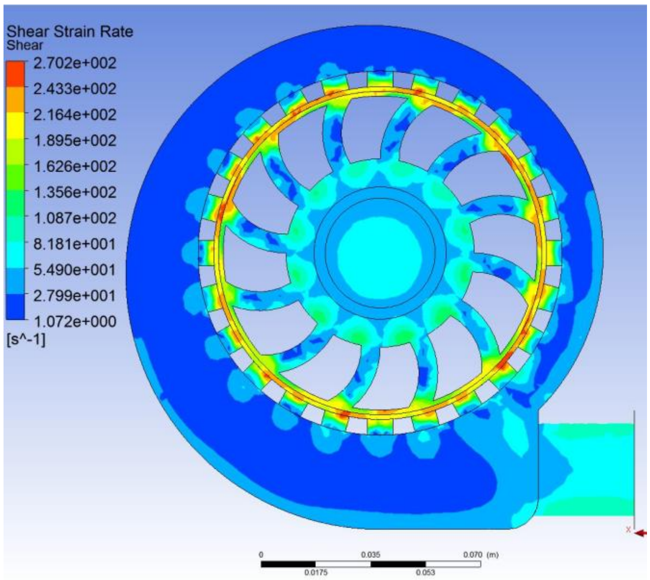

</td></tr>
<tr><th colspan="2">800 RPM</th></tr>
<tr><th>Velocity</th><th>Shear Strain Rate</th></tr>
<tr><td>
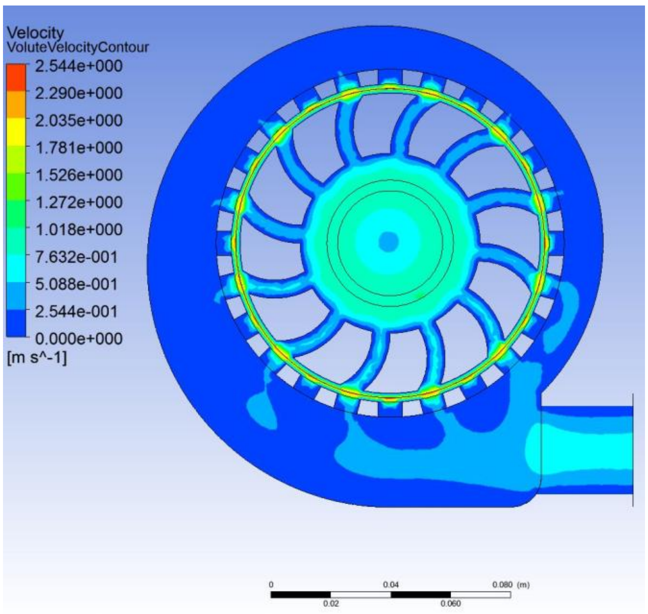

</td><td>
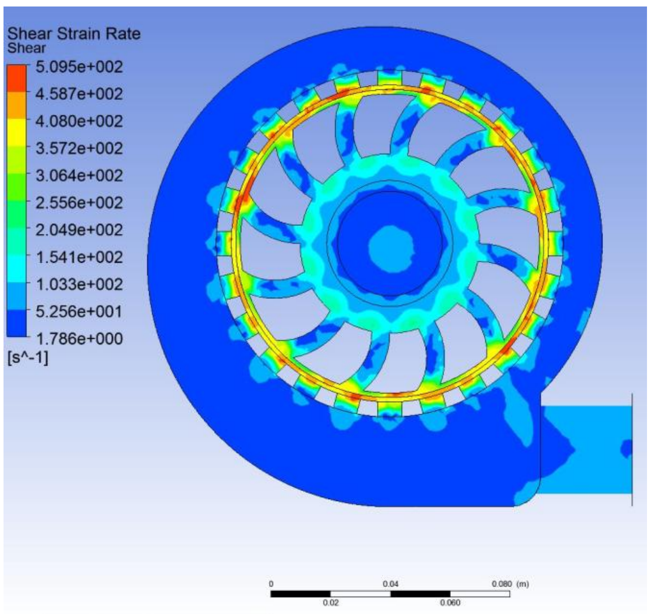

</td></tr>
</table>

<table>
<tr><th colspan="2">Mass Flow Rate = 1.0 kg/s</th></tr>
<tr><th colspan="2">1200 RPM</th></tr>
<tr><th>Velocity</th><th>Shear Strain Rate</th></tr>
<tr><td>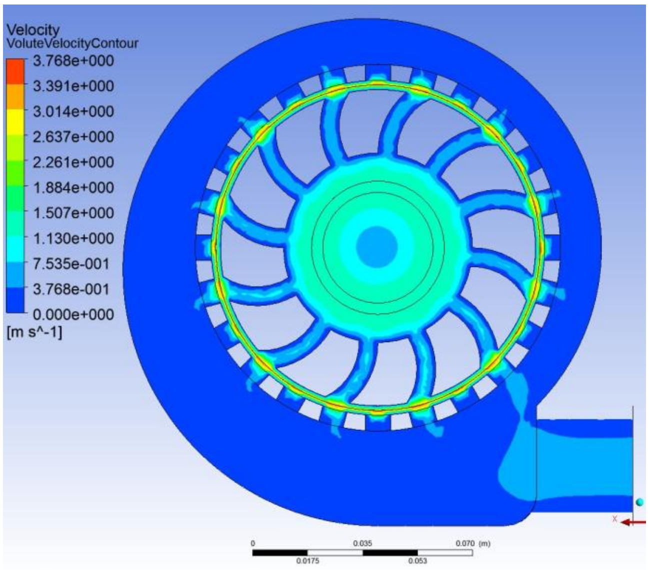
</td><td>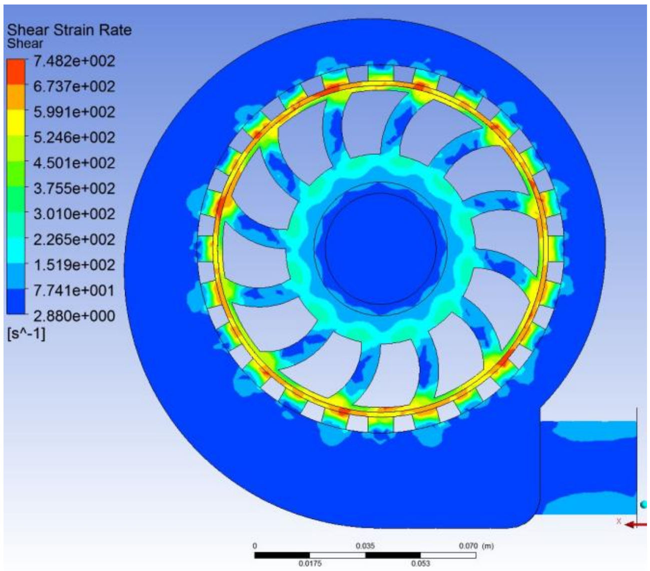
</td></tr>
<tr><th colspan="2">1600 RPM</th></tr>
<tr><th>Velocity</th><th>Shear Strain Rate</th></tr>
<tr><td>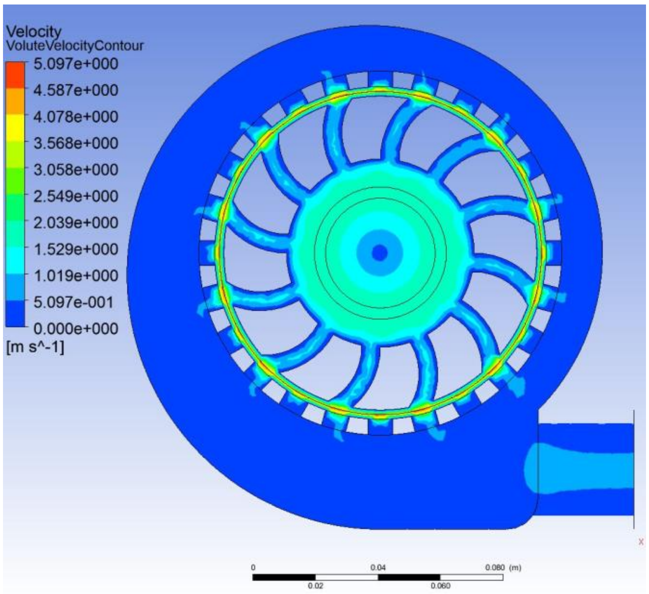
</td><td>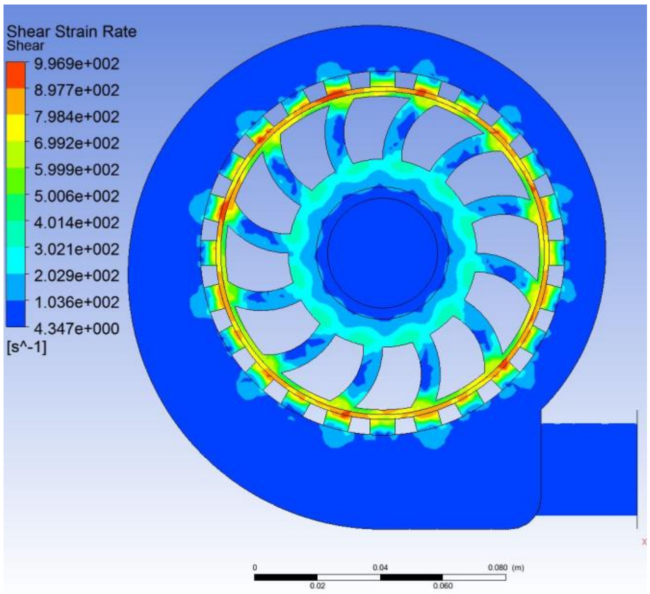
</td></tr>
</table>

<table>
<tr><th colspan="2">Mass Flow Rate = 1.2 kg/s</th></tr>
<tr><th colspan="2">400 RPM</th></tr>
<tr><th>Velocity</th><th>Shear Strain Rate</th></tr>
<tr><td>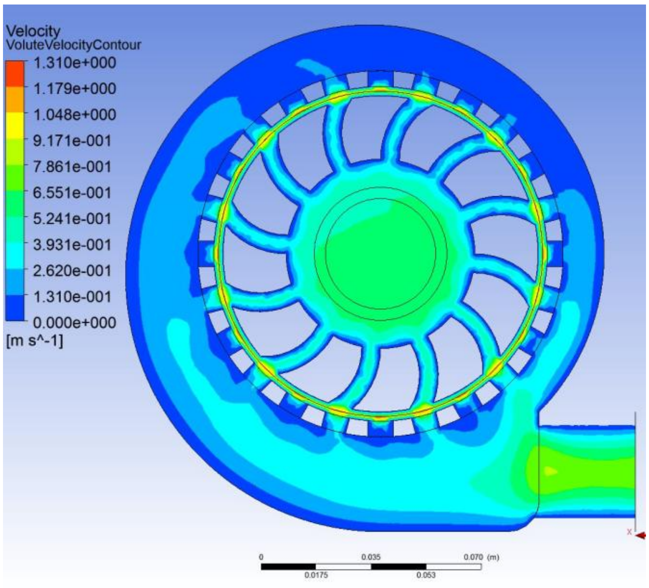
</td><td>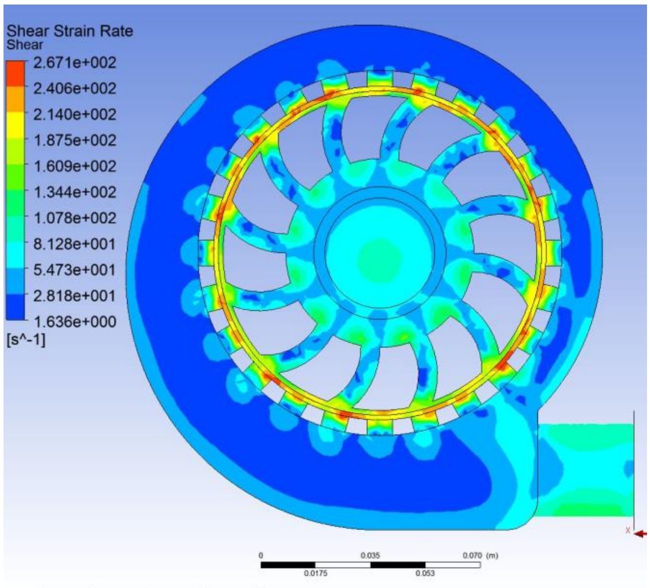
</td></tr>
<tr><th colspan="2">800 RPM</th></tr>
<tr><th>Velocity</th><th>Shear Strain Rate</th></tr>
<tr><td>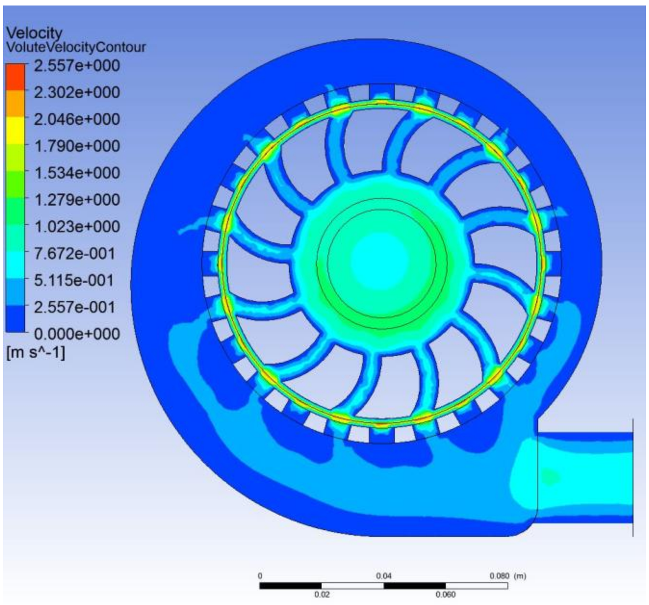
</td><td>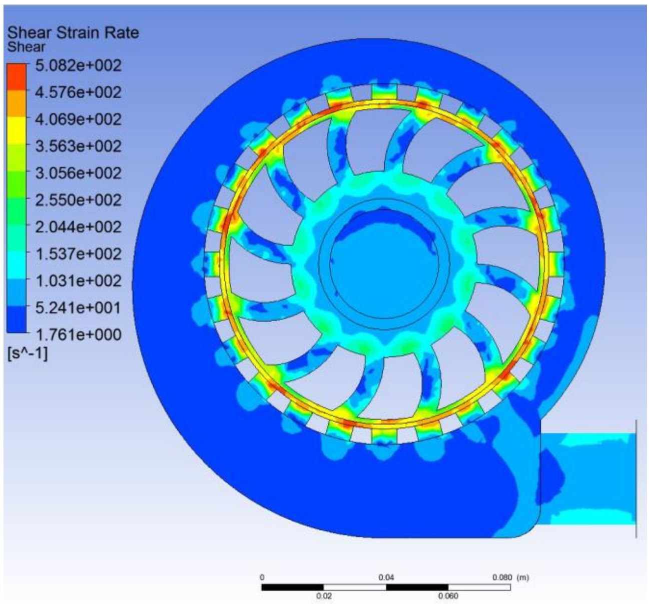
</td></tr>
</table>

<table>
<tr><th colspan="2">Mass Flow Rate = 1.2 kg/s</th></tr>
<tr><th colspan="2">1200 RPM</th></tr>
<tr><th>Velocity</th><th>Shear Strain Rate</th></tr>
<tr><td>
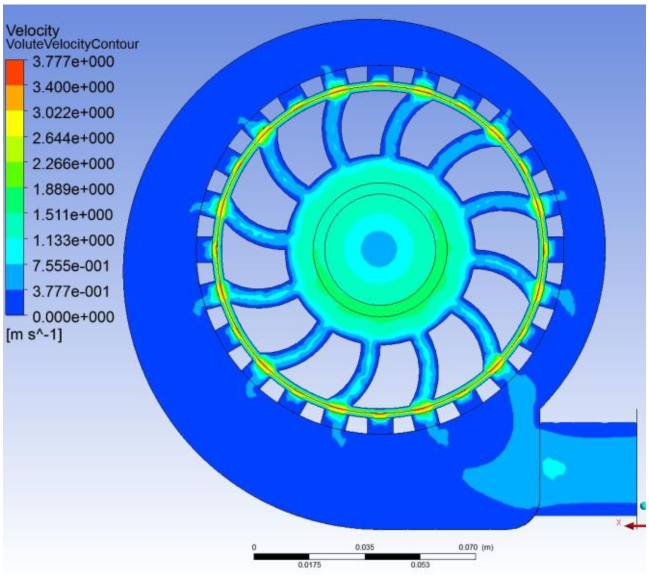

</td><td>
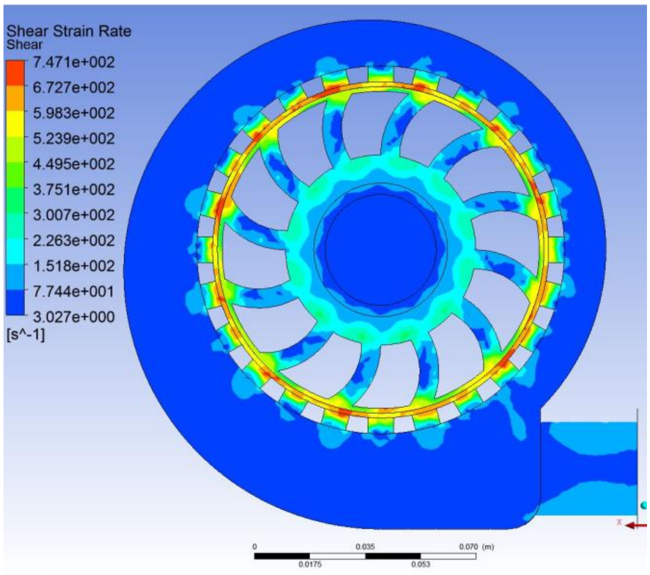

</td></tr>
<tr><th colspan="2">1600 RPM</th></tr>
<tr><th>Velocity</th><th>Shear Strain Rate</th></tr>
<tr><td>
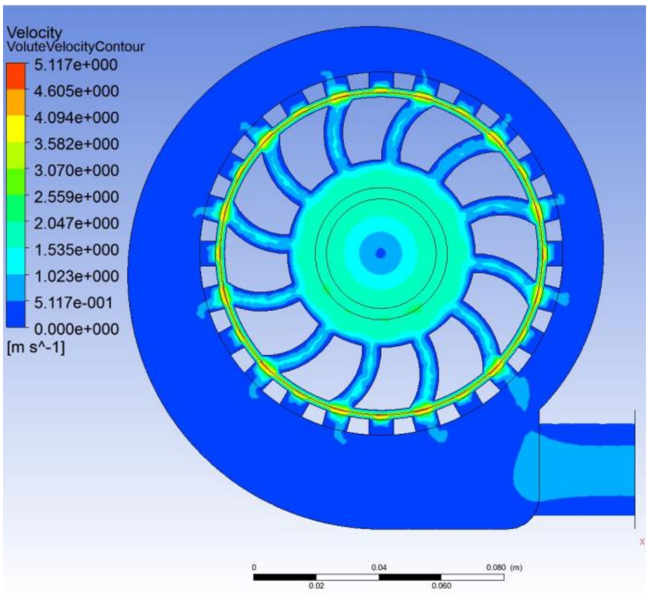

</td><td>
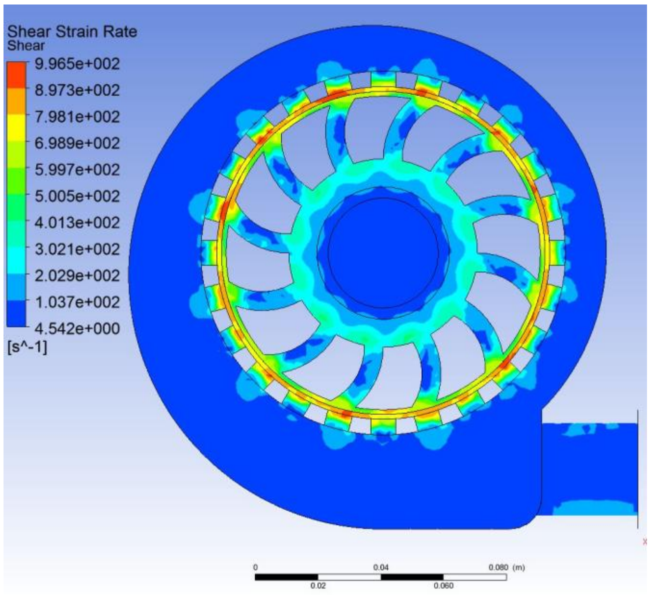

</td></tr>
</table>

Mass Flow Rate = 1.4 kg/s

400 RPM

Velocity	Shear Strain Rate
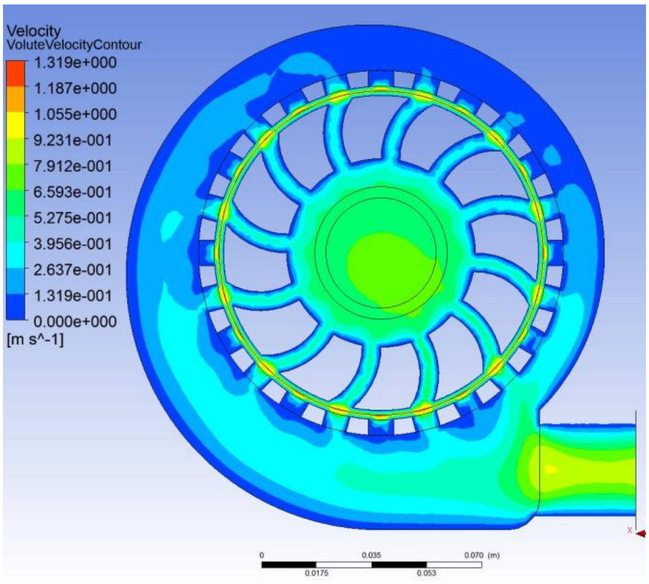	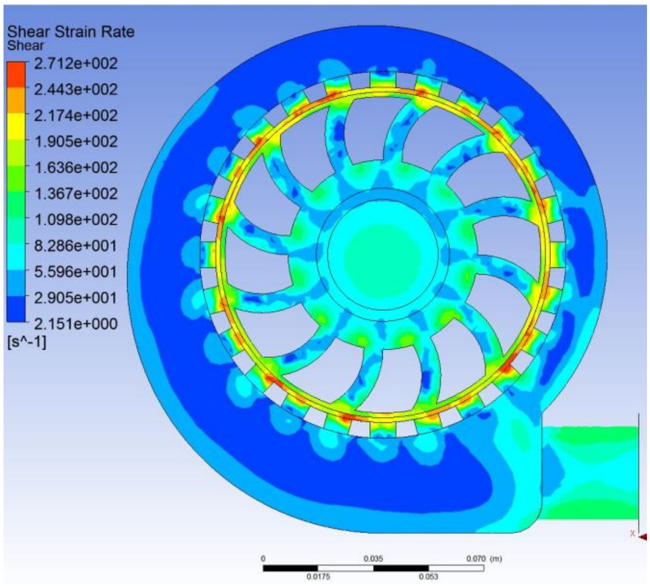

800 RPM

Velocity	Shear Strain Rate
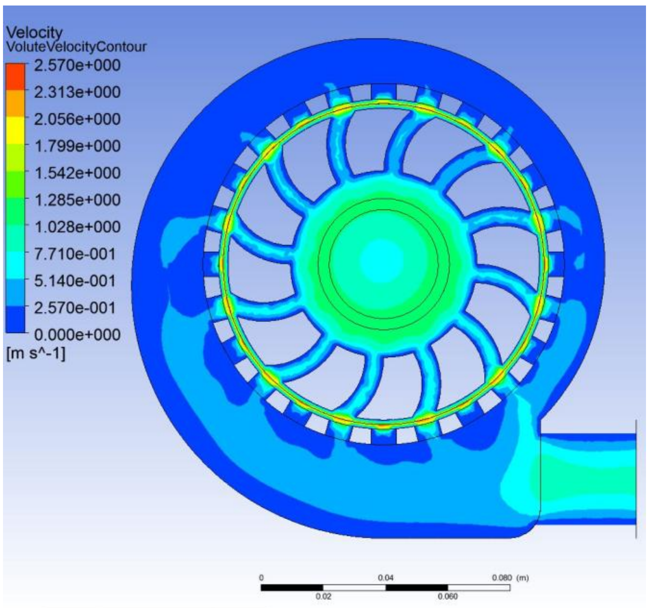	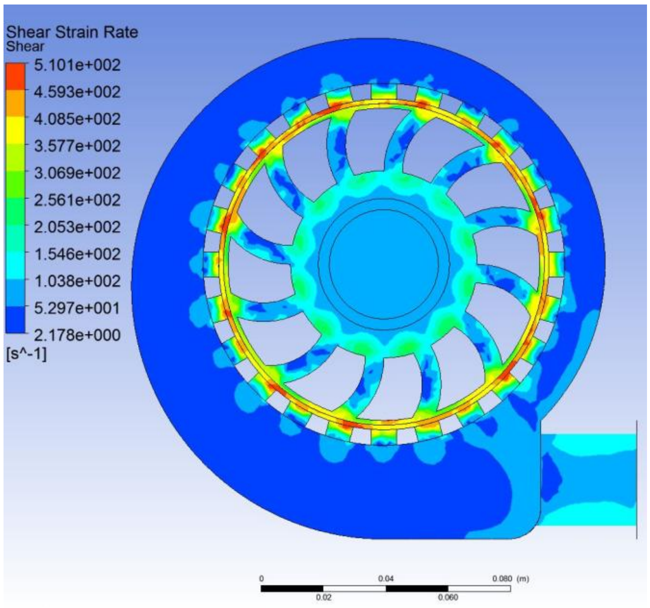

<table>
<tr><th colspan="2">Mass Flow Rate = 1.4 kg/s</th></tr>
<tr><th colspan="2">1200 RPM</th></tr>
<tr><th>Velocity</th><th>Shear Strain Rate</th></tr>
<tr><td>
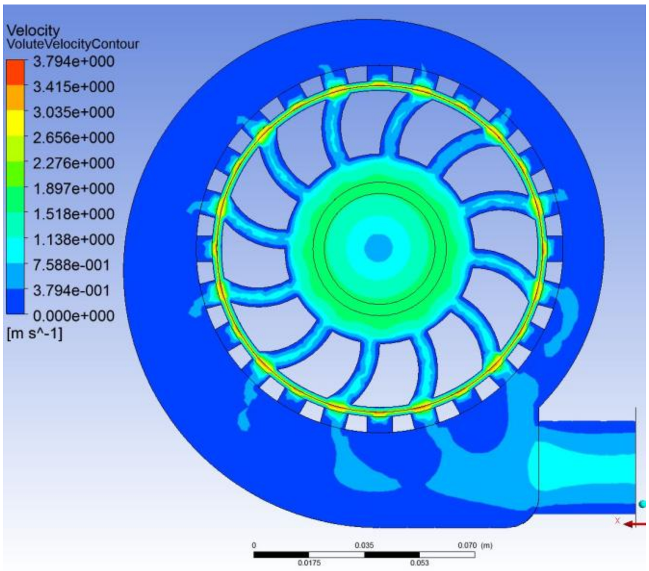

</td><td>
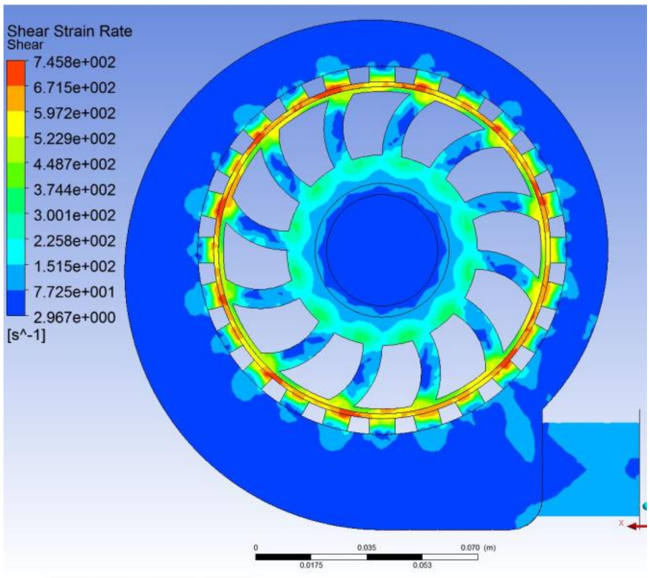

</td></tr>
<tr><th colspan="2">1600 RPM</th></tr>
<tr><th>Velocity</th><th>Shear Strain Rate</th></tr>
<tr><td>
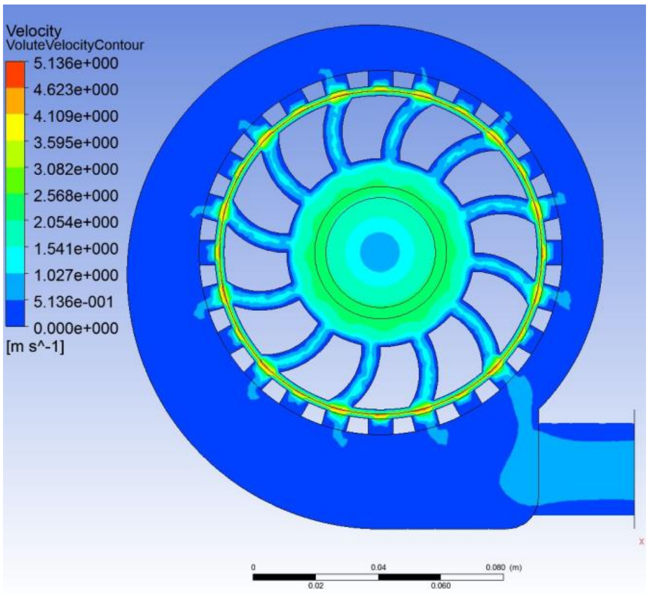

</td><td>
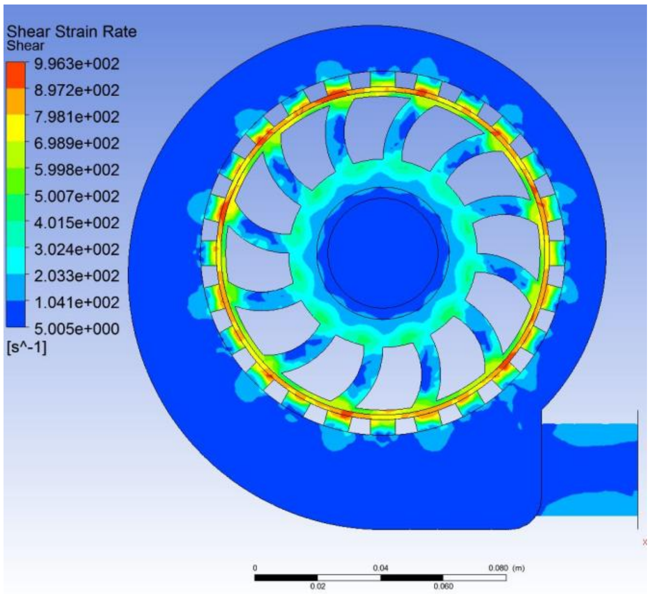

</td></tr>
</table>